Cruise Report ZDLM3-02-2018

Ground Fish survey

Michaël Gras, Haseeb Randhawa, Alex Blake, Tom Busbridge, Irina Chemshirova, Amy Guest

Falkland Islands Government
Directorate of Natural Resources
Fisheries
Stanley, Falkland Islands

Participating Scientific Staff

Dr Michaël Gras	Chief scientist
Tom Busbridge	Trawl survey supervisor
Alex Blake	Oceanography and Trawl Survey
Dr Haseeb Randhawa	Trawl survey
Irina Chemshirova	Trawl survey, data handling and training
Amy Guest	Trawl survey and training

Acknowledgements

We thank Captain José Vincente Santos Reiriz, officers and crew of the FV Monteferro for all of their work and assistance.

For citation purposes, this publication should be referenced as follows:
Gras, M., Randhawa, H.S., Blake, A., Busbridge, T., Chemshirova, I. and Guest, A., 2018. Report of the 2018 ground fish survey ZDLM3–02–2018. Stanley, Directorate of Natural Resources – Fisheries, Falkland Islands Government.

Contents

1.0 Introduction

Falkland Island waters are part of the Patagonian shelf large marine ecosystem, one of the most productive zones of the world (Bakun, 1993). The Falkland Islands declared the Falkland Interim Conservation Zone (FICZ) in 1986 and the Falkland Islands Fisheries Department (now Directorate of Natural Resources – Fisheries; DNRF) was created in 1987 to regulate and manage the fisheries. In 1990, the Falkland Outer Conservation Zone (FOCZ) extended the FICZ. Fishing vessels that want to operate in Falkland waters have to be licensed by the DNRF. The finfish fleet is managed using a total allowable effort (TAE) which is in theory derived from the five–year average effort required to reach the catch limit of the main finfish species (FIFD, 2016). Southern blue whiting (*Micromesistius australis*) was the main species and used to calculate TAE. However, when southern blue whiting crashed in the 2010s, rock cod (*Patagonotothen ramsayi*) took over and became the most abundant species exploited by the finfish fleet (Laptikhovsky et al., 2013). Since 2007, rock cod total annual catches ranged from 2,530 to 76,451 t.

Since 2010, six research cruises were conducted to estimate the biomass of the rock cod stock in February 2010 (Brickle and Laptikhovsky, 2010), 2011 (Arkhipkin et al., 2011), October–November 2014 (Pompert et al., 2014), and February 2015 - 2017 (Gras et al., 2015; 2016; 2017), prior to this survey. From 2011 to 2013, six research cruises were also undertaken to test various fishing gears. The objective was to find a new setup for the trawl to fish more efficiently by reducing the bycatch of undersized rock cod and non–commercial species (Brickle and Winter, 2011; Roux et al., 2012a; b; 2013a; b; c). The outcome was the publication of the new regulation in 2014 that came into force on 1 January 2015 to increase the mesh size from 90 to 110 mm in the cod-end.

The finfish fishery is a multi-species fishery where vessels work under licences A (unrestricted finfish), G (combined *Illex* and restricted finfish), and W (restricted finfish). While rock cod was the primary target species from 2007 to 2012, and in 2014, vessels also targeted or took as bycatch other finfish species such as common (*Merluccius hubbsi*) and Patagonian (*Merluccius australis*) hakes, kingclip (*Genypterus blacodes*), hoki (*Macruronus magellanicus*), red cod (*Salilota australis*), southern blue whiting, and one species of cephalopod, the Argentine shortfin squid (*Illex argentinus*). In recent years, the TAE estimation based on the primary species rock cod has shown its limitations, especially in years when rock cod was not the primary targeted stock, i.e. 2013, 2015–2017 (FIFD, 2014; 2015; 2016; 2017). It was then advised to not only focus on rock cod but also to collect as much data as possible about all the other species encountered throughout the survey, i.e. moving from single-species to multi-species surveys and management.

Over the last three decades, scientists have emphasized that trophic relationships play an important role in marine ecosystems (Bax, 1998) and that the ecological role of individual species within an ecosystem is dependent on trophic interactions, geographical distribution, other species present in the community, and type of feeding guild (Vaudo and Heithaus, 2011). Understanding the trophic interactions within marine ecosystems is linked to ecosystem function and is crucial for developing sustainable models to inform ecosystem-based management decisions in fisheries science (Link, 2002; Corrales et al., 2015). Hence, the data time series spent sampling the entire community over most of the finfish area, supported by occasional collection of stomach content data (as per Gras et al., 2017) and parasite survey, can help identify ecosystem shifts and changes in trophic interactions over time; crucial elements for moving towards an ecosystem-based management of the Falkland Islands fishery.

The primary objective of the survey was to assess the biomass and abundance of demersal commercial species encountered in the survey zone. Biological data (length, sex, maturity, and otoliths) were collected for a sample of each species at each station and used to describe the stock in February. In the present report, biological data are presented for all the species that more than 30 specimens were assessed throughout the cruise. Parasite data were collected for rock cod from every station and these data will be presented in a separate report. Finally, this report presents the maps of the oceanographic situation based on data collected in the vicinity of each trawl station.

2.0 Material and methods

2.1 Cruise vessel and surveyed area

The ground fish survey ZDLM3–02–2018 was conducted on board the F/V Monteferro (LOA 63.7 m, GRT 1499) from 3 to 24 February 2018. Embarking and disembarking occurred on 2 and 25 February respectively. In order to be able to compare data with previous biomass estimate surveys carried out since 2010 (Brickle and Laptikhovsky, 2010; Arkhipkin et al., 2011; Pompert et al., 2014; Gras et al. 2015; 2016; 2017a; b) it was decided to repeat stations already explored in 2011, 2014, 2015, 2016 and 2017. The map of the stations sampled during the cruise is presented in Figure 1 and coordinates are given in Table 1. Because the survey was firstly designed to study rock cod, it did not cover the deep water zone to the southwest and to the south of West Falkland. In order to better monitor southern blue whiting, hoki, grenadier, and toothfish, 23 stations were added in the south of the FICZ and 10 stations were removed in the east of the survey area in the north western part of the *Loligo* box since this region was already covered by the *Loligo* pre–recruitment survey running concurrently. The total number of trawl station was 102. However, in 2018 an unusual high abundance of jellyfish was observed to the west of West Falkland. Several tonnes of jellyfish were caught at 7 stations. After close examination of the catchlogs and length frequency data of species caught at these stations, scientists on board concluded that catchability of the net was altered at stations 143, 144, 156, and 164. Consequently, these stations were removed from the dataset used to study length frequency and to estimate biomass. At station 183, the portside wing and the belly of the net were damaged by an unidentified object. Although the catch seemed to be OK, it was decided to discard this station as well.

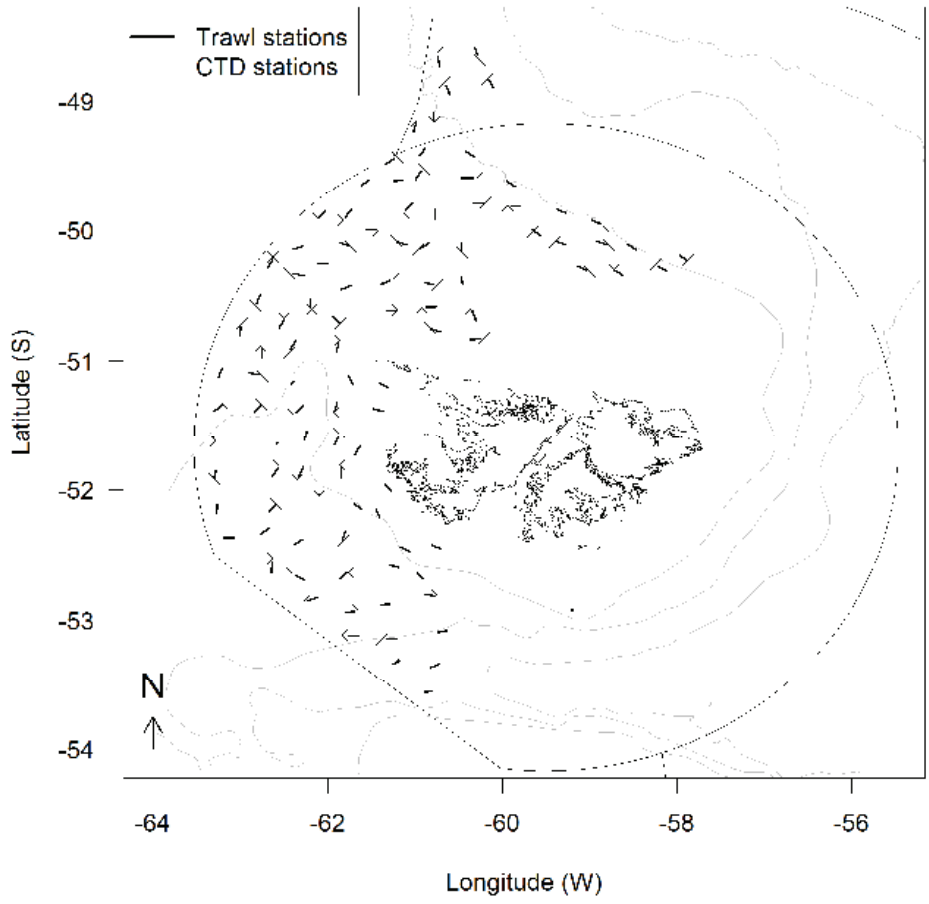

Figure 1: Location of trawl, plankton and CTDO stations

Table 1: Trawl stations number, date, geographical coordinates, depth, duration and associated comments. A CTD was also carried out before or after each trawl.

Station	Date	Longitude Start	Latitude Start	Longitude finish	Latitude Finish	Modal Depth (m)	Duration (min)	Activity	Comments
8	03/02/2018	57.97	50.19	57.89	50.23	271	60	B	
10	03/02/2018	58.12	50.31	58.23	50.27	161	60	B	
12	03/02/2018	58.46	50.15	58.56	50.11	166	60	B	
15	03/02/2018	58.81	50.11	58.92	50.08	154	60	B	
17	03/02/2018	58.88	49.95	58.98	49.92	190	60	B	
18	04/02/2018	58.62	50.35	58.72	50.31	143	60	B	
21	04/02/2018	59.04	50.31	59.15	50.27	149	60	B	
22	04/02/2018	59.28	50.11	59.39	50.09	157	60	B	
24	04/02/2018	59.56	50.05	59.66	50.00	159	60	B	
27	04/02/2018	59.28	49.87	59.38	49.84	185	60	B	
28	05/02/2018	60.33	49.80	60.21	49.80	165	60	B	
31	05/02/2018	59.91	49.81	59.80	49.82	167	60	B	
33	05/02/2018	59.85	49.65	59.95	49.61	185	60	B	
35	05/02/2018	60.34	49.59	60.47	49.59	169	60	B	
36	05/02/2018	60.32	49.43	60.42	49.39	197	60	B	
38	06/02/2018	60.11	48.89	60.17	48.83	371	60	B	
41	06/02/2018	60.28	48.65	60.32	48.59	375	60	B	
43	06/02/2018	60.74	48.66	60.72	48.73	241	60	B	
45	06/02/2018	60.65	48.88	60.60	48.96	238	60	B	
46	08/02/2018	60.79	49.09	60.79	49.15	188	60	B	
49	08/02/2018	60.99	49.17	61.02	49.23	170	60	B	
51	08/02/2018	60.88	49.36	60.95	49.42	167	60	B	
53	08/02/2018	60.93	49.53	60.99	49.60	164	60	B	
55	08/02/2018	61.24	49.44	61.35	49.48	160	60	B	
56	09/02/2018	61.62	49.65	61.53	49.60	157	60	B	
59	09/02/2018	61.25	49.61	61.14	49.60	161	60	B	
61	09/02/2018	61.11	49.85	61.02	49.79	162	60	B	
63	09/02/2018	60.77	49.84	60.77	49.91	162	60	B	
64	09/02/2018	60.85	50.10	60.95	50.14	158	60	B	
66	10/02/2018	60.47	50.10	60.46	50.17	157	60	B	
69	10/02/2018	60.47	50.35	60.46	50.42	152	60	B	
71	10/02/2018	60.35	50.62	60.30	50.69	142	60	B	
73	10/02/2018	60.25	50.83	60.37	50.84	134	60	B	
74	10/02/2018	60.71	50.78	60.82	50.76	133	60	B	
76	11/02/2018	61.33	50.62	61.21	50.61	149	60	B	
79	11/02/2018	60.88	50.59	60.76	50.59	148	60	B	
81	11/02/2018	60.78	50.42	60.89	50.40	149	60	B	
83	11/02/2018	61.29	50.38	61.40	50.42	159	60	B	
84	11/02/2018	61.73	50.43	61.85	50.45	165	60	B	
86	12/02/2018	61.10	50.11	61.21	50.09	158	60	B	
89	12/02/2018	61.45	50.00	61.57	50.00	156	60	B	
91	12/02/2018	61.76	50.12	61.87	50.09	156	60	B	

93	12/02/2018	61.80	49.90	61.73	49.84	155	60	B	
94	12/02/2018	62.03	49.85	62.11	49.91	145	60	B	
96	13/02/2018	62.00	50.25	62.12	50.25	157	60	B	
99	13/02/2018	62.29	50.13	62.40	50.15	146	60	B	
101	13/02/2018	62.63	50.23	62.68	50.29	145	60	B	
103	13/02/2018	62.40	50.33	62.27	50.35	151	60	B	
104	13/02/2018	62.20	50.53	62.19	50.60	163	60	B	
106	14/02/2018	62.77	50.49	62.82	50.56	147	60	B	
109	14/02/2018	62.99	50.74	63.01	50.81	152	60	B	
111	14/02/2018	62.76	50.91	62.75	50.98	163	60	B	
113	14/02/2018	62.43	50.91	62.36	50.85	179	60	B	
114	14/02/2018	62.56	50.75	62.50	50.68	162	60	B	
116	15/02/2018	61.95	50.66	61.87	50.71	179	60	B	
119	15/02/2018	61.87	50.87	61.90	50.93	172	60	B	
121	15/02/2018	61.77	51.11	61.70	51.18	178	60	B	
123	15/02/2018	61.41	51.17	61.31	51.20	134	60	B	
124	15/02/2018	61.37	51.39	61.48	51.36	142	60	B	
126	16/02/2018	61.89	51.32	61.93	51.39	197	60	B	
129	16/02/2018	61.87	51.58	61.92	51.65	169	60	B	
131	16/02/2018	62.26	51.61	62.24	51.54	247	60	B	
133	16/02/2018	62.36	51.40	62.28	51.34	207	60	B	
134	16/02/2018	62.42	51.18	62.38	51.16	187	30	B	Jellyfish
136	17/02/2018	62.84	51.39	62.77	51.34	181	60	B	
139	17/02/2018	62.78	51.11	62.90	51.09	168	60	B	
141	17/02/2018	63.21	51.05	63.25	51.12	153	60	B	
143	17/02/2018	63.21	51.34	63.31	51.39	163	55	B	Jellyfish
144	17/02/2018	63.31	51.59	63.31	51.61	178	15	B	Jellyfish
146	18/02/2018	63.28	51.85	63.30	51.91	200	55	B	Jellyfish
149	18/02/2018	63.26	52.11	63.27	52.18	227	60	B	
151	18/02/2018	63.19	52.37	63.07	52.36	257	60	B	
153	18/02/2018	62.77	52.34	62.68	52.29	266	60	B	
154	18/02/2018	62.68	52.17	62.60	52.12	254	60	B	
156	19/02/2018	62.57	51.64	62.59	51.65	208	15	B	Jellyfish
159	19/02/2018	62.58	51.83	62.64	51.90	229	60	B	
161	19/02/2018	62.33	51.90	62.28	51.82	262	60	B	
163	19/02/2018	61.85	51.83	61.84	51.91	184	60	B	
164	19/02/2018	62.08	52.03	62.09	52.04	287	10	B	Jellyfish
166	20/02/2018	61.63	51.67	61.69	51.73	146	60	B	
169	20/02/2018	61.35	51.96	61.28	52.01	120	60	B	
171	20/02/2018	61.45	52.14	61.41	52.21	184	60	B	
173	20/02/2018	61.61	52.15	61.70	52.10	249	60	B	
174	20/02/2018	61.79	52.31	61.83	52.38	317	60	B	Jellyfish
176	21/02/2018	62.28	52.38	62.38	52.42	291	60	B	
179	21/02/2018	62.64	52.55	62.65	52.64	298	60	B	
181	21/02/2018	62.37	52.65	62.26	52.69	321	60	B	
183	21/02/2018	62.24	52.85	62.12	52.83	342	60	B	Net broke

184	21/02/2018	61.86	52.68	61.78	52.63	340	60	B	
186	22/02/2018	61.29	52.87	61.40	52.88	368	60	B	
189	22/02/2018	61.70	52.93	61.80	52.94	381	60	B	
191	22/02/2018	61.76	53.11	61.65	53.12	479	60	B	
193	22/02/2018	61.33	53.14	61.21	53.14	505	60	B	
194	22/02/2018	61.17	53.31	61.26	53.34	578	60	B	
196	23/02/2018	60.90	52.80	60.77	52.81	399	60	B	
199	23/02/2018	60.64	53.08	60.74	53.09	495	60	B	
201	23/02/2018	60.72	53.33	60.82	53.36	704	60	B	
202	23/02/2018	60.80	53.55	60.90	53.56	733	60	B	
204	24/02/2018	60.90	52.68	60.98	52.64	375	60	B	
207	24/02/2018	61.19	52.59	61.29	52.57	366	60	B	
209	24/02/2018	61.17	52.44	61.06	52.47	263	60	B	
211	24/02/2018	60.81	52.42	60.70	52.45	182	60	B	

2.2 Trawl gear

The DNRF owns a bottom trawl fitted with rockhopper gear and used the Monteferro's Injector cobra 6.5 m² 2,600 kg bottom doors. The cod–end has a 90 mm mesh size. The cod–end was also fitted with a 10–15 mm cod end liner. The MarPort Net Monitoring System was used to monitor the geometry of the net. Originally sensors were fitted on both the trawl doors to monitor door depth, door horizontal spread, angle and tilt as well as one on the net to monitor vertical net opening. Of these data, only door horizontal spread and vertical net opening were recorded. Until the 2015 research cruise, the only information about the horizontal net opening was the wing spread derived as follows:

$$Wing\ spread = \frac{Door\ Spread\ \times Net\ Length}{Bridle\ Length + Net\ Length}$$

In 2016, two additional sensors were bought by the DNRF and attached 2 m behind the trawl wings to monitor the horizontal net opening at the same time as the door spread. Significant differences between calculated and measured values of the horizontal net opening were noted during the research cruise. A method was therefore developed to correct historical geometry net data (Gras, 2016).

During the research cruise ZDLT1–10–2014 (Pompert et al., 2014), a discussion with the captain about the gear configuration revealed that trawl setup was the same from 2011 to 2017 (ZDLT1–02–2011), but not the same as in 2010 (ZDLT1–02–2010) when Morgère Ovalfoil OF12.5 (3400 x 2200 cm) doors were used. According to the captain, the doors used from 2011 to 2017 on the F/V Castelo opened the trawl a bit more than previously. The trawl setup was asked to be rigorously the same as from 2014 to 2017 and especially the bridle length, which was 115 m. During ZDLT1–02–2010 and ZDLT1–02–2011 surveys, the bridle length was 100 and 120 m, respectively.

2.3 Biological sampling

For all the trawled stations, the entire catch was weighed by species (for finfish, squids, skates and sharks) or by the lowest taxonomic level (for invertebrates) using the electronic marine adjusted POLS balance. In the past, at some stations, when the catch was too large to be weighed, the crew processed the catch, a sample of the species concerned was taken before factory processing, weighed (green weight; GW), processed by the crew and weighed again (processed weight; PW) to estimate the conversion factor (CF) as:

$$CF = \frac{GW}{PW}$$

The catch (C) for this species was then estimated using the number of filled boxes (BN), the average box weight (BW) and the conversion factor as:

$$C = BN \times BW \times CF$$

At each station, random samples were taken from all finfish species as well as squids *Illex argentinus, Doryteuthis gahi*, and *Moroteuthis ingens*. When it was possible, 100 specimens of each finfish and squid species were randomly taken. All skates were sampled for total length, disk width, weight, sex, and maturity. Maturity stages were determined for all sampled specimens using an 8 stage maturity scale for finfish (see observer manual), a 6 stage maturity scale for both species of squid (see observer manual), and a 6 stage maturity scale for chondrichthyans (see observer manual). Length frequencies were recorded using fish measuring board and paper form.

Otolith extraction was undertaken for 29 finfish species and statoliths were extracted ashore from *I. argentinus, D. gahi*, and *M. ingens* (associated information were length, weight, sex and maturity). No vertebrae/thorn samples were collected from skates this year.

Skate specimens from the genus *Psammobatis* were not identified to species, due to confusion with available identification guides and available literature (i.e. McEachran, 1983). It is likely that the most common species found in waters deeper than 120 m is *Psammobatis normani* (slender claspers) whereas in shallower waters the most common species is *Psammobatis rudis* (short and stout claspers). During the survey there were no shallow stations and all specimens are most likely *P. normani.*

2.4 Biomass estimation

Biomass estimations using trawl surveys generally generate auto–correlated data (Rivoirard et al., 2000). To avoid processing biased data and overestimating the biomass of fish in the survey area, geostatistical methods were used to firstly describe and model data autocorrelation and secondly to estimate by kriging an unbiased mean of the studied variable to provide an interpolated map of the studied variable.

The variable used in this report is the density of each species of interest (derived from the catch and swept–area). The methodology described below uses R scripts developed to perform the 2010 rock cod assessment (Winter et al. 2010) in packages rgdal (geographical coordinates projection) (Bivand et al., 2017) and geoR (geostatistics) (Ribeiro Jr and Diggle, 2016).

The distance covered by the trawl was estimated using the geographical coordinates of the stations. For each station, coordinates of the start were extracted from the database fields

DegS_Start_Seabed, MinS_Start_Seabed, DegW_Start_Seabed, MinW_Start_Seabed and end from the database fields DegS_Finish_Seabed, MinS_Finish_Seabed, DegW_Finish_Seabed, MinW_Finish_Seabed and transformed first in decimal degrees (deg) and then in radians (rad) as:

$$rad = \frac{deg \times \pi}{180}$$

Radian coordinates were then used to calculate the distance between the start and end of the trawl track as:

$$d = \text{acos}(\sin(latS) \times \sin(latF) + \cos(latS) \times \cos(latF) \times \cos(lonF - lonF) \times R$$

where *d* is the distance covered in km, *latS* is the start latitude, *lonS* is the start longitude, *latF* is the end latitude, *lonF* is the end longitude and *R* is the radius of the earth (6,371 km). Density of the studied species (*D* in kg·km^{-2}) was finally derived using the catch (*C*), the distance covered (*d*) and the horizontal net opening (*HNO*; see Gras (2016) for details)

$$D = \frac{C}{d \times HNO}$$

Densities at stations were then used as input data in the geostatistical procedure to estimate the abundance of each species.

2.5 Geographical coordinates

Station's geographical coordinates were collected using the World Geodetic System of 1984 (WGS 84). However, as the Earth is a sphere and because the Falkland Islands are situated at relatively high latitudes (the study area in our case ranges from 48° to 52°S), one longitude degree does not have the same length as one latitude degree. Data were therefore projected in the Universal Transverse Mercator Coordinate System (zone 21; UTM 21) which keeps the distances between stations both in latitude and longitude. The projection was carried out using the project function (with following argument proj="+proj=utm +zone=21 +south +ellps=WGS84 +towgs84=0,0,0,0,0,0,0 +units=m +no_defs") of the rgdal R package. Previously in the Falkland Islands Fisheries Department, the Easting Northing system was used. A comparison between the UTM 21 projection and Easting Northing system showed no significant differences (Pompert et al., 2014).

2.6 Geostatistics methods

Geostatistic methods must be performed in 4 steps, (i) plotting and (ii) modelling the semi–variogram, (iii) using the variogram model to krige data in order to estimate an unbiased mean of the studied variable, and (iv) mapping the estimated data. The following criteria were used at different steps of the process to fit the right variogram model and estimate a realistic biomass for each species of interest.

- Various numbers of distance classes (from 10 to 50 classes) and 3 lambda parameters of the Box–Cox transformation (0, 0.5 and 1) were tested to obtain a scatter plot best describing the auto–correlation at short distances. The semi-variance values should increase with distance and reach the sill. The only accepted exception is the pure nugget effect.
- The range must be shorter than the maximum distance observed on the semi-variogram. In the studied dataset, some models can fit log transformed data (lambda=0) well, however they exhibit a range further than 400 km which is not biologically consistent in our case.

- Exponential, Gaussian and spherical models were fitted to the semi-variogram data and residual sum of square (RSS) were used as a basis to choose the most suitable model. The lowest RSS suggesting the most suitable model.
- Finally the kriging was performed and accepted if the range of estimated biomass was positive and reasonably close to the range of observed values. If not, another variogram model exhibiting higher RSS was tested until estimated and observed values were close enough.

The kriging area was 122,494 km^2. It was recently changed and extended from the survey area to the whole finfish zone. Biomass estimations for common rock cod, red cod, common hake, toothfish, kingclip, southern blue whiting, and Argentine shortfin squid were estimated using derived horizontal net opening for data collected in 2010, 2011, 2014 and 2015 (Gras, 2016) and using measured horizontal net opening for 2016–2018 datasets and time series displayed for every species.

2.7 Abundance estimation

At each survey station, a random sample of 100 specimens was assessed for total length, sex, and maturity. The total number of fish–at–station N_s was estimated using the number of fish in the sample (n_s), the station catch weight (C_s) and the sample weight (W_s) as

$$N_s = \frac{n_s \times C_s}{W_s}$$

The total abundance in the water N_t was estimated using the total biomass B (estimated following protocol of section 2.6)

$$N_t = \frac{B \times \sum N_s}{\sum C_s}$$

The total number of fish–at–length l for each station ($N_{l,s}$) was then estimated using the total number of fish–at–station (N_s) and the number of fish per size class in the sample

$$N_{l,s} = \frac{n_{l,s} \times C_s}{W_s}$$

Finally the total abundance of fish–at–length in the water was estimated using the biomass estimation (B; see section 2.6)

$$N_{l,t} = \frac{B \times \sum N_{l,s}}{\sum C_{l,s}}$$

The numbers–at–length were then presented in histograms to show how the structures of the stocks have changed over the years.

2.8 Oceanography

A single CTD (SBE-25, Sea-Bird Electronics Inc., Bellevue, USA) instrument, Serial No 0247, was used to collect oceanographic data in the vicinity of all trawl stations. Soak time was one minute at *c.*10 m depth to allow flushing of the system. Once flushing completed, the CTD was raised to a minimum depth of 5 m below surface, then lowered towards the sea bed at a speed of 1 $m \cdot sec^{-1}$. The CTD collected: (1) pressure in dbar; (2) temperature in °C; (3) conductivity in mS/cm; (4) Oxygen voltage; and (5) fluorescence. At the first station the CTD wrote the data to a greater number of columns than was recorded, and this has not been recovered. Luckily this was noticed before the second CTD station, and resetting the CTD back to factory settings and rebuilding the internal configuration allowed for good data to be collected at all subsequent stations. The raw .hex files were converted and processed using SBE Data Processing (version.7.22.5) using the CON file 0247_2017_06.xmlcon. Up-cast data was filtered out. Depth was derived from pressure using the latitude of each station, with dissolved oxygen in ml/L derived at the same time as depth. Practical salinity (PSU) and density (sigma-t [σ-t]) were derived following derivation of depth. Further derived variables of conservative temperature (°C) and absolute salinity (g/kg) were calculated in Ocean Data View version 4.5.4 (Schlitzer, 2013).

3.0 Results

3.1 Catch composition

Bottom trawling was conducted at 102 stations (97 stations were considered good to study stock structure and estimate biomass) as shown in Figure 1 and Table 1. Seabed trawling times during the survey was 60 minutes for 96 of the trawls. At stations 134, 143, 144, 146, 156, and 164 the time of trawling ranged from 15 to 55 min (see Table 1 for exact values). As a result of the high abundance of jellyfish in the west of the FICZ, the net catchability was altered and the doors closed leading to an anticipated hauling and the discard of stations 143, 144, 156 and 164.

During the survey a total of 130,402.1 kg of biomass was caught comprising 125 species or taxa (Appendix Table 2). The largest catches by weight, all exceeding 950 kg in total, were in order of importance: jellyfish (37,476 kg); hoki (29,335 kg); red cod (12,734 kg); rock cod (11,383 kg); Argentine shortfin squid (10,694 kg); banded whiptail grenadier (*Coelorhynchus fasciatus*) (6.854 kg); ridge scaled rattail (*Macrourus carinatus*) (3,945 kg); kingclip (3,351 kg); lobster krill (*Munida* spp.) (2,522 kg); southern blue whiting (2,201 kg); common hake (1,732 kg); toothfish (1,389 kg); and Falkland calamari (*D. gahi*) (968 kg).

3.2 Biological information of finfish species

Species summaries are presented in alphabetical order (based on species code) of commercial species (BAC [3.2.1] to WHI [3.2.9]) followed by non-commercial species (BUT [3.2.10] to SAR [3.2.21]).

3.2.1 *Salilota australis* – red cod – BAC (Figure 2)

The total catch of red cod was 12,734 kg. It was caught at 81 of the 97 stations (Figure 2A) sampled throughout the research cruise. Catches ranged from 0.02 to 7,559 kg. Among the 81 stations, 34 yielded >10 kg, 14 >100 kg, and one >1 t. Densities ranged from 0.09 to 34,512 kg·km^{-2} (CPUE ranged 0.02–7,559 kg·h^{-1}). Catches of red cod occurred almost everywhere across the survey area, but in small quantities except to the west of West Falkland between 50°30'S and 53°00'S where higher abundances were observed. The number of fish sampled for length frequency was 3,188 (2,025 females and 1,163 males) and 255 were taken for otoliths including 11 as non–random. Total length ranged from 14 to 80 cm for females and from 13 to 72 cm for males (Figure 2C). The histogram exhibits a series of modes, but due to the overlap between them it is difficult to identify individual cohorts. Females were observed immature (10%), resting (87%), early developing (2%), spent (0.1%) and recovering spent (1%) (Figure 2B). Males were immature (13%), resting (83%), early developing (4%) and late developing (0.3%) (Figure 2B).

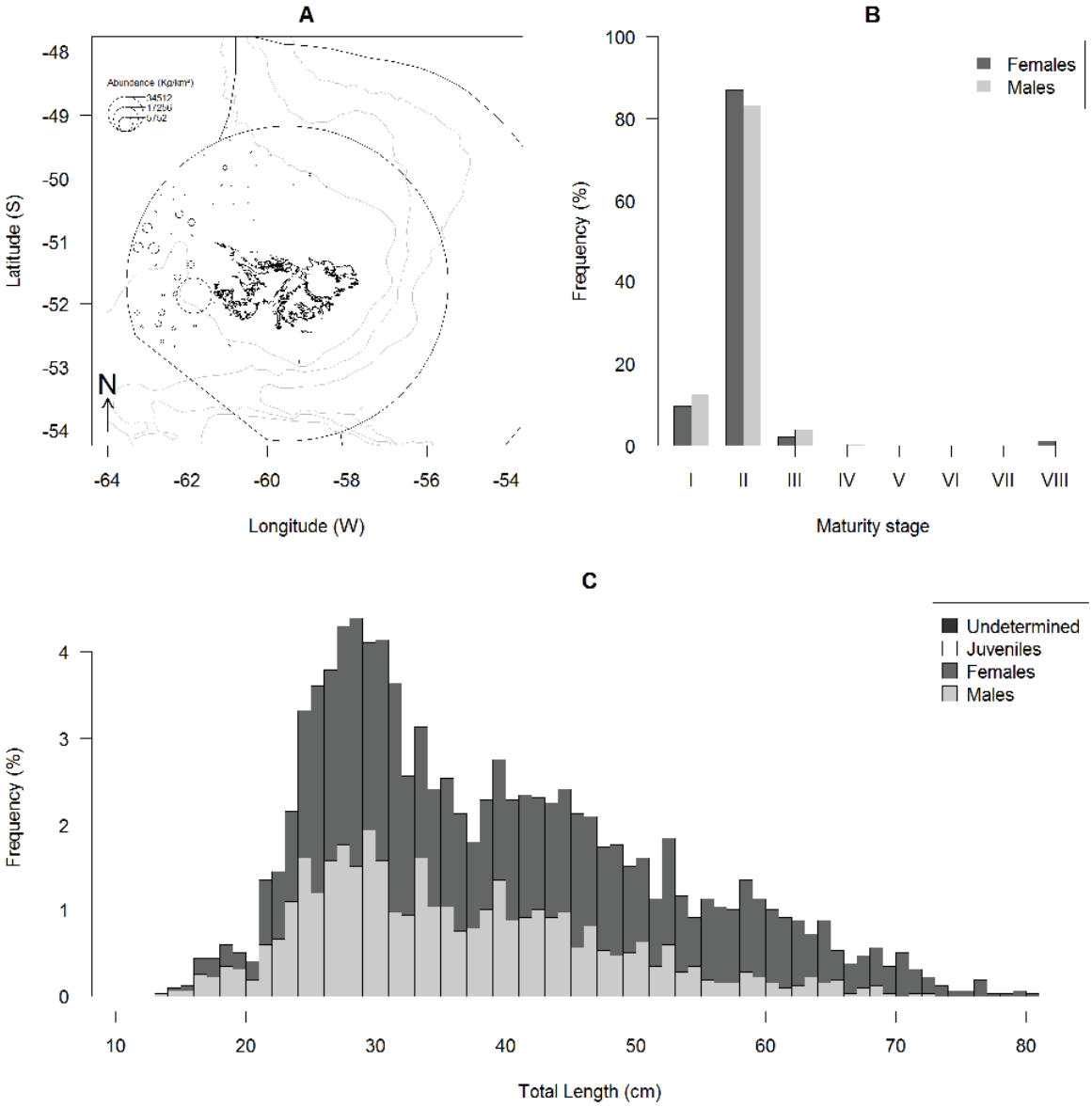

Figure 2: Biological data of *Salilota australis* (red cod; BAC), map of the densities in kg·km^{-2} (A), percentage of specimens of each sex per maturity stage (B; I, immature; II, resting; III, early developing; IV, late developing; V, ripe; VI, running; VII, spent; VIII, recovering spent), and length frequency (in percentage of the total sample assessed) of each sex with 1 cm size class (C; n= 3,188).

3.2.2 *Micromesistius australis* – southern blue whiting – BLU (Figure 3)

The total catch of southern blue whiting was 2,201 kg. It was caught at 62 of the 97 trawl stations sampled throughout the research cruise (Figure 3A). Catches ranged from 0.01 to 420 kg. Among the 62 stations, 20 yielded >10 kg and six yielded >100 kg. Densities ranged from 0.04 to 2,017 kg·km^{-2} (CPUE ranged 0.01–420 kg·h^{-1}). Highest densities were observed in the southwest of the survey area, especially at stations that were added to this year's survey (Figure 3A). The highest densities were observed along the border between the FICZ and Argentine waters at deep water stations. The number of fish sampled for length frequency was 2,704 (38 juveniles, 1,157 females and 1,509 males) and 249 were sampled for otolith including 76 taken non–randomly. Total lengths ranged from six to 11 cm for juveniles, from 19 to 65 cm for females, and from 20 to 63 cm for males (Figure 3C). Four cohorts were easily identifiable on the length frequency histogram with modes at ten, 24, 32 and 42 cm (Figure 3C). Females were observed immature (70%), resting (25%), early developing (0.1%), and recovering spent (5%) (Figure 3B). Males were immature (64%), resting (23%), and recovering spent (13%) (Figure 3B).

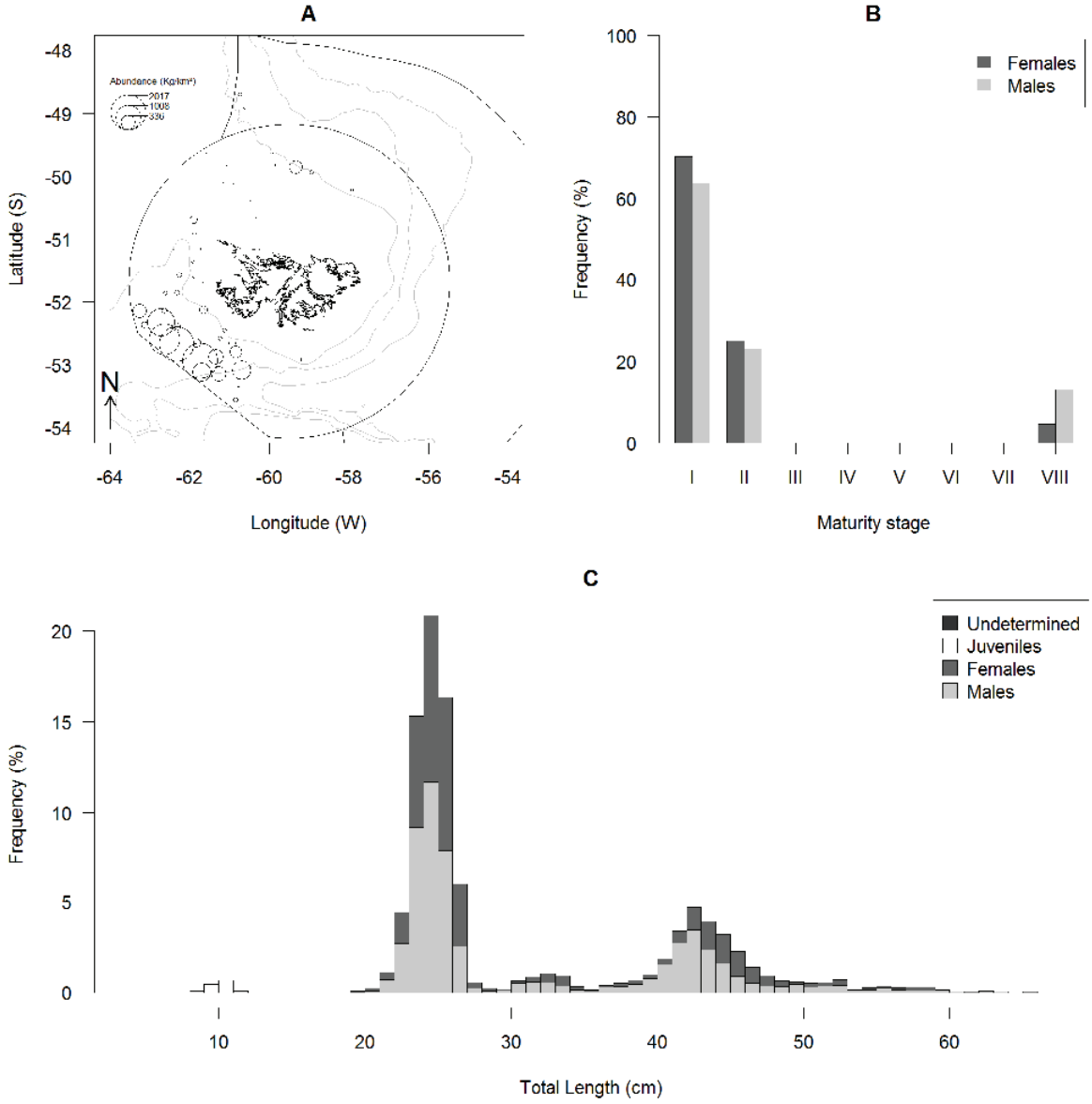

Figure 3: Biological data of *Micromesistius australis* (southern blue whiting; BLU), map of the densities in kg·km^{-2} (A), percentage of specimens of each sex per maturity stage (B; I, immature; II, resting; III, early developing; IV, late developing; V, ripe; VI, running; VII, spent; VIII, recovering spent), and length frequency (in percentage of the total sample assessed) of each sex with 1 cm size class (C; n= 2,704).

3.2.3 *Macrourus carinatus* – grenadier-ridge scaled rattail – GRC (Figure 4)

The total catch of grenadier–ridge scaled rattail was 3,945 kg. It was caught at 15 of the 97 trawl stations sampled throughout the research cruise (Figure 4A). Catches ranged from 1.00 to 936 kg. Among the 15 stations, 13 yielded >10 kg and eight >100 kg. Densities ranged from 5.39 to 5,783 kg·km^{-2} (CPUE ranged 1.00–936 kg·h^{-1}). Highest densities were observed in the south-western part of the survey zone, especially in deeper waters, the usual habitat for this species. The number of fish sampled for length frequency was 1,072 (one juvenile, 715 females, 355 males, and one unsexed), 135 were taken for collection of otoliths; all of them were taken as part of the random sample. Pre-anal lengths were six cm for the juvenile and 21 for the undetermined, and ranged from six to 33 cm for females and from six to 28 cm for males (Figure 4C). Cohorts were difficult to identify on the length frequency histogram as they are most likely overlapping (Figure 4C). Overall, males appeared to be smaller than females. Females were observed immature (1%), resting (18%), early developing (16%), late developing (30%), ripe (12%), spent (7%), and recovering spent (16%) (Figure 4B). Males were immature (4%), resting (7%), early developing (12%), late developing (77%), and spent (0.3%) (Figure 4B).

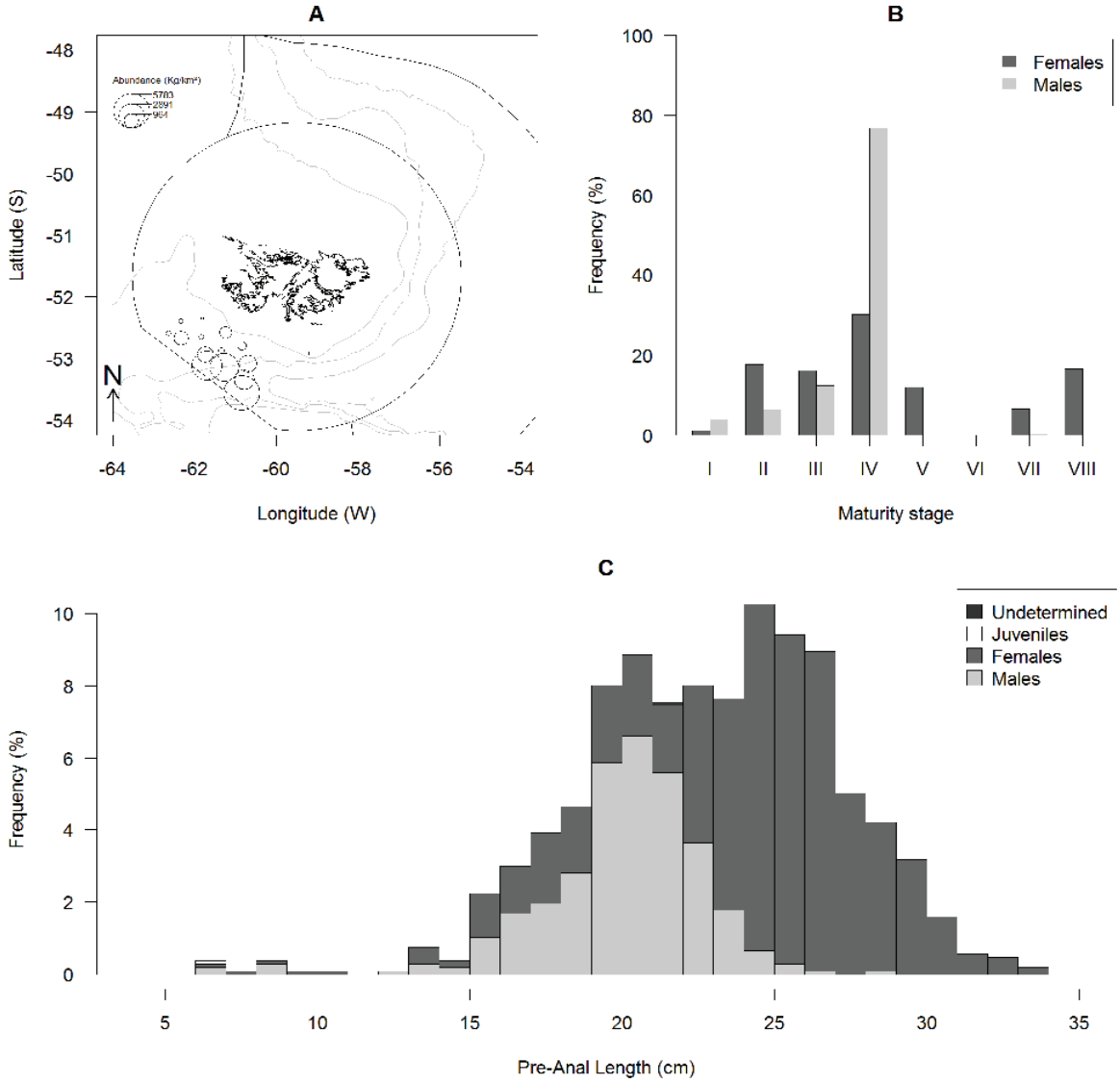

Figure 4: Biological data of *Macrourus carinatus* (Grenadier-Ridge Scaled Rattail; GRC), map of the densities in kg·km^{-2} (A), percentage of specimens of each sex per maturity stage (B; I, immature; II, resting; III, early developing; IV, late developing; V, ripe; VI, running; VII, spent; VIII, recovering spent), and length frequency (in percentage of the total sample assessed) of each sex with 1 cm size class (C; n= 1,072).

3.2.4 *Merluccius hubbsi* – common hake – HAK (Figure 5)

The total catch of common hake was 1,732 kg. It was caught at 56 of the 97 trawl stations sampled throughout the research cruise (Figure 5A). Catches ranged from 0.23 to 223 kg. Among the 56 stations, 36 yielded >10 kg and three >100 kg. Densities ranged from 1.07 to 1,046 kg·km^{-2} (CPUE ranged 0.23–223 kg·h^{-1}). Common hake was observed to the west of 60°W and to the north of 51°S, an area where hake has historically been observed at this time of the year. The number of fish sampled for length frequency was 2,508 (2,105 females, 401 males and two unsexed), 160 were taken for otolith including one non–randomly chosen individual. Total length was 28 and 38 cm for two unsexed individuals, respectively, and ranged from 23 to 75 cm for females and from 25 to 70 cm for males (Figure 5C). Two cohorts can be distinguished on the length frequency histogram (Figure 5C). The first one most likely consists of three–year old animals. The other cohorts most likely overlap each other, but a clear second cohort can be seen at 43 cm (Figure 5C). Females were observed immature (0.2%), resting (34%), early developing (59%), late developing (0.1%), spent (1%), and recovering spent (6%) (Figure 5B). Males were immature (0.2%), resting (29%), early developing (1%), late developing (0.2%), ripe (0.2%), running (0.2%), spent (65%), and recovering spent (4%) (Figure 5B).

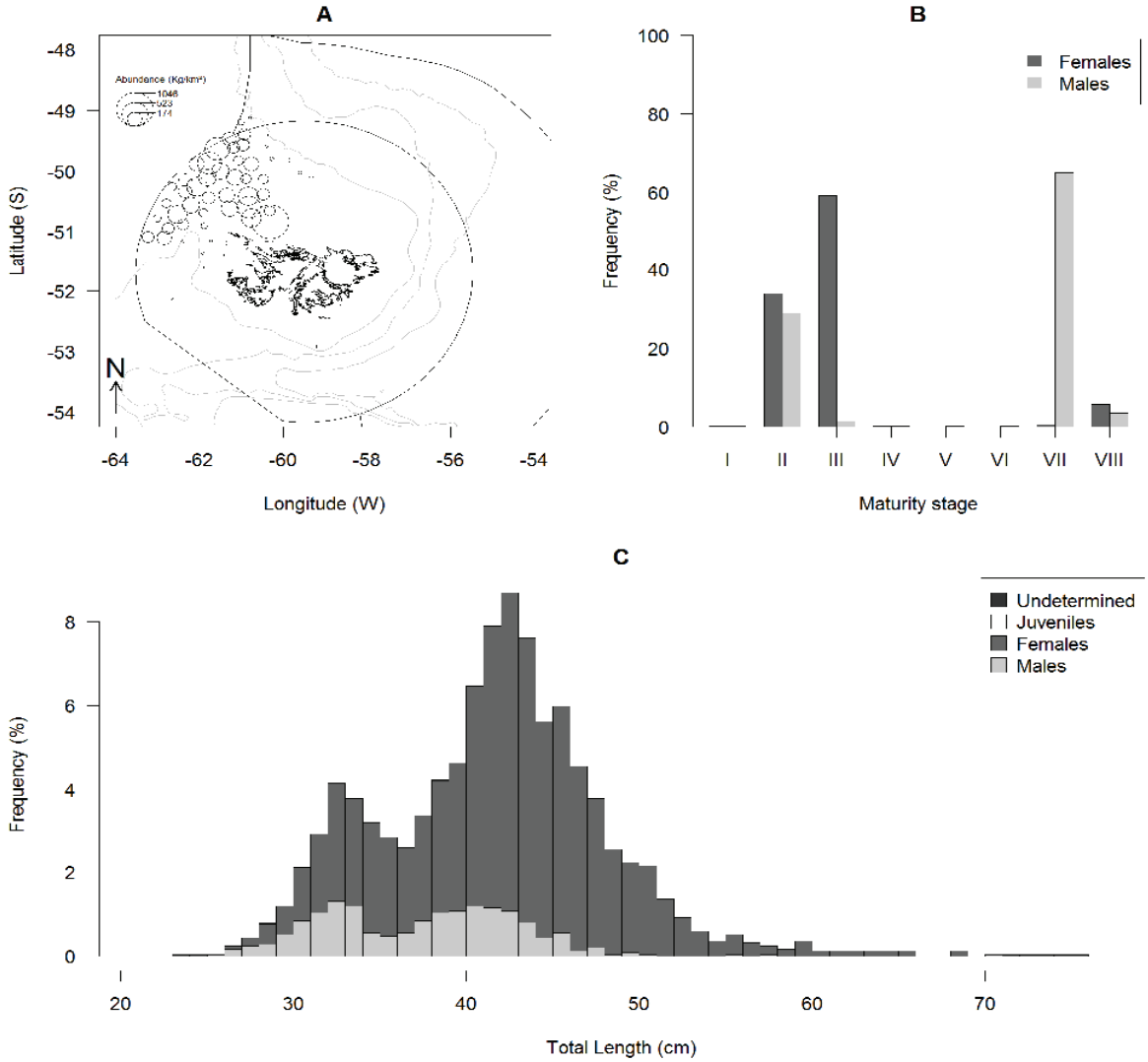

Figure 5: Biological data of *Merluccius hubbsi* (common hake; HAK), map of the densities in kg·km^{-2} (A), percentage of specimens of each sex per maturity stage (B; I, immature; II, resting; III, early developing; IV, late developing; V, ripe; VI, running; VII, spent; VIII, recovering spent), and length frequency (in percentage of the total sample assessed) of each sex with 1 cm size class (C; n= 2,508).

3.2.5 *Genypterus blacodes* – kingclip – KIN (Figure 6)

The total catch of kingclip was 3,351 kg. It was caught at 81 of the 97 trawl stations sampled throughout the research cruise (Figure 6A). Catches ranged from 0.44 to 389 kg. Among the 81 stations, 54 yielded >10 kg and nine >100 kg. Densities ranged from 2.11 to 1,667 kg·km^{-2} (CPUE ranged 0.44–389 kg·h^{-1}). Highest densities were observed in three different areas of the survey zone, one in the north along the border between the FICZ and the FOCZ where high densities of kingclip are usually observed, and two were in the west and exhibited lower densities (Figure 6A). The number of fish sampled for length frequency was 2,871 (one juvenile, 1,623 females, 1,245 males and two unsexed), 381 were taken for otolith (all of them were randomly sampled). Total length was 23 cm for the juvenile, and ranged from 27 to 134 cm for females and from 25 to 125 cm for males (Figure 6C). One cohort can be seen on the histogram and the others are difficult to identify due to overlap (Figure 6C). Females were observed immature (4%), resting (76%), early developing (14%), late developing (4%), ripe (1%), spent (0.1%) and recovering spent (0.2%) (Figure 6B). Males were immature (14%), resting (72%), early developing (11%), late developing (3%), and recovering spent (0.1%) (Figure 6B).

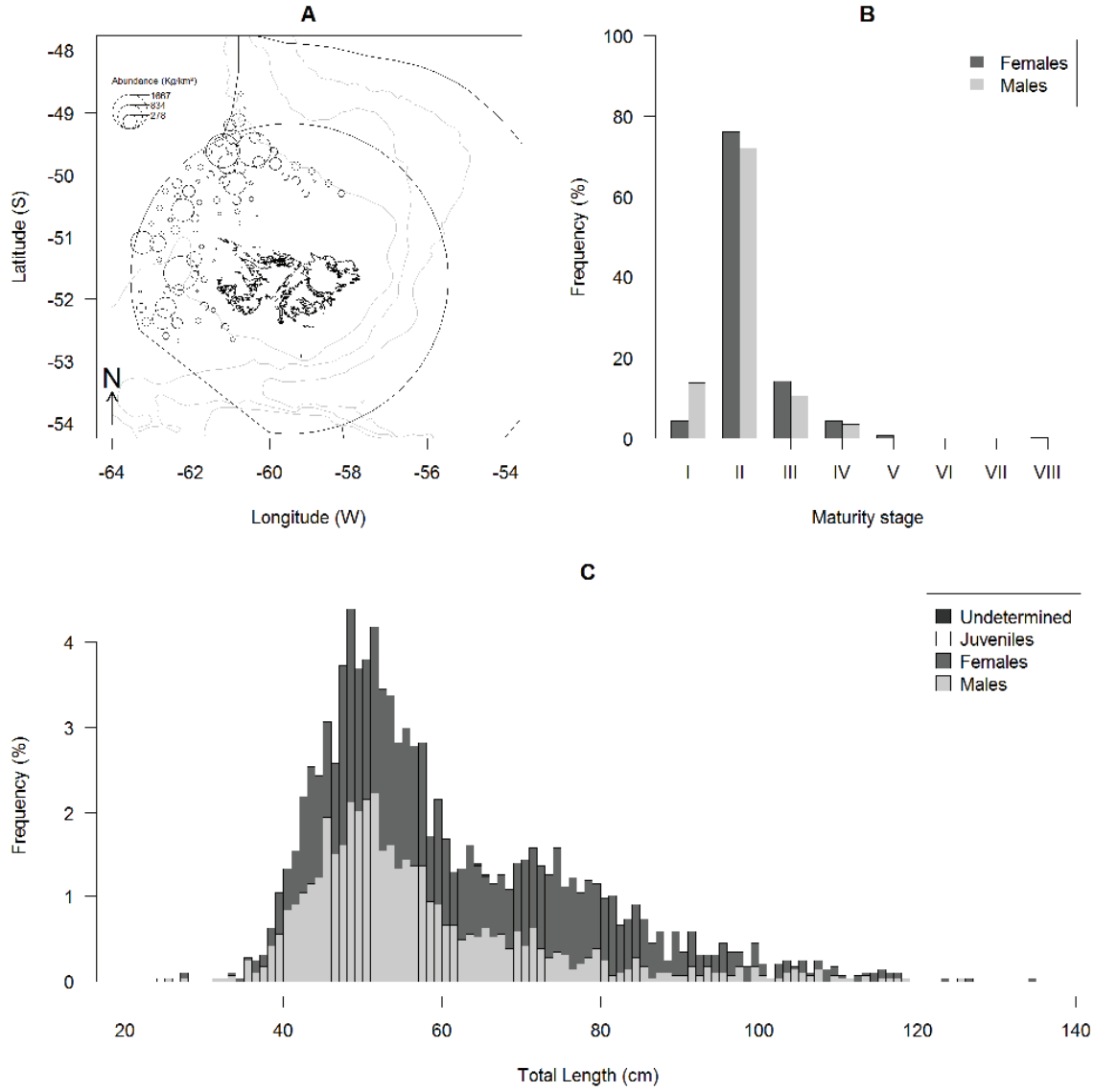

Figure 6: Biological data of *Genypterus blacodes* (kingclip; KIN), map of the densities in kg·km^{-2} (A), percentage of specimens of each sex per maturity stage (B; I, immature; II, resting; III, early developing; IV, late developing; V, ripe; VI, running; VII, spent; VIII, recovering spent), and length frequency (in percentage of the total sample assessed) of each sex with 1 cm size class (C; n= 2,871).

3.2.6 *Patagonotothen ramsayi* – common rock cod – PAR (Figure 7)

The total catch of common rock cod was 11,383 kg. It was the only species caught at all 97 trawl stations sampled throughout the research cruise (Figure 7A). Catches ranged from 0.09 to 2,035 kg. Among the 97 stations, 81 yielded >10 kg, 24 >100 kg and three >1 t. Densities ranged from 0.56 to 8,753 kg·km^{-2} (CPUE ranged 0.09–2,035 kg·h^{-1}). Highest densities were observed to the north of East Falkland where young fish are generally sampled and to the northwest of West Falkland where bigger fish are found (Figure 7A). The latter is where the bulk of the commercial exploitation occurred between 2007 and 2014. The number of fish sampled for length frequency was 9,834 (ten juveniles, 4,875 females, 4,927 males, and 22 unsexed), 12 were sampled for length–weight, and 673 for otolith including 39 taken as non–random samples. Total length ranged from five to 12 cm for juveniles, from nine to 39 cm for females, and from ten to 38 cm for males (Figure 7C). The histogram exhibits two different cohorts with modes at 14 and 20 cm, respectively. Females were observed immature (17%), resting (80%), early developing (1%), ripe (0.1%), spent (0.6%), and recovering spent (1%) (Figure 7B). Males were immature (21%), resting (78%), and early developing (1%) (Figure 7B).

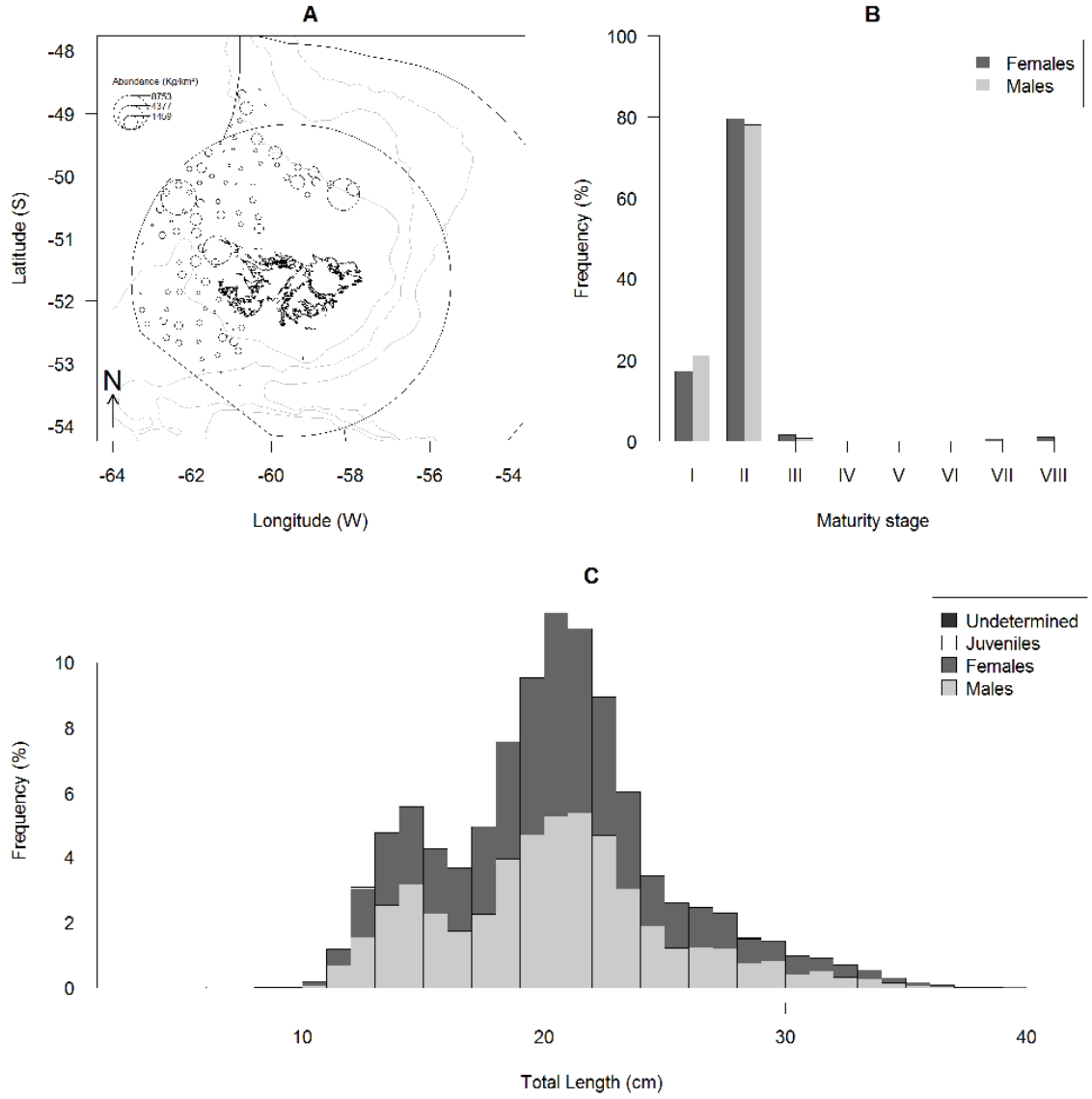

Figure 7: Biological data for *Patagonotothen ramsayi* (common rock cod; PAR), map of the densities in kg·km^{-2} (A), percentage of specimens of each sex per maturity stage (B; I, immature; II, resting; III, early developing; IV, late developing; V, ripe; VI, running; VII, spent; VIII, recovering spent), and length frequency (in percentage of the total sample assessed) of each sex with 1 cm size class (C; n=9,834).

3.2.7 *Merluccius australis* – Patagonian hake – PAT (Figure 8)

The total catch of Patagonian hake was 268 kg. It was caught at 20 of the 97 trawl stations sampled throughout the research cruise (Figure 8A). Catches ranged from 0.89 to 34.2 kg. Among the 20 stations, nine yielded >10 kg. Densities ranged from 4.09 to 185 kg·km^{-2} (CPUE ranged 0.89–34.2 kg·h^{-1}). Almost all the stations where Patagonian hake were observed were in the southwest of the survey zone between the 200 m isobath and the border between the FICZ and Argentine waters (Figure 8A). This area is in deep waters where Patagonian hake are the most abundant. Patagonian hake was also sampled at one station to the north of West Falkland in waters shallower than 200 m (Figure 8A). The number of fish sampled was 79 (78 females and a single male) and otoliths were taken from all of them. Total length ranged from 54 to 98 cm for females and was 83 cm for the lone male (Figure 8C). The small number of fish and the large size range did not enable us to identify cohorts on the length frequency histogram. Females were observed resting (33%), early developing (38%), late developing (28%) and recovering spent (1%) (Figure 8B). The male was late developing (Figure 8B).

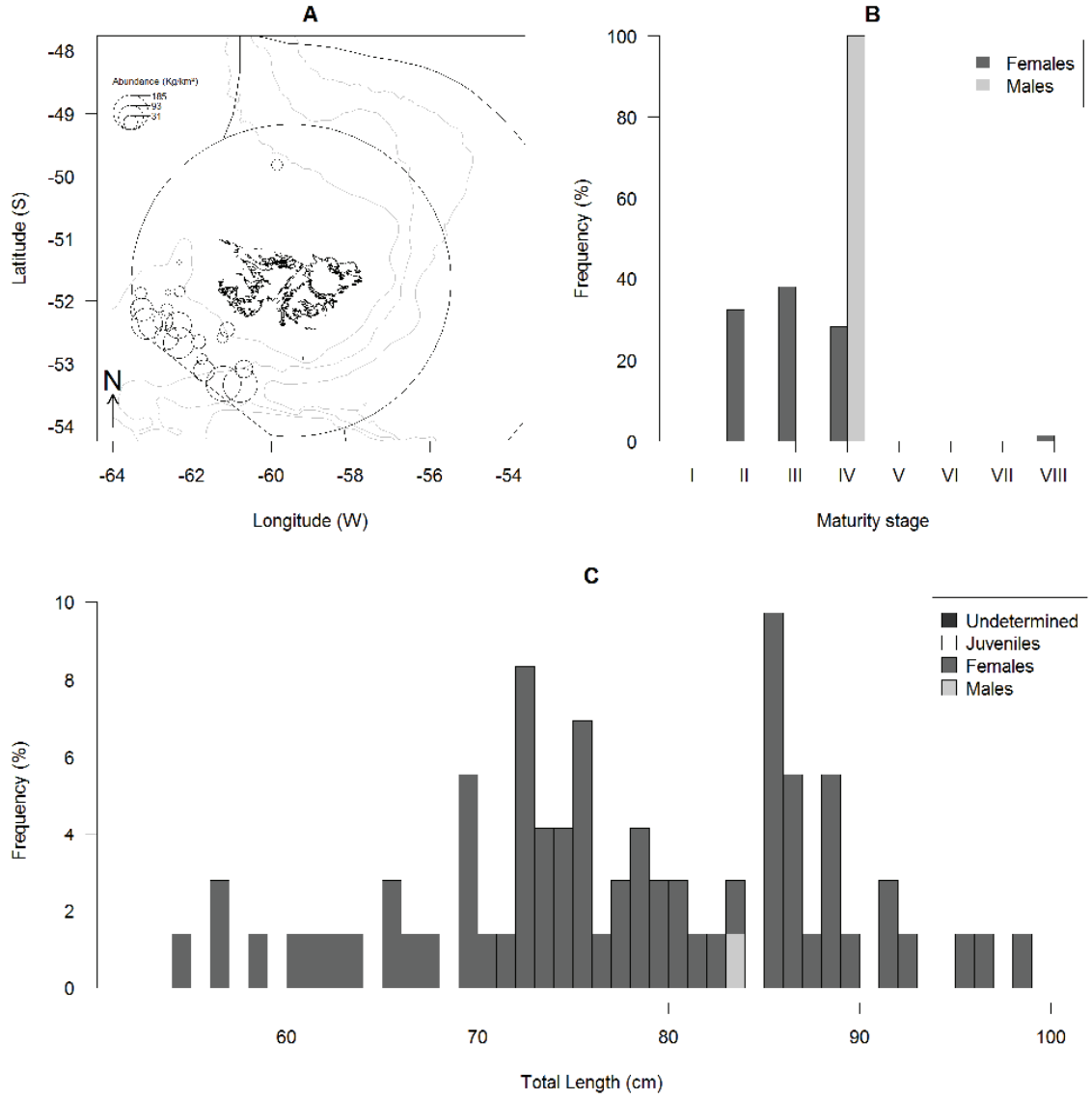

Figure 8: Biological data of *Merluccius australis* (Patagonian hake; PAT), map of the densities in kg·km^{-2} (A), percentage of specimens of each sex per maturity stage (B; I, immature; II, resting; III, early developing; IV, late developing; V, ripe; VI, running; VII, spent; VIII, recovering spent), and length frequency (in percentage of the total sample assessed) of each sex with 1 cm size class (C; n= 79).

3.2.8 *Dissostichus eleginoides* – Patagonian toothfish – TOO (Figure 9)

The total catch of Patagonian toothfish was 1,389 kg. It was caught at 77 of the 97 trawl stations sampled throughout the research cruise (Figure 9A). Catches ranged from 0.36 to 198 kg. Among the 77 stations, 28 yielded >10 kg and three yielded >100 kg. Densities ranged from 1.71 to 902 kg·km^{-2} (CPUE ranged 0.36–198 kg·h^{-1}). Highest densities were observed in the southwest of the survey zone, especially at stations sampled for the first time in 2018 (Figure 9A). A high density station was also observed to the south of the Jason Islands and consisted of young toothfish. The number of fish sampled for length frequency was 1,123 (657 females, 460 males, and six unsexed), 77 were sampled for length–weight and 533 for otoliths; all of them taken as random samples. Total length ranged from 24 to 82 cm for females and from 23 to 70 cm for males (Figure 9C). The first cohort is easily identifiable on the length frequency histogram with its mode at 30 cm (Figure 9C). Two other cohorts might appear with modes at 49 and 57 cm but are difficult to identify (Figure 9C). Females were observed immature (36%), and resting (63%) (Figure 9B). Males were immature (44%), resting (55%), and early developing (1%) (Figure 9B).

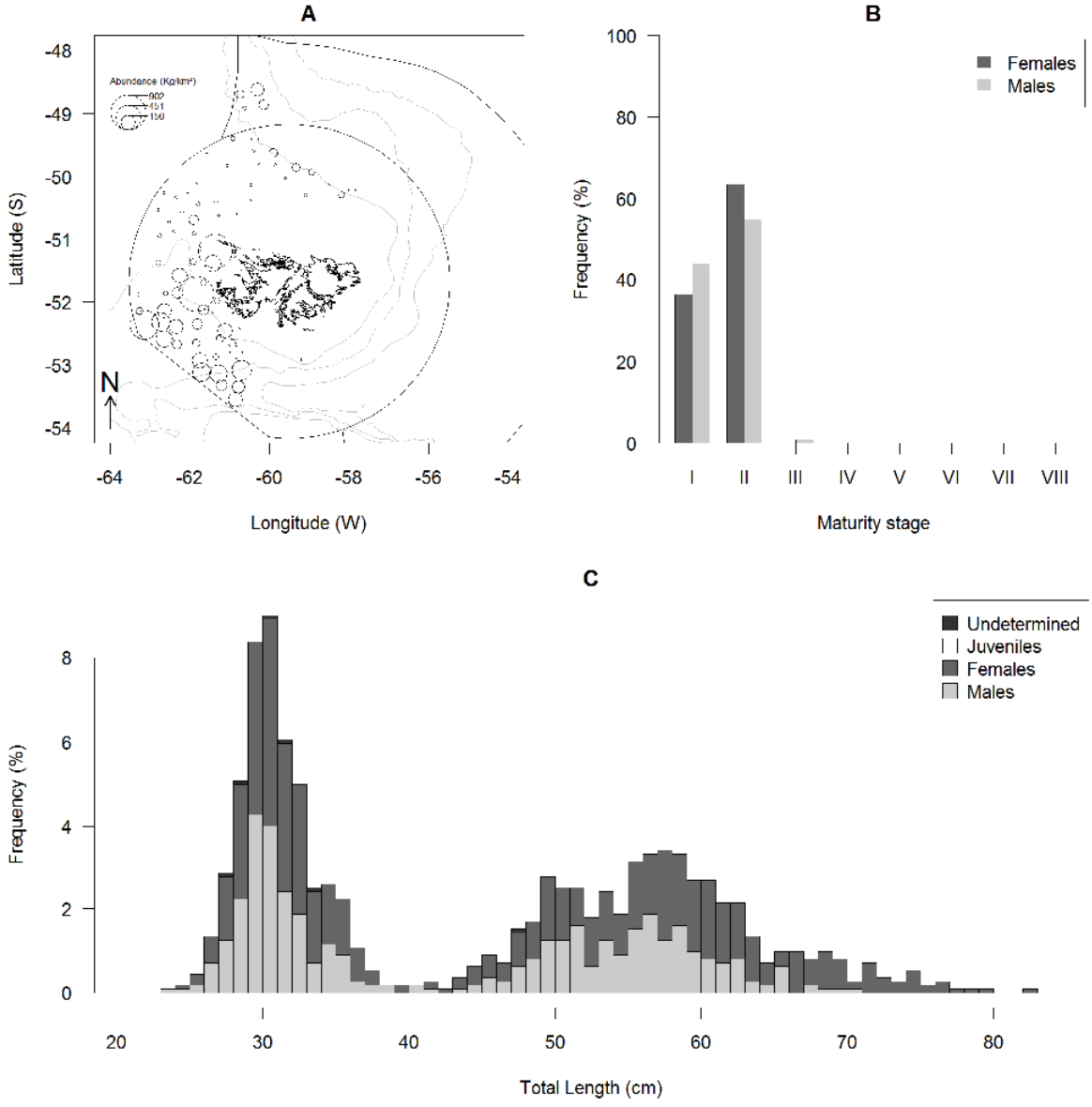

Figure 9: Biological data of *Dissostichus eleginoides* (toothfish; TOO), map of the densities in kg·km^{-2} (A), percentage of specimens of each sex per maturity stage (B; I, immature; II, resting; III, early developing; IV, late developing; V, ripe; VI, running; VII, spent; VIII, recovering spent), and length frequency (in percentage of the total sample assessed) of each sex with 1 cm size class (C; n=1,123).

3.2.9 *Macruronus magellanicus* – hoki – WHI (Figure 10)

The total catch of hoki was 29,335 kg. It was caught at 75 of the 97 stations sampled throughout the research cruise (Figure 10A). Catches ranged from 0.2 to 4,663 kg. Among the 75 stations, 31 yielded >10 kg, 24 >100 kg, and eight >1 t. Densities ranged from 0.96 to 21,245 kg·km^{-2} (CPUE ranged 0.2–4,663 kg·h^{-1}). Highest densities were observed in the southwest of the survey area to the south of 52°S (Figure 10A). This area is characterised by deeper waters and it is the fishing grounds where hoki is generally targeted. One station exhibited a high density in the northwest (Figure 10A). The number of fish sampled for length frequency was 2,970 (1,778 females and 1,192 males), 223 were taken for otoliths including 68 non–randomly. Pre-anal length ranged from 14 to 41 cm for females and from 13 to 37 cm for males (Figure 10C). The length frequency histogram exhibits two well identified cohorts with modes at 19 cm and 28 cm (Figure 10C). Females were observed immature (1%), resting (97%), early developing (1%), and recovering spent (1%) (Figure 10B). Males were immature (6%), resting (92%), early developing (2%), and recovering spent (0.1%) (Figure 10B).

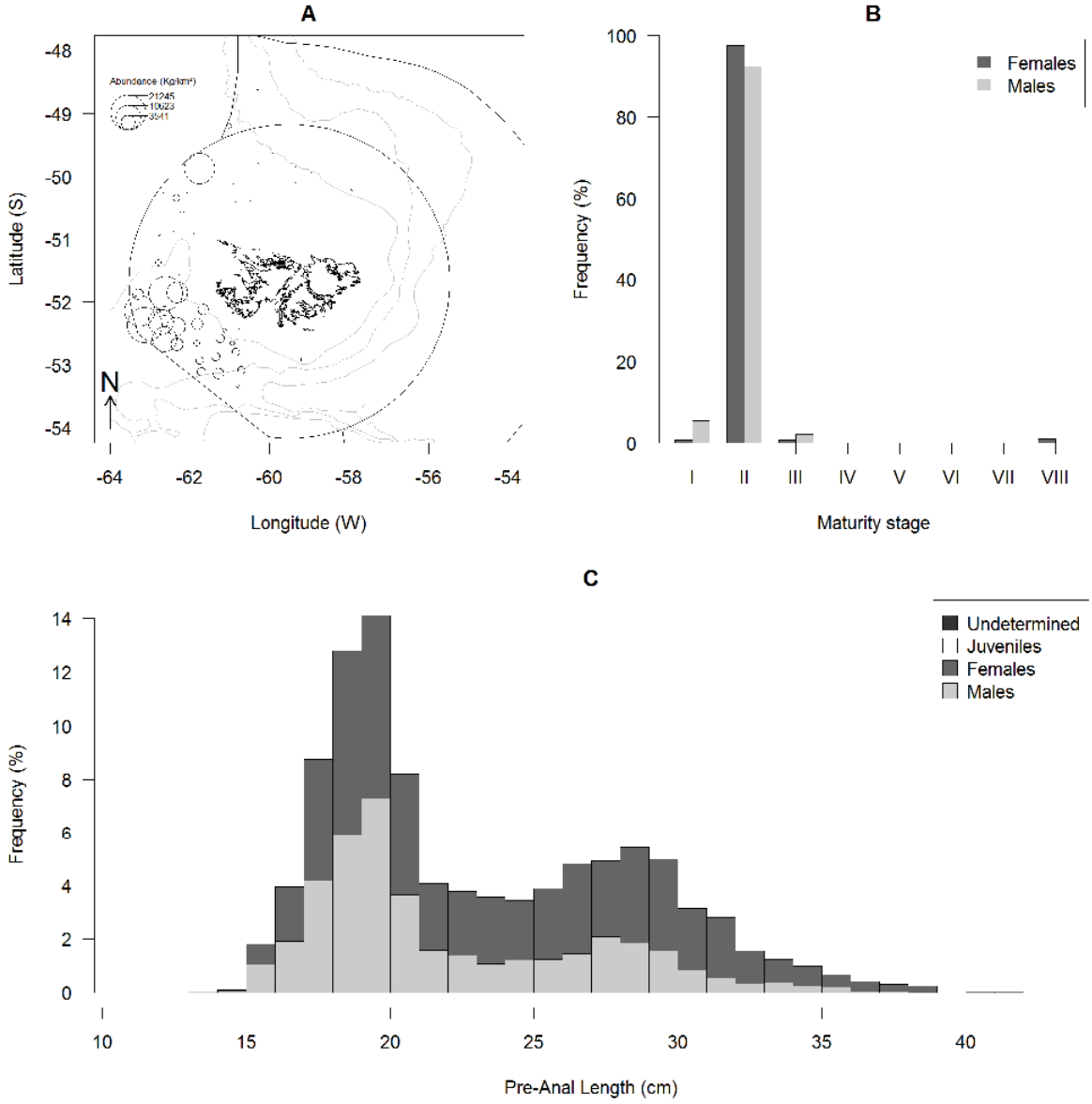

Figure 10: Biological data of *Macruronus magellanicus* (hoki; WHI), map of the densities in kg·km^{-2} (A), percentage of specimens of each sex per maturity stage (B; I, immature; II, resting; III, early developing; IV, late developing; V, ripe; VI, running; VII, spent; VIII, recovering spent), and length frequency (in percentage of the total sample assessed) of each sex with 1 cm size class (C; n= 2,970).

3.2.10 *Stromateus brasiliensis* – butterfish – BUT (Figure 11)

The total catch of butterfish was 169 kg. It was caught at 21 of the 97 trawl stations sampled throughout the research cruise (Figure 11A). Catches ranged from 0.67 to 23.2 kg. Among the 21 stations, six yielded >10 kg. Densities ranged from 3.57 to 114 kg·km^{-2} (CPUE ranged 0.67–23.2 kg·h^{-1}). Butterfish was caught to the northwest of West Falkland along the border between the FICZ and Argentine waters (Figure 11A). The number of fish sampled for length frequency was 319 (298 females and 21 males), none were sampled for otoliths or for length–weight. Total length ranged from 12 to 38 cm for females and from 25 to 34 cm for males (Figure 11C). The histogram exhibited possibly two different cohorts with modes 28 cm and 31 cm (Figure 11C). However, if there were two cohorts the overlap between them did not ease their discrimination. Females were observed immature (0.3%), early developing (89%) and late developing (10%) (Figure 11B). Males were resting (5%), early developing (48%) and late developing (48%) (Figure 11B).

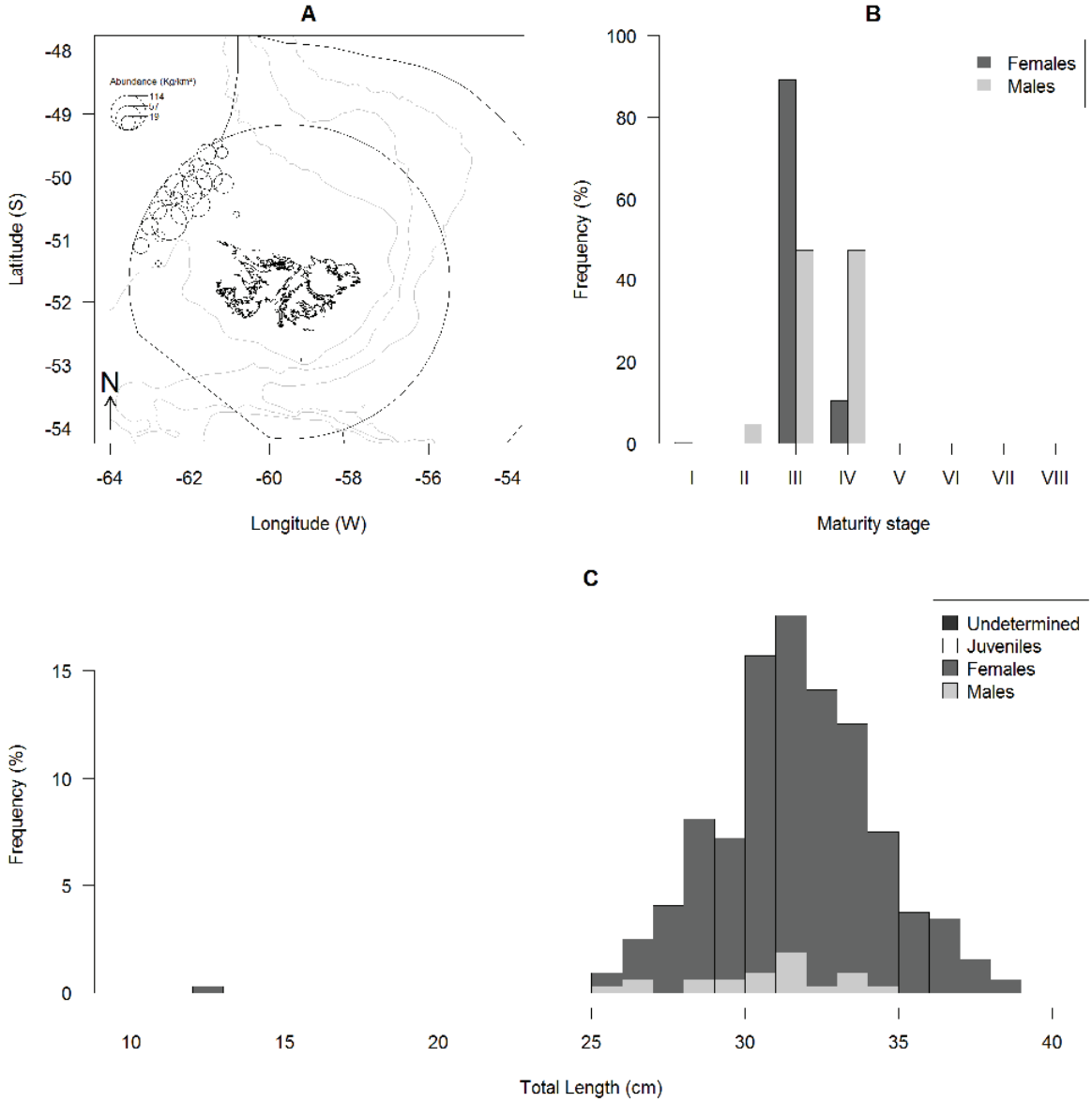

Figure 11: Biological data of *Stromateus brasiliensis* (butterfish; BUT), map of the densities in kg·km^{-2} (A), percentage of specimens of each sex per maturity stage (B; I, immature; II, resting; III, early developing; IV, late developing; V, ripe; VI, running; VII, spent; VIII, recovering spent), and length frequency (in percentage of the total sample assessed) of each sex with 1 cm size class (C; n= 319).

3.2.11 *Cottoperca gobio* – frogmouth – CGO (Figure 12)

The total catch of frogmouth was 255 kg. It was caught at 58 of the 97 trawl stations sampled throughout the research cruise (Figure 12A). Catches ranged from 0.05 to 26 kg. Among the 58 stations, seven yielded >10 kg. Densities ranged from 0.23 to 123 kg·km^{-2} (CPUE ranged 0.05–26 kg·h^{-1}). Frogmouth was observed to the west of 60°W primarily in waters shallower than 200 m (Figure 12A). The number of fish sampled for length frequency was 618 (300 females, 289 males, and 29 unsexed), 29 were sampled for length–weight and kept alive in a tank in the framework of the project "*Evolution of microRNA regulation of gene expression in Antarctic and Sub-Antarctic notothenioid fish*". Total length ranged from 18 to 48 cm for unsexed, from eight to 50 cm for females, and from eight to 58 cm for males (Figure 12C). The histogram exhibited a series of modes but cohorts were not discernible (Figure 12C). Females were observed immature (9%), resting (46%), early developing (37%), late developing (7%), ripe (0.3%), spent (0.3%), and recovering spent (0.3%) (Figure 12B). Males were immature (30%), resting (67%), and early developing (3%) (Figure 12B).

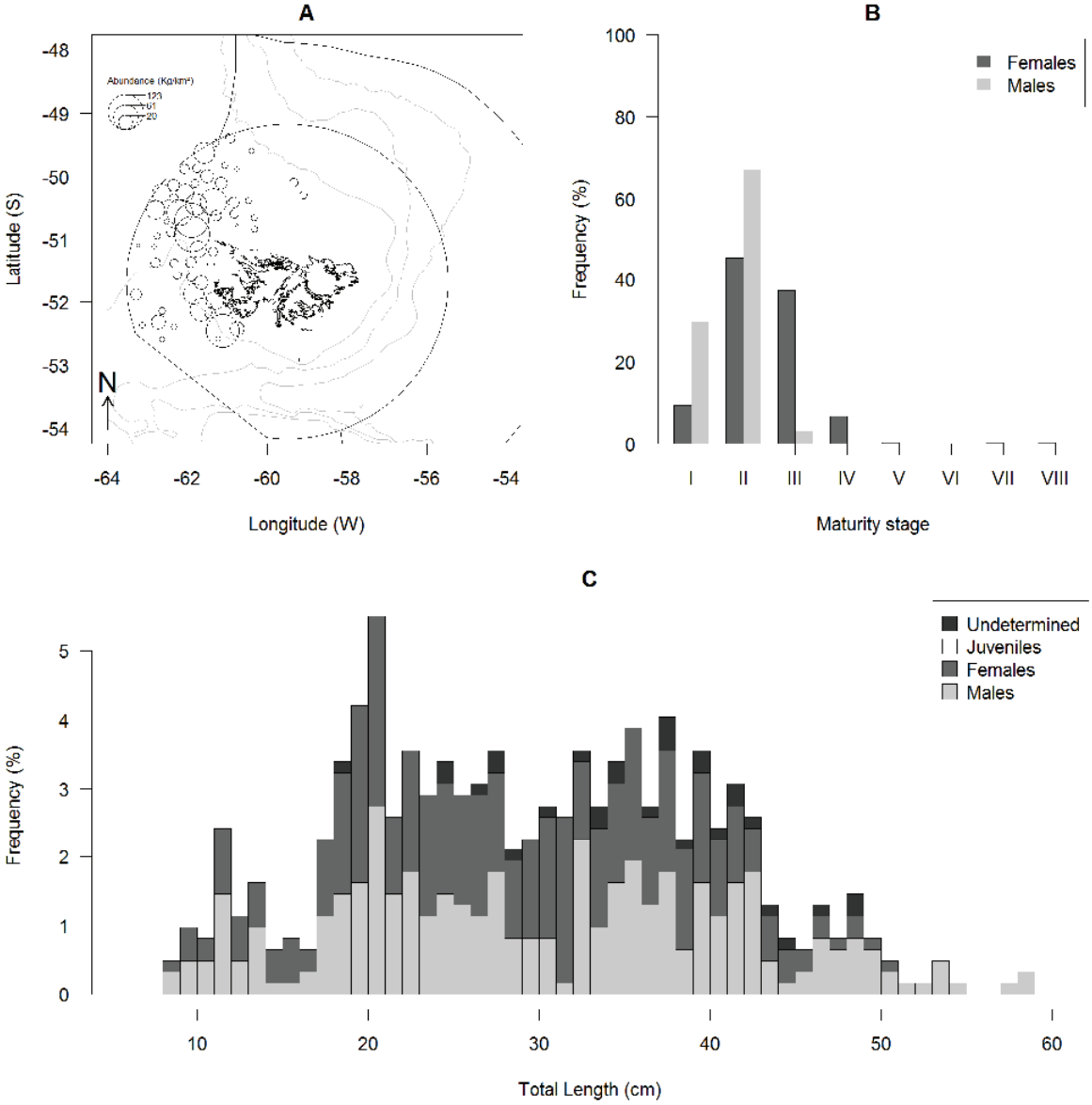

Figure 12: Biological data of *Cottoperca gobio* (frogmouth; CGO), map of the densities in kg·km^{-2} (A), percentage of specimens of each sex per maturity stage (B; I, immature; II, resting; III, early developing; IV, late developing; V, ripe; VI, running; VII, spent; VIII, recovering spent), and length frequency (in percentage of the total sample assessed) of each sex with 1 cm size class (C; n= 618).

3.2.12 *Champsocephalus esox* – icefish – CHE (Figure 13)

The total catch of icefish was 129 kg. It was caught at six of the 97 trawl stations sampled throughout the research cruise (Figure 13A). Catches ranged from 0.18 to 64.6 kg. Among the six stations, two yielded >10 kg. Densities ranged from 0.84 to 311 kg·km^{-2} (CPUE ranged 0.18–64.6 kg·h^{-1}). Icefish were observed to the west and the southwest of West Falkland in shallow waters and highest densities were observed to the south of the Jason Islands (Figure 13A). The number of fish sampled for length frequency was 396 (234 females, 157 males, and five unsexed), 141 were sampled for length–weight, one was taken for otoliths and non–randomly chosen. Total length ranged from 28 to 32 cm for unsexed individuals, from 13 to 37 cm for females, and from 14 to 34 cm for males (Figure 13C). The histogram exhibited one cohort with a mode at 30 cm (Figure 13C). Specimens of 13, 14 and 20 cm also appeared in the sample and could belong to two other cohorts, however the number of specimens does not enable us to identify them (Figure 13C). Females were observed immature (0.4%), resting (85%), early developing (1%), spent (1%), and recovering spent (12%) (Figure 13B). Males were resting (94%), and recovering spent (6%) (Figure 13B).

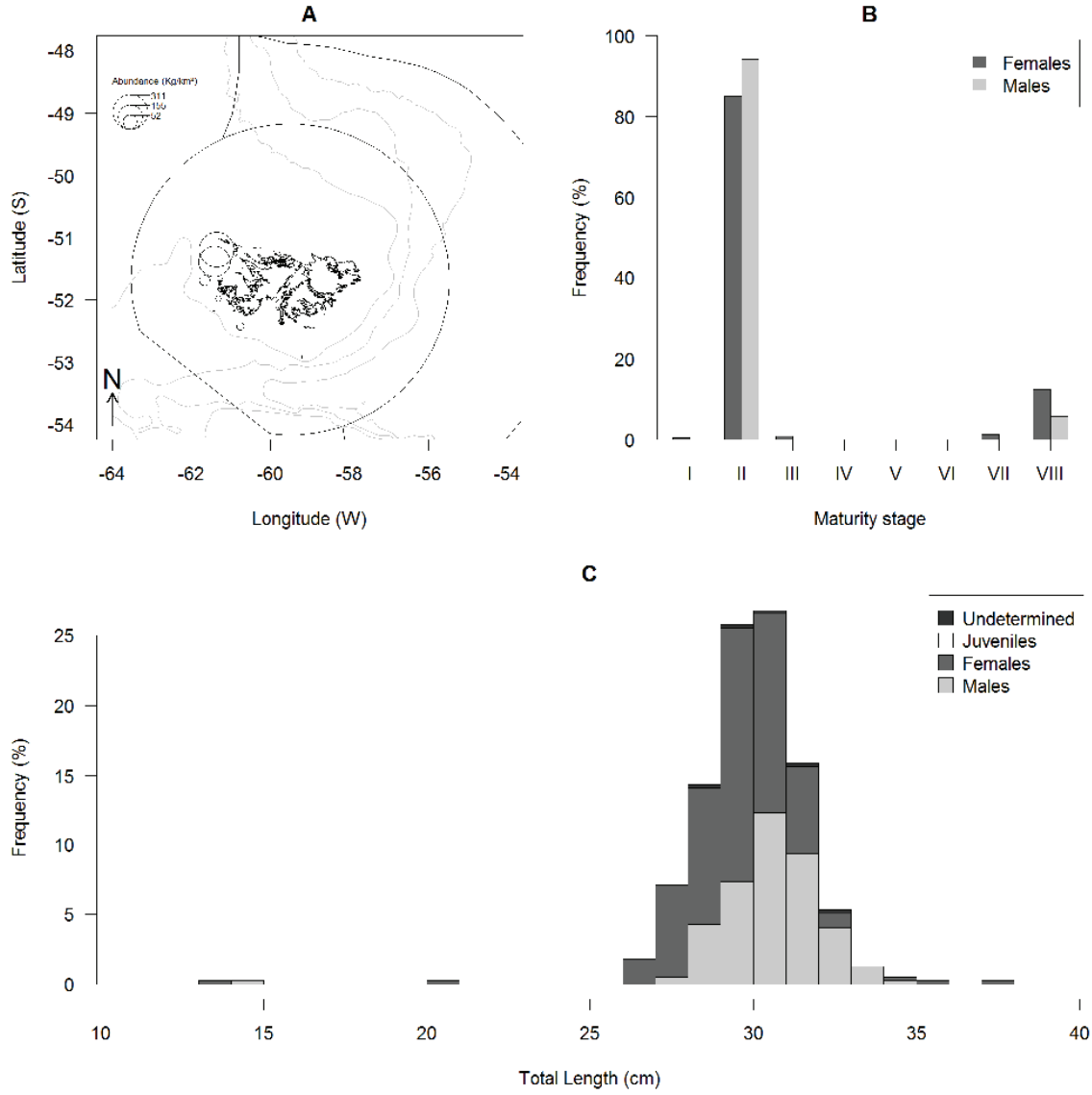

Figure 13: Biological data of *Champsocephalus esox* (icefish; CHE), map of the densities in kg·km^{-2} (A), percentage of specimens of each sex per maturity stage (B; I, immature; II, resting; III, early developing; IV, late developing; V, ripe; VI, running; VII, spent; VIII, recovering spent), and length frequency (in percentage of the total sample assessed) of each sex with 1 cm size class (C; n= 396).

3.2.13 *Coelorinchus kaiyomaru* – Campbell whiptail – COK (Figure 14)

The total catch of Campbell whiptail was 2.09 kg. It was caught at two of the 97 trawl stations sampled throughout the research cruise (Figure 14A). Catches were 0.23 and 2.67 kg, respectively. Densities were 1.45 and 13.8 kg·km^{-2} (CPUE were 0.24–2.67 kg·h^{-1}). The two stations where this species was sampled were the two stations at the southern end of the survey area (Figure 14A). The number of fish sampled for length frequency was 30 (23 females and seven males), all of them had their otoliths extracted. Pre–anal length ranged from five to 11 cm for females and from six to nine cm for males (Figure 14C). The histogram exhibited a single cohort with a mode at eight cm (Figure 14C). Females were observed immature (4%), resting (48%), early developing (17%), and recovering spent (31%) (Figure 14B). Males were resting (43%), spent (43%), and recovering spent (14%) (Figure 14B).

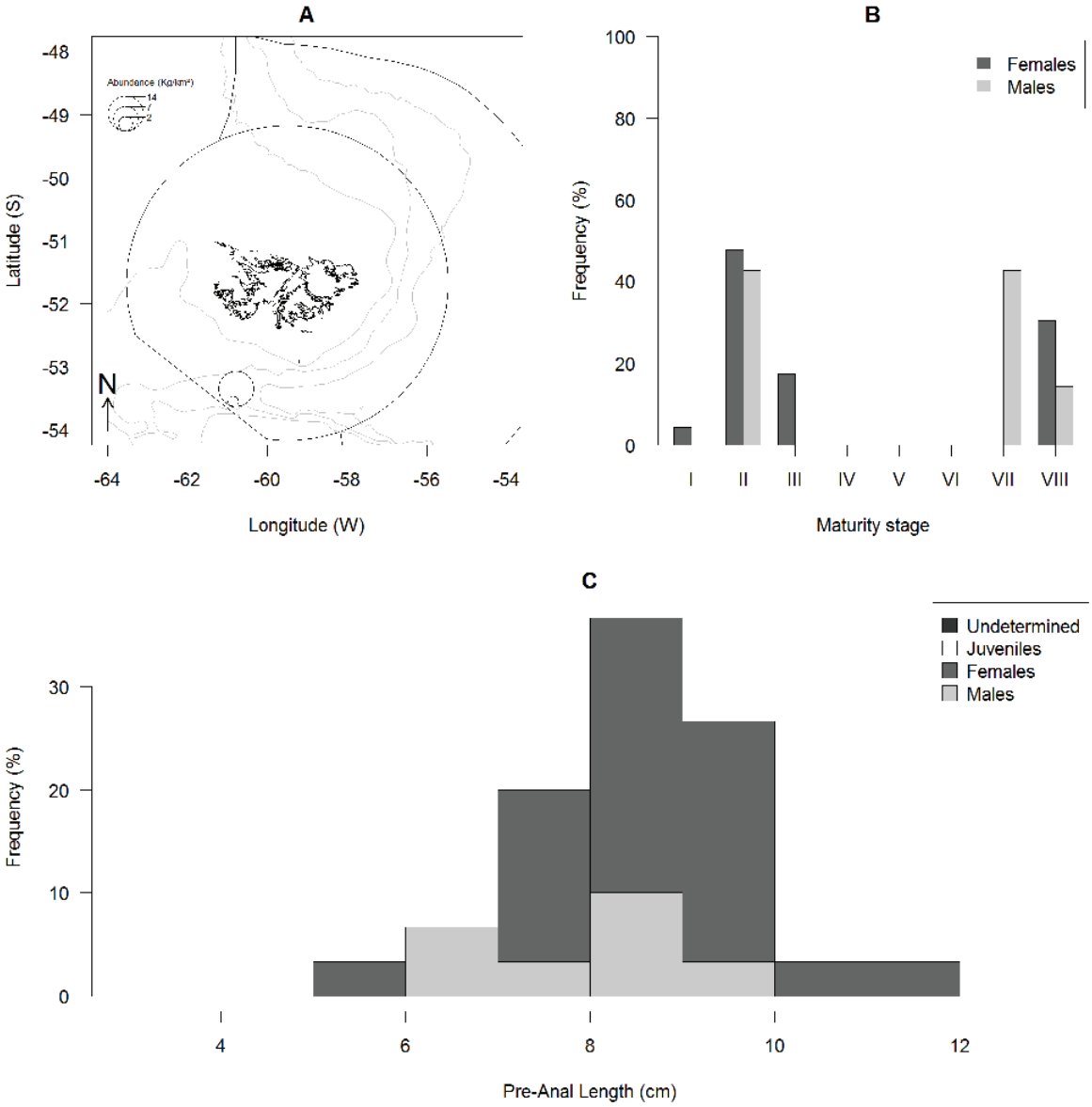

Figure 14: Biological data of *Coelorinchus kaiyomaru* (Campbell whiptail; COK), map of the densities in kg·km^{-2} (A), percentage of specimens of each sex per maturity stage (B; I, immature; II, resting; III, early developing; IV, late developing; V, ripe; VI, running; VII, spent; VIII, recovering spent), and length frequency (in percentage of the total sample assessed) of each sex with 1 cm size class (C; n=30).

3.2.14 Congiopodus peruvianus – Pigfish – COP (Figure 15)

The total catch of pigfish was 33.4 kg. It was caught at 13 of the 97 trawl stations sampled throughout the research cruise (Figure 15A). Catches ranged from 0.45 to 5.23 kg. Among the 13 stations, ten yielded >1 kg and one >5 kg. Densities ranged from 2.13 to 24.6 kg·km^{-2} (CPUE ranged 0.45–5.23 kg·h^{-1}). Highest densities were observed in the northwest of the FICZ along the border between the FICZ and Argentine waters. The number of fish sampled for length frequency was 89 (28 females and 61 males), none were sampled for length–weight data or for otolith collection. Total length ranged from 23 to 39 cm for females and from 22 to 35 cm for males (Figure 15C). The histogram exhibits potentially two cohorts (modes at 24 and 27 cm) (Figure 15C). However, due to the low number of fish, cohorts are not distinctly discernible (Figure 15C). Females were observed early developing (4%), late developing (14%), ripe (82%) (Figure 15B). Males were resting (2%), early developing (48%), and late developing (51%) (Figure 15B).

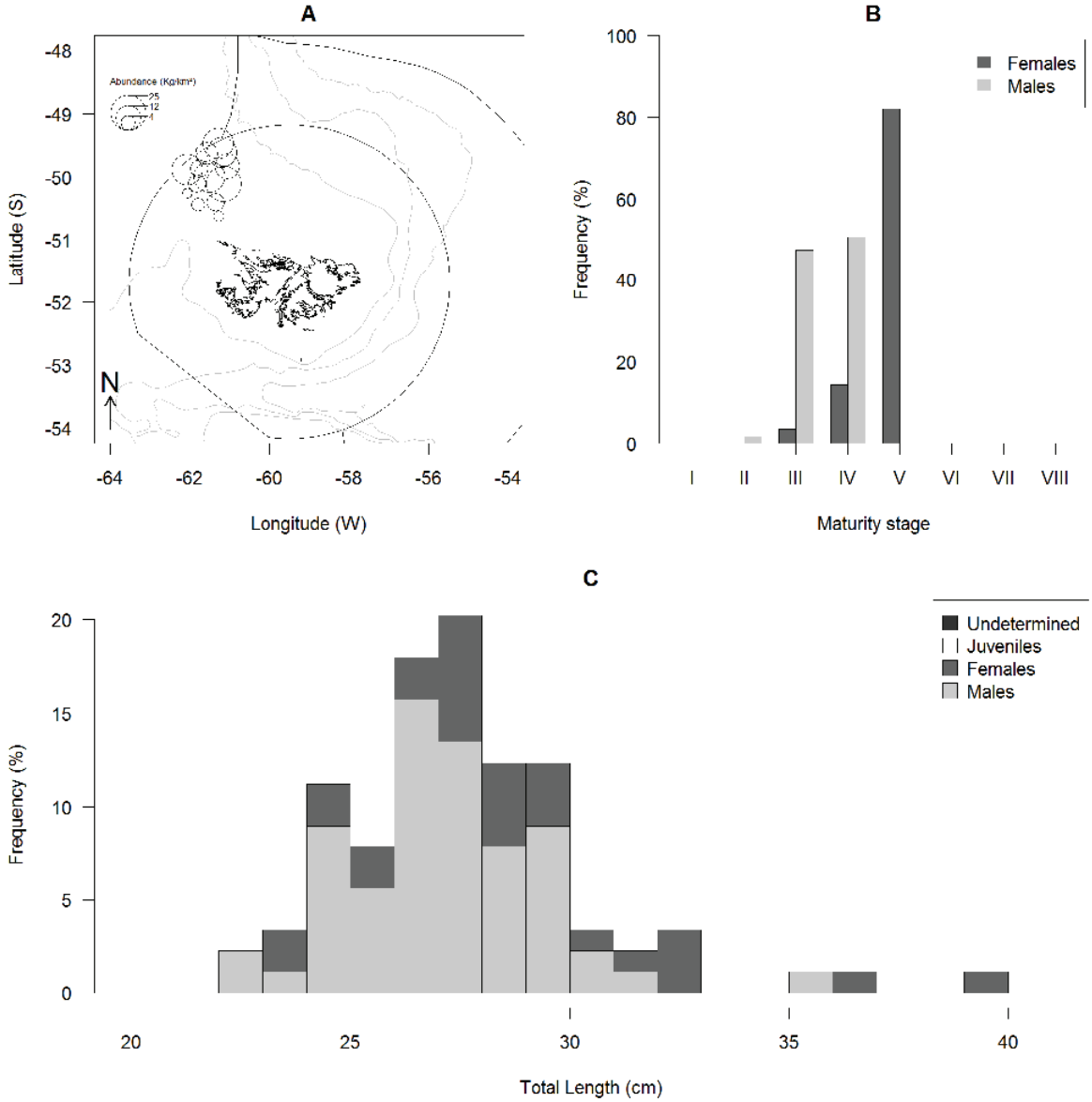

Figure 15: Biological data of *Congiopodus peruvianus* (Pigfish; COP), map of the densities in kg·km^{-2} (A), percentage of specimens of each sex per maturity stage (B; I, immature; II, resting; III, early developing; IV, late developing; V, ripe; VI, running; VII, spent; VIII, recovering spent), and length frequency (in percentage of the total sample assessed) of each sex with 1 cm size class (C; n= 89).

3.2.15 *Cottunculus granulosus* – fathead – COT (Figure 16)

The total catch of fathead was 15.2 kg. It was caught at 14 of the 97 trawl stations sampled throughout the research cruise (Figure 16A). Catches ranged from 0.01 to 7.45 kg. Among the 14 stations, three yielded >1 kg, and one >5 kg. Densities ranged from 0.05 to 34.8 kg·km^{-2} (CPUE ranged 0.01–7.45 kg·h^{-1}). Highest densities were observed in the north of the FICZ, in the north of the FOCZ, and to the south of West Falkland (Figure 16A). Most of the stations where this species was observed were in deeper waters (> 200 m). The number of fish sampled for length frequency was 81 (34 females and 47 males), no length–weight data were recorded nor otoliths extracted for this species. Total length ranged from ten to 28 cm for both sexes (Figure 16C). The histogram exhibited at least two modes at 18 and 25 cm most likely representing two separate cohorts (Figure 16C). Other cohorts were difficult to discern due to the low number of fish sampled (Figure 16C). Females were observed immature (15%), early developing (3%), late developing (6%), ripe (6%), spent (65%) and recovering spent (6%) (Figure 16B). Males were immature (38%), resting (13%), early developing (4%), spent (23%) and recovering spent (21%) (Figure 16B).

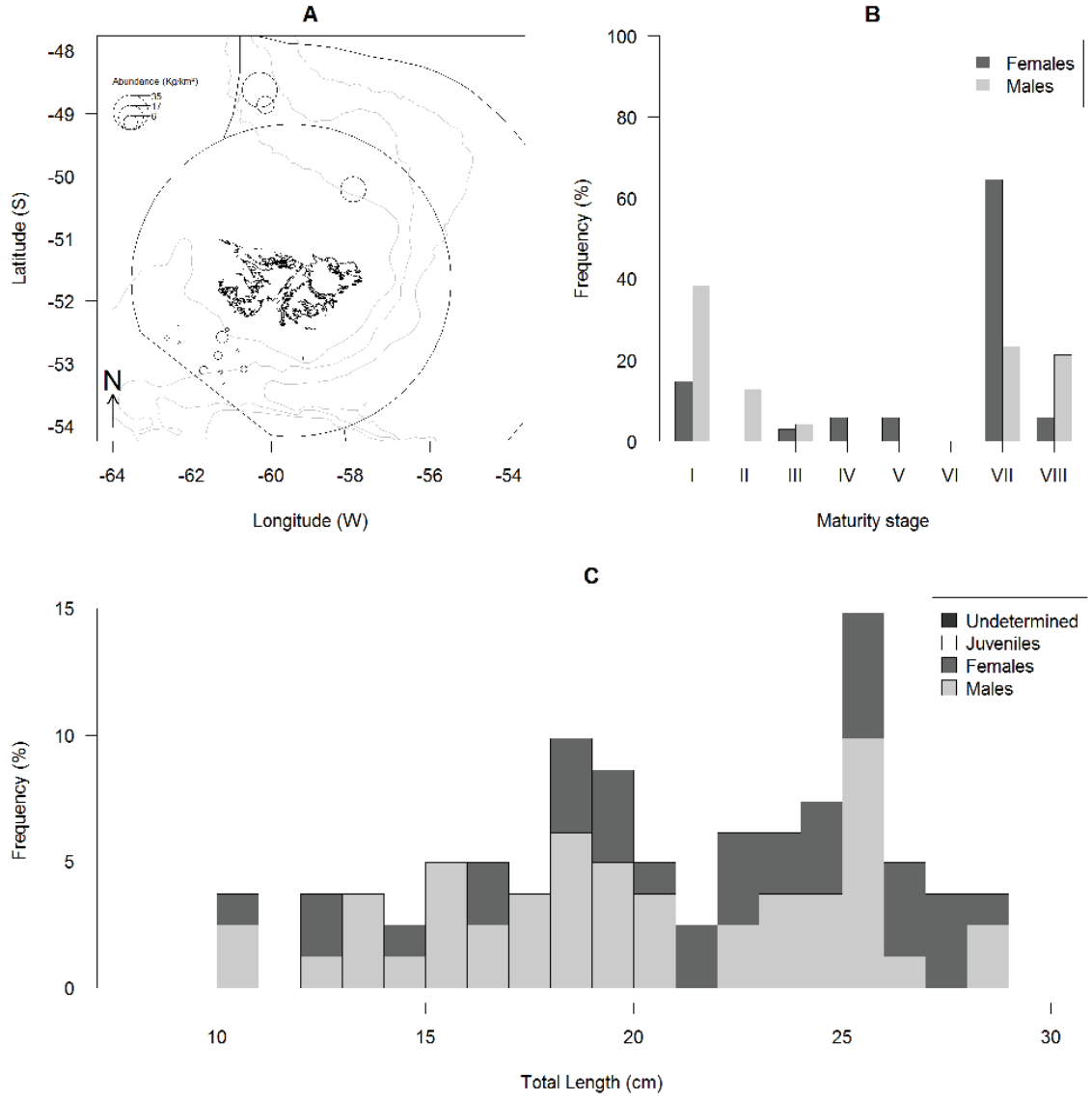

Figure 16: Biological data of *Cottunculus granulosus* (fathead; COT), map of the densities in kg·km^{-2} (A), percentage of specimens of each sex per maturity stage (B; I, immature; II, resting; III, early developing; IV, late developing; V, ripe; VI, running; VII, spent; VIII, recovering spent), and length frequency (in percentage of the total sample assessed) of each sex with 1 cm size class (C; n= 81).

3.2.16 *Coelorinchus fasciatus* – banded whiptail grenadier – GRF (Figure 17)

The total catch of banded whiptail grenadier was 6,854 kg. It was caught at 29 of the 97 trawl stations sampled throughout the research cruise (Figure 17A). Catches ranged from 2.88 to 642 kg. Among the 29 stations, 26 yielded >10 kg and 22 >100 kg. Densities ranged from 12.8 to 3,216 kg·km^{-2} (CPUE ranged 2.88–642 kg·h^{-1}). Highest densities were observed in the southwest of the survey zone between the 200 m isobath and the border between the FICZ and Argentine waters at stations deeper than 200 m (Figure 17A). The number of fish sampled for length frequency was 2,610 (1,502 females, 1,102 males, and six unsexed), 91 were sampled for otolith including 12 non–randomly selected. Pre–anal length ranged from nine to 11 cm for unsexed individuals, from three to 14 cm for females and from four to 12 cm for males (Figure 17C). The histogram exhibited a single cohort (mode at nine cm) (Figure 17C). Females were observed immature (1%), resting (46%), early developing (36%), late developing (5%), ripe (1%), spent (1%), and recovering spent (10%) (Figure 17B). Males were immature (1%), resting (98.6%), early developing (0.3%), and spent (0.1%) (Figure 17B).

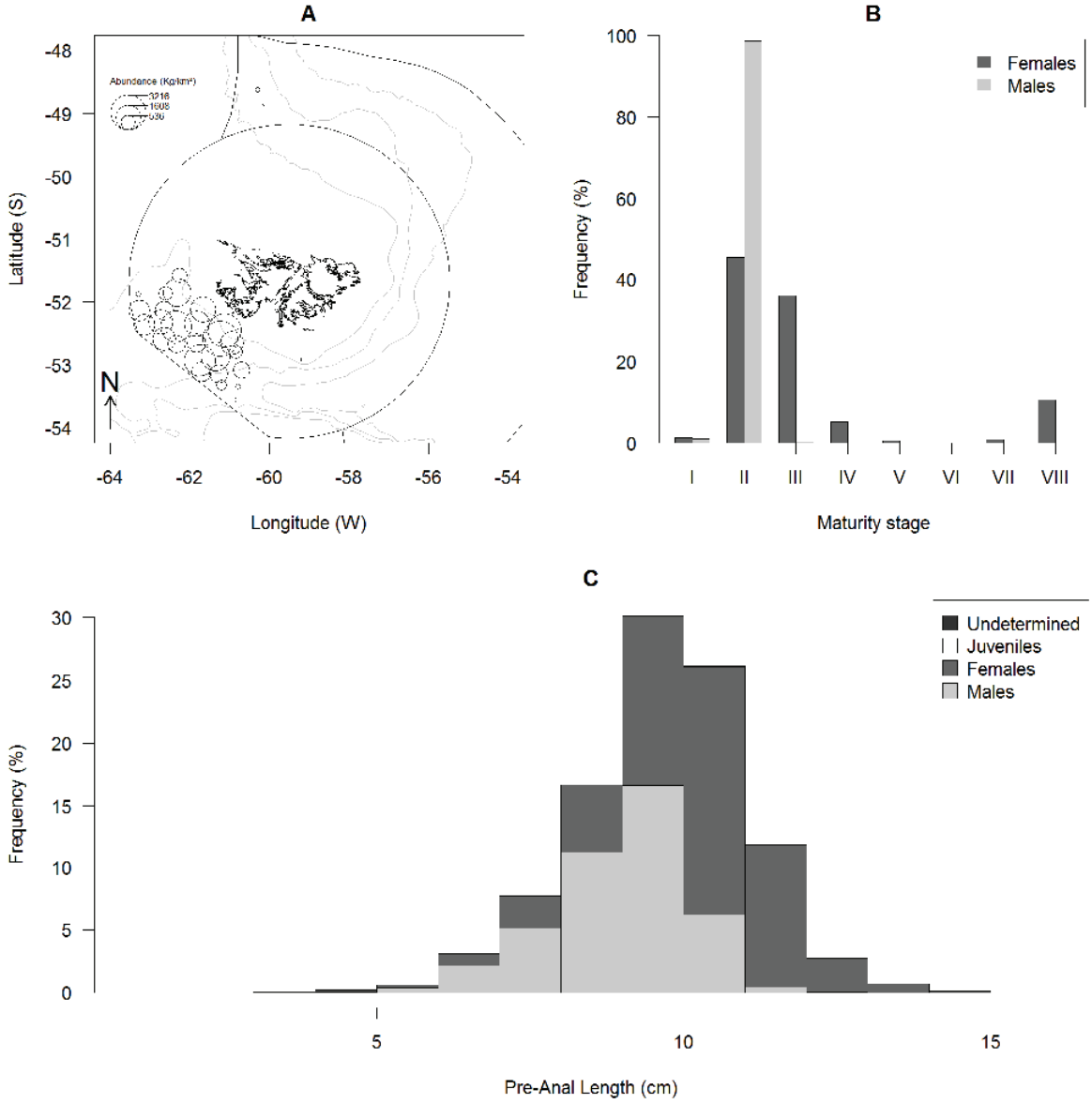

Figure 17: Biological data of *Coelorinchus fasciatus* (banded whiptail grenadier; GRF), map of the densities in kg·km^{-2} (A), percentage of specimens of each sex per maturity stage (B; I, immature; II, resting; III, early developing; IV, late developing; V, ripe; VI, running; VII, spent; VIII, recovering spent), and length frequency (in percentage of the total sample assessed) of each sex with 1 cm size class (C; n= 2,610).

3.2.17 *Gymnoscopelus nicholsi* – Nichol's lanternfish – GYN (Figure 18)

The total catch of Nichol's lanternfish was 35.6 kg. It was caught at five of the 97 stations sampled throughout the research cruise (Figure 18A). Catches ranged from 0.03 to 35.21 kg. Among the 5 stations, a single station yielded >1 kg. Densities ranged from 0.16 to 157 kg·km^{-2} (CPUE ranged 0.03–35.2 kg·h^{-1}). Highest densities were observed in the north of the FOCZ at one station (Figure 18A). The number of fish sampled for length frequency was 100 and none of the sampled fish were sexed. Total length ranged from 13 to 17 cm (Figure 18C). The histogram exhibited a single cohort (mode at 15 cm) (Figure 18C).

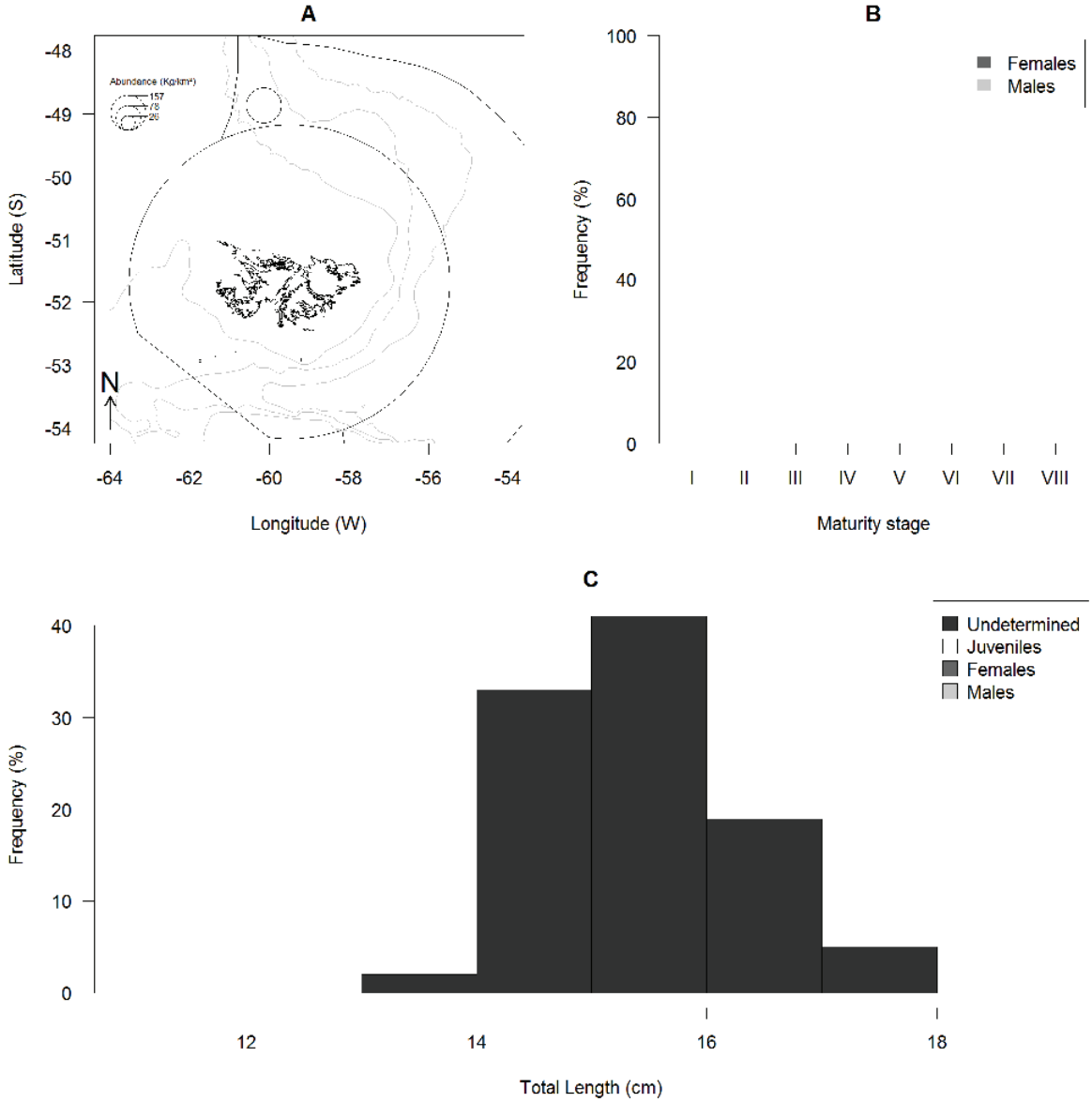

Figure 18: Biological data of *Gymnoscopelus nicholsi* (Nichol's lanternfish; GYN), map of the densities in kg·km^{-2} (A), percentage of specimens of each sex per maturity stage (B; I, immature; II, resting; III, early developing; IV, late developing; V, ripe; VI, running; VII, spent; VIII, recovering spent) and length frequency (in percentage of the total sample assessed) of each sex with 1 cm size class (C; n= 100).

3.2.18 *Patagolycus melastomus* – Black–mouthed eelpout – PAU (Figure 19)

The total catch of black–mouthed eelpout was 117 kg. It was caught at 30 of the 97 trawl stations sampled throughout the research cruise (Figure 19A). Catches ranged from 0.05 to 38.9 kg. Among the 30 stations, 11 yielded >10 kg and three >10 kg. Densities ranged from 0.22 to 185 kg·km^{-2} (CPUE ranged 0.05–38.9 kg·h^{-1}). Highest densities were observed in the north and south of the survey area in waters as deep as 200 m (Figure 19A). The number of fish sampled for length frequency was 93 (52 females and 41 males), and six fish randomly sampled had their otoliths extracted. Total length ranged from 12 to 37 cm for females and from 26 to 38 cm for males (Figure 19C). The length frequency histogram exhibited one clear cohort (mode at 27 cm) and potentially two others at 22 and 32 cm (Figure 19C). Females were observed immature (2%), early developing (11%), late developing (64%), ripe (19%) and spent (4%) (Figure 19B). Males were resting (59%), and early developing (42%) (Figure 19B).

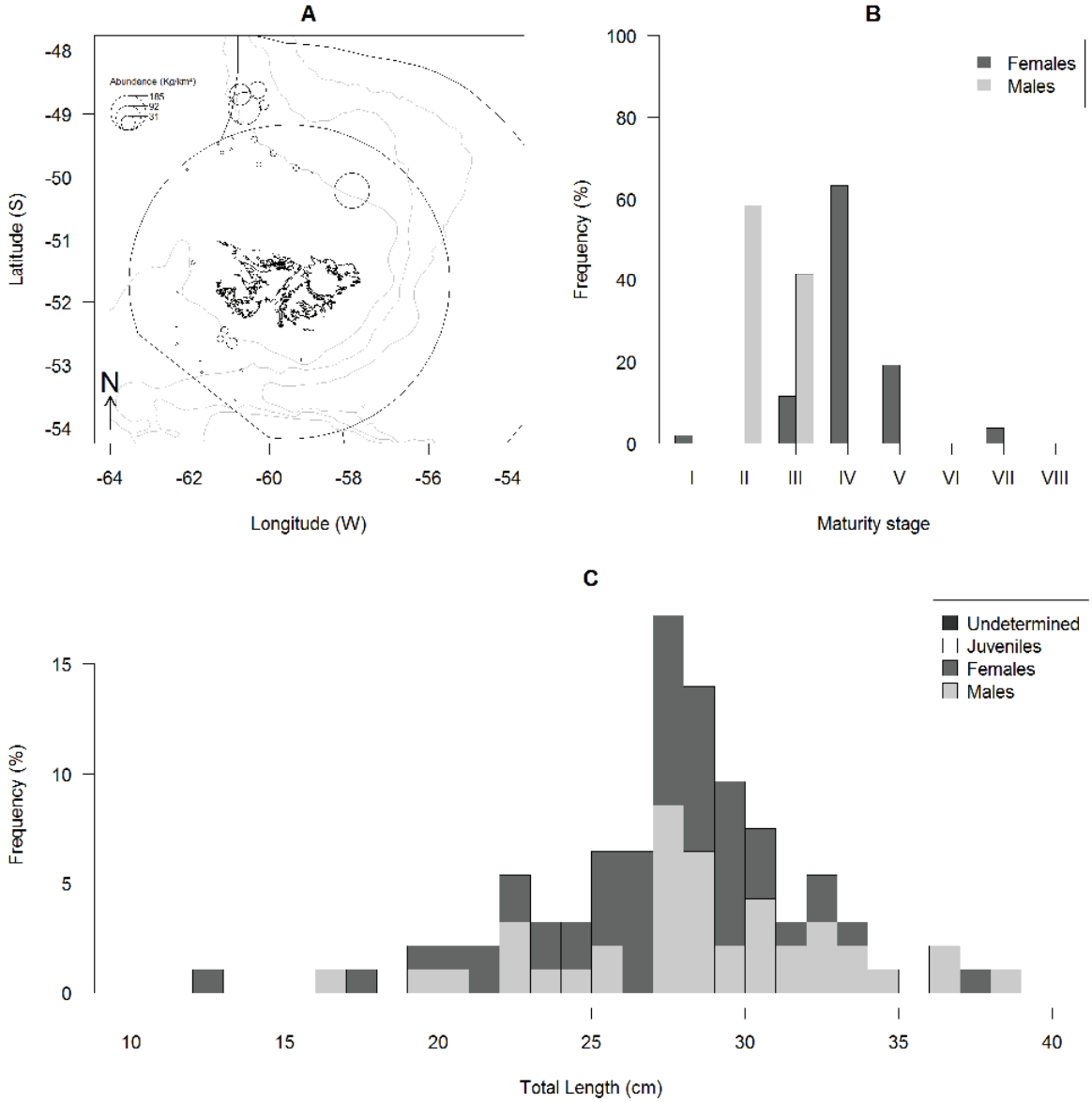

Figure 19: Biological data of *Patagolycus melastomus* (eelpout; PAU), map of the densities in kg·km^{-2} (A), percentage of specimens of each sex per maturity stage (B; I, immature; II, resting; III, early developing; IV, late developing; V, ripe; VI, running; VII, spent; VIII, recovering spent), and length frequency (in percentage of the total sample assessed) of each sex with 1 cm size class (C; n= 93).

3.2.19 *Physiculus marginatus* – dwarf codling – PYM (Figure 20)

The total catch of dwarf codling was 807 kg. It was caught at 23 of the 97 trawl stations sampled throughout the research cruise (Figure 20A). Catches ranged from 0.03 to 146 kg. Among the 23 stations, 13 yielded >10 kg, and two >100 kg. Densities ranged from 0.15 to 782 kg·km^{-2} (CPUE ranged 0.03–146 kg·h^{-1}). Highest densities were observed in deep waters either in the north of the FOCZ or in the south of the FICZ (Figure 20A). The number of fish sampled for length frequency was 2,175 and none of them were sexed. Total length ranged from 11 to 23 cm (Figure 20C). The histogram exhibited one cohort (mode at 17 cm) (Figure 20C).

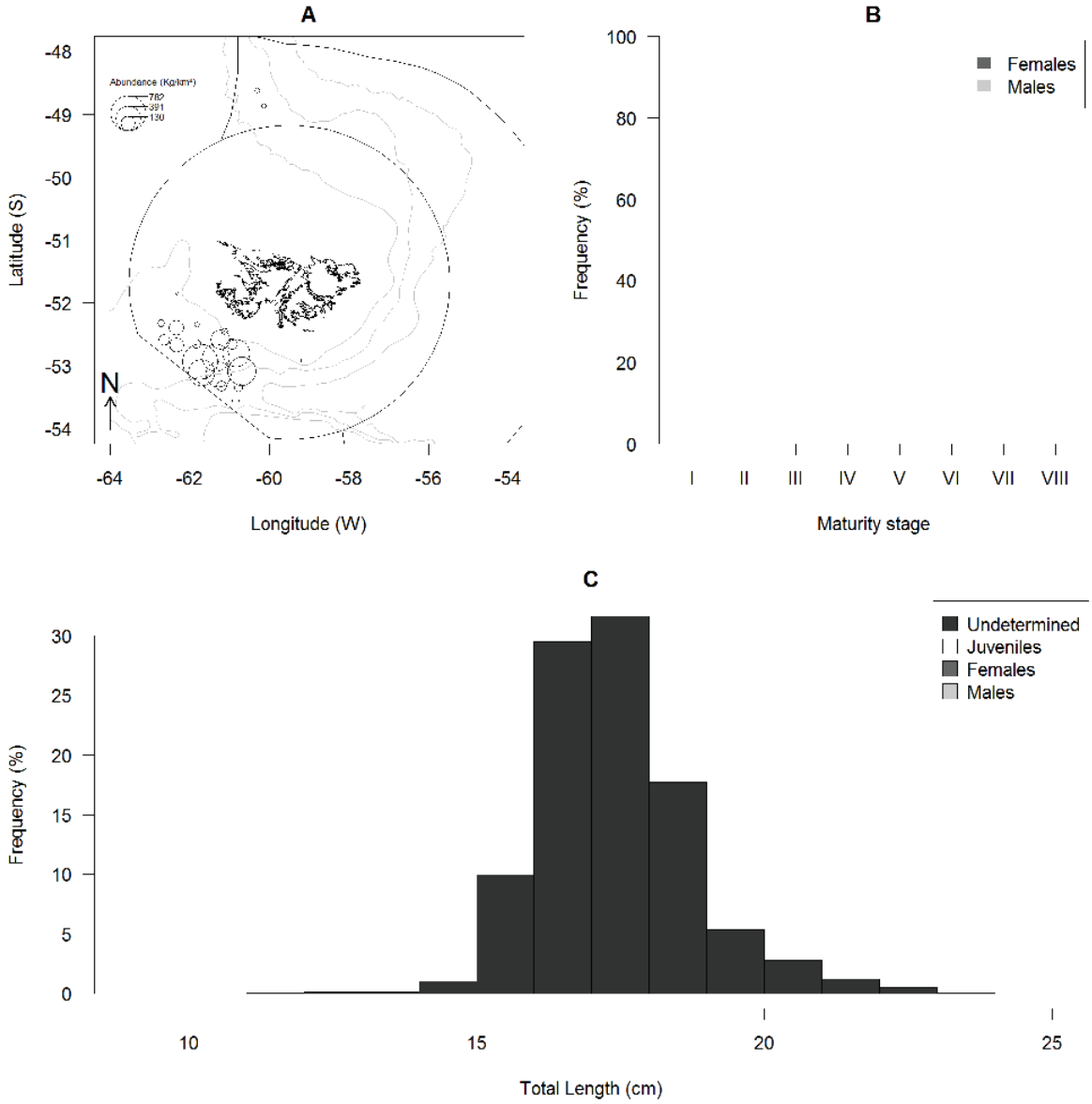

Figure 20: Biological data of *Physiculus marginatus* (dwarf codling; PYM), map of the densities in kg·km^{-2} (A), percentage of specimens of each sex per maturity stage (B; I, immature; II, resting; III, early developing; IV, late developing; V, ripe; VI, running; VII, spent; VIII, recovering spent), and length frequency (in percentage of the total sample assessed) of each sex with 1 cm size class (C; n= 2,175).

3.2.20 *Sebastes oculatus* – redfish – RED (Figure 21)

The total catch of redfish was 16.1 kg. It was caught at seven of the 97 trawl stations sampled throughout the research cruise (Figure 21A). Catches ranged from 0.39 to 5.45 kg. Among the seven stations, five yielded >1 kg, and one >5 kg. Densities ranged from 1.78 to 28.2 kg·km^{-2} (CPUE ranged 0.39–5.45 kg·h^{-1}). Highest densities were observed to the north and to the northwest of West Falkland (Figure 21A). The number of fish sampled for length frequency was 33 (19 females and 14 males), and 18 for otoliths. Total length ranged from 26 to 38 cm for females and from 16 to 38 cm for males (Figure 21C). Due to the low number of fish in the sample it was difficult to identify cohorts on the length frequency histogram. Females were observed resting (16%), early developing (5%), late developing (11%), ripe (16%), running (5%) and recovering spent (47%) (Figure 21B). Males were immature (7%), resting (64%), early developing (14%), late developing and recovering spent (14%) (Figure 21B).

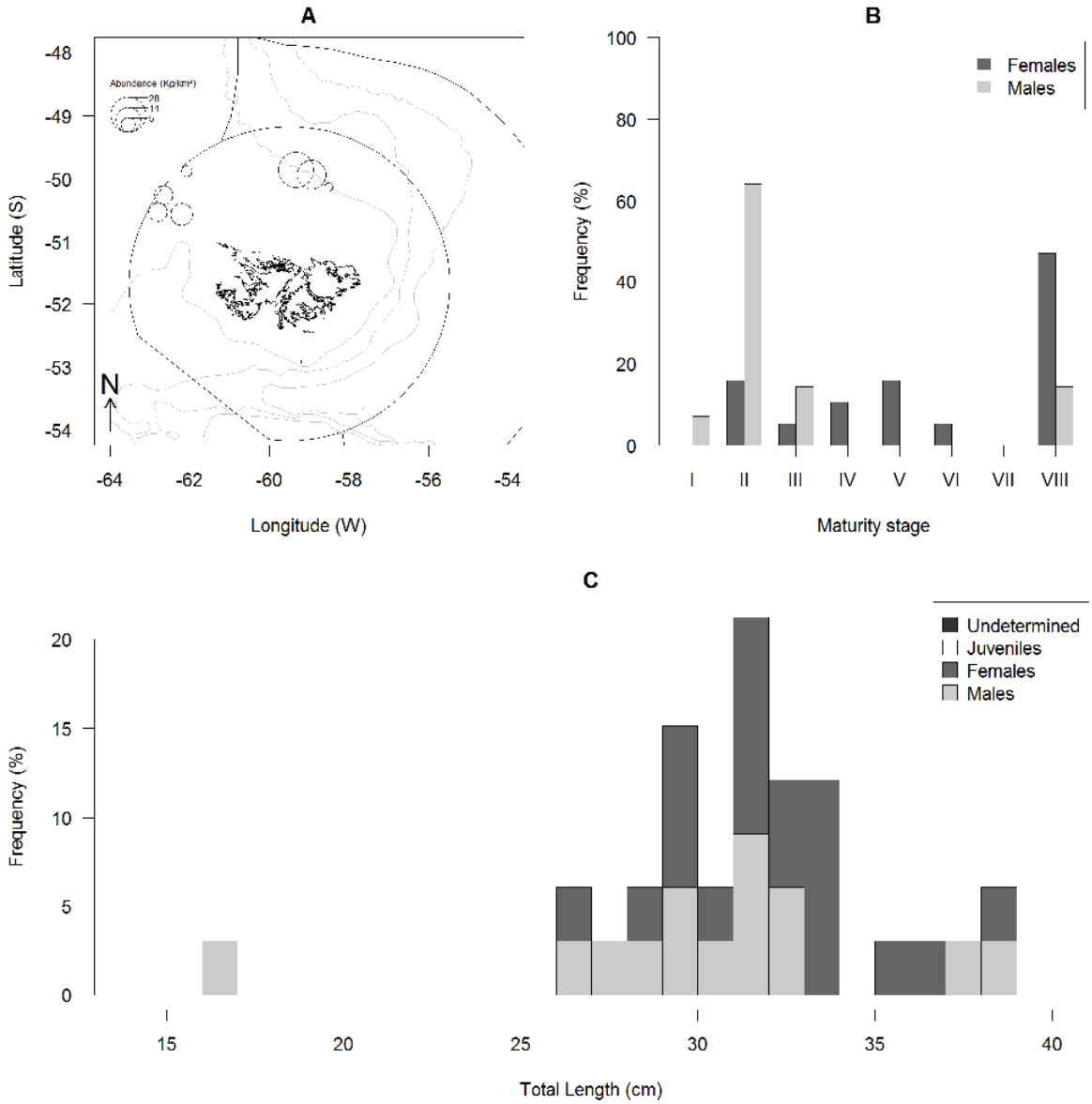

Figure 21: Biological data of *Sebastes oculatus* (redfish; RED), map of the densities in kg·km^{-2} (A), percentage of specimens of each sex per maturity stage (B; I, immature; II, resting; III, early developing; IV, late developing; V, ripe; VI, running; VII, spent; VIII, recovering spent), and length frequency (in percentage of the total sample assessed) of each sex with 1 cm size class (C; n= 33).

3.2.21 *Sprattus fuegensis* – Falkland herring – SAR (Figure 22)

The total catch of Falkland herring was 208 kg. It was caught at eight of the 97 trawl stations sampled throughout the research cruise (Figure 22A). Catches ranged from 0.01 to 201 kg. Among the eight stations, two yielded > 6 kg and one yielded >200 kg. Densities ranged from 0.04 to 954 kg·km^{-2} (CPUE ranged 0.01–201 kg·h^{-1}). Stations with presence of Falkland herring were observed to the northwest of the West Falkland and two inshore stations to the south of the Jason Islands exhibited the highest densities (Figure 22A). The number of fish sampled for length frequency was 206 (110 females and 96 males) and no length–weight data were collected nor were any otoliths extracted. Total length ranged from 15 to 22 cm for both sexes (Figure 22C). The histogram exhibited a single clear cohort with a mode at 20 cm and two specimens of 15 cm might have belonged to another cohort (Figure 22C). Females were observed resting (82%), early developing (14%), late developing (4%) (Figure 22B). Males were all resting (Figure 22B).

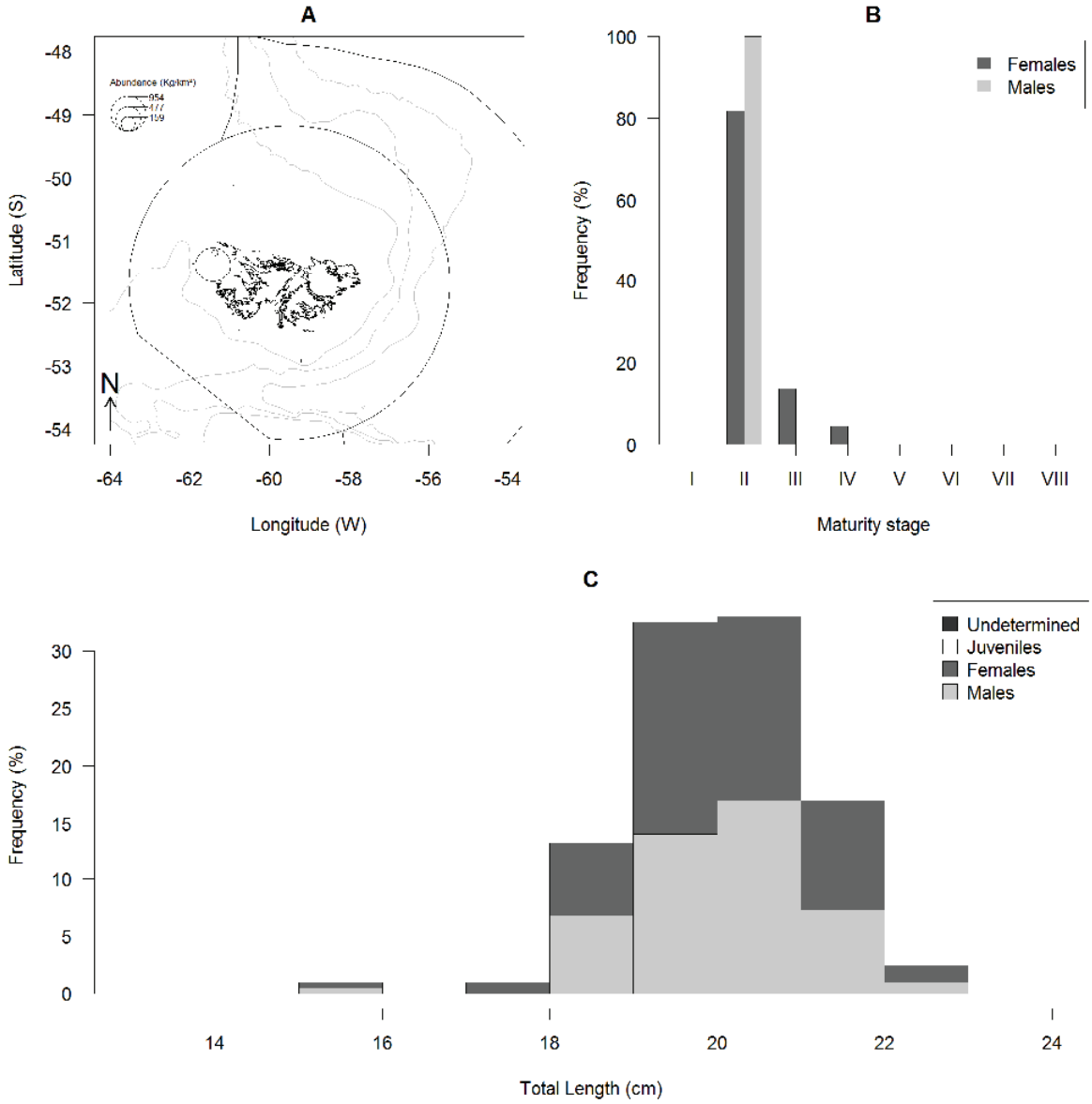

Figure 22: Biological data of *Sprattus fuegensis* (Falkland herring; SAR), map of the densities in kg·km^{-2} (A), percentage of specimens of each sex per maturity stage (B; I, immature; II, resting; III, early developing; IV, late developing; V, ripe; VI, running; VII, spent; VIII, recovering spent), and length frequency (in percentage of the total sample assessed) of each sex with 1 cm size class (C; n= 206).

3.3 Biological information of squids

3.3.1 *Illex argentinus* – Argentine shortfin squid – ILL (Figure 23)

The total catch of Argentine shortfin squid was 10,694 kg. It was caught at 68 of the 97 trawl stations sampled throughout the research cruise (Figure 23A). Catches ranged from 0.02 to 1,905 kg. Among the 68 stations, 44 yielded >10 kg, 23 >100 kg, and two >1 t. Densities ranged from 0.09 to 8,662 kg·km^{-2} (CPUE ranged 0.02–1905 kg·h^{-1}). Highest densities were observed in the northwest of the survey zone, especially to the west of 60°W and to the north of 51°30'S (Figure 23A). Argentine shortfin squid was caught in small quantities at many other stations to the south and to the east of the perimeter outlined above (Figure 23A). The number of squid sampled for length frequency was 4,844 (three juveniles, 3,238 females, and 1,603 males), 141 were sampled for length–weight, 122 for statoliths (including four non–randomly selected individuals). Dorsal mantle lengths ranged from 8.5 to 10 cm for juveniles, from 8 to 29 cm for females, and from 8.5 to 27 cm for males (Figure 23C). The histogram exhibited two different cohorts with modes at 11 cm and 23–24 cm (Figure 23C). The smaller cohort was also observed in 2016 and 2017 (Gras et al., 2016; 2017). Females were observed young (6%), immature (75%), preparatory (13%), maturing (2%), and mature (4%) (Figure 23B). Males were young (8%), immature (3 %), preparatory (6%), maturing (17%), and mature (66 %) (Figure 23B).

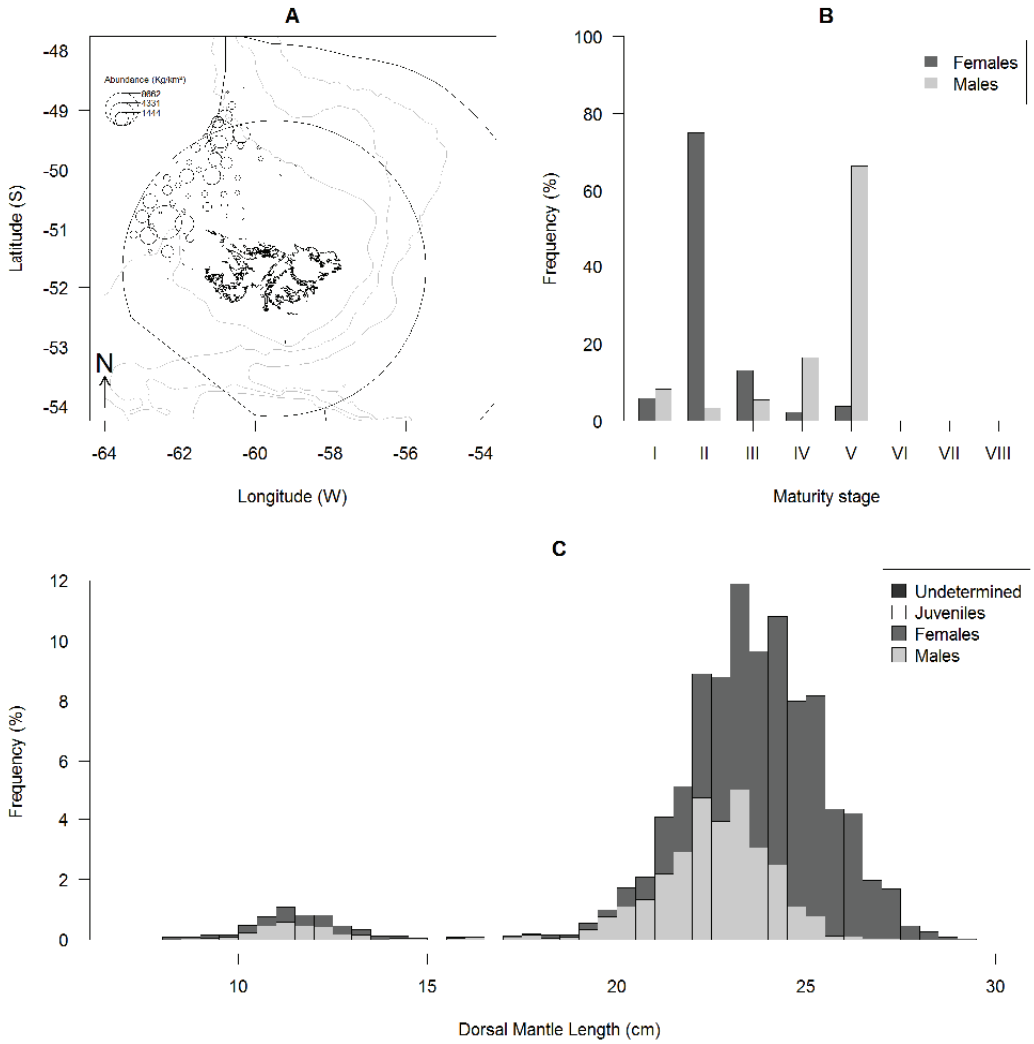

Figure 23: Biological data of *Illex argentinus* (Argentine shortfin squid; ILL), map of the densities in kg·km^{-2} (A), percentage of specimens of each sex per maturity stage (B; I, young; II, immature; III, preparatory; IV, maturing; V, mature; VI, spent), and dorsal mantle length frequency (in percentage of the total sample assessed) of each sex with 0.5 cm size class (C; n= 4,844).

3.3.2 *Moroteuthis ingens* – greater hooked squid – ING (Figure 24)

The total catch of greater hooked squid was 397 kg. It was caught at 50 of the 97 trawl stations sampled throughout the research cruise (Figure 24A). Catches ranged from 0.24 to 118 kg. Among the 50 stations, eight yielded >10 kg and one >100 kg. Densities ranged from 1.11 to 570 kg·km^{-2} (CPUE ranged 0.24–118 kg·h^{-1}). Greater hooked squid were caught almost throughout the research cruise. However higher densities of this species were observed to the north of East Falkland and to the south of West Falkland (Figure 24A). In the south, the species was caught at deep water stations (i.e. deeper than 200 m) (Figure 24A). The number of squid sampled for length frequency was 708 (one juvenile, three unsexed, 398 females and 306 males), two taken from the random sample were sampled for statoliths. Dorsal mantle length was 13.5 cm for the juvenile, ranged from 19.5 to 22 cm for the unsexed individuals, from 13 to 36.5 cm for females, and from 9.5 to 34.5 cm for males (Figure 24C). It is difficult to identify cohorts on the histograms and length–at–age should rather be derived from statoliths. The smaller cohort was also observed in 2016 and 2017 (Gras et al., 2016; 2017). Females were observed young (6%), immature (75%), preparatory (13%), maturing (2%) and mature (4%) (Figure 24B). Males were young (8%), immature (3%), preparatory (6%), maturing (17%) and mature (66 %) (Figure 24B).

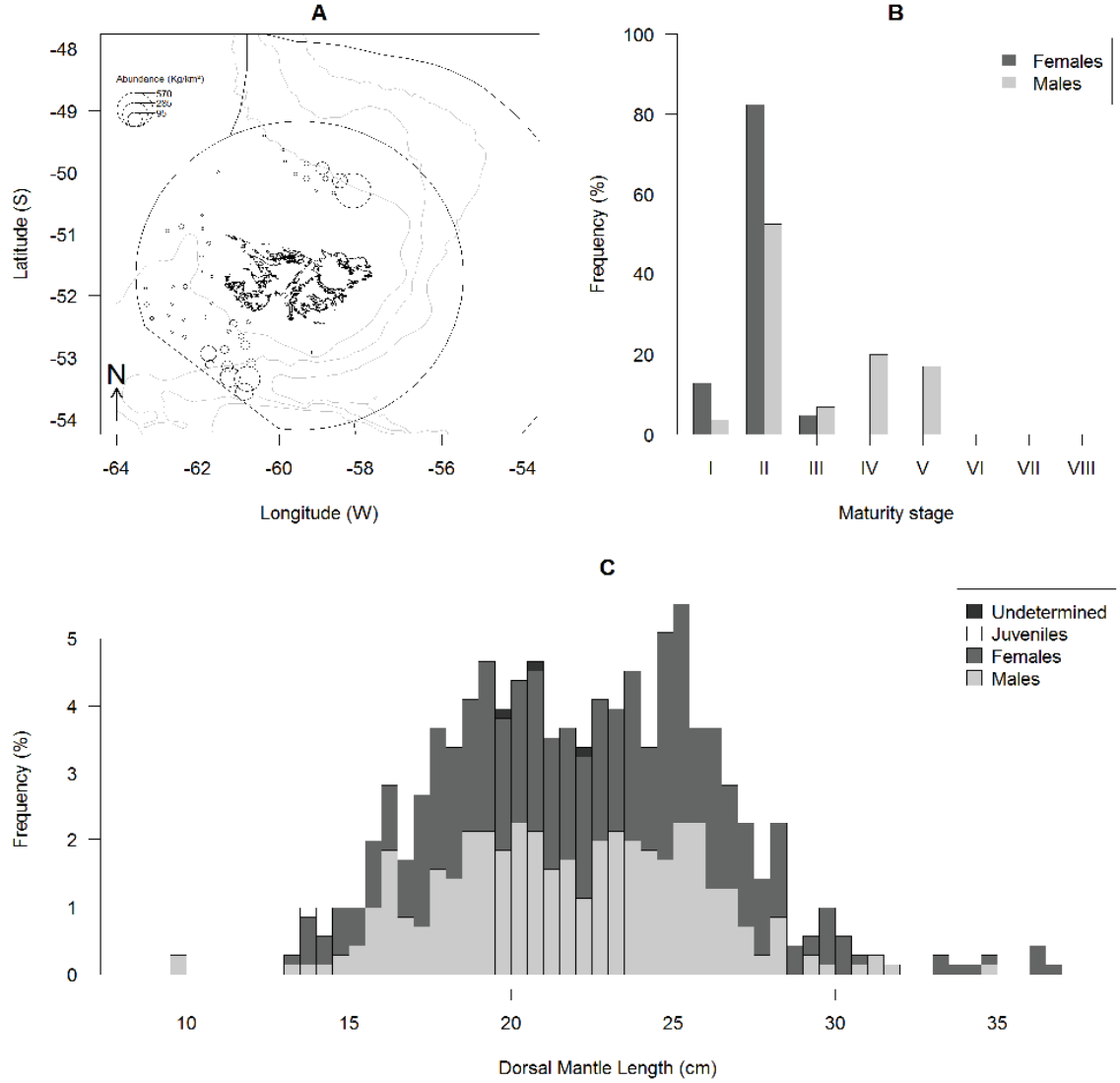

Figure 24: Biological data of *Illex argentinus* (greater hooked squid; ILL), map of the densities in kg·km^{-2} (A), percentage of specimens of each sex per maturity stage (B; I, young; II, immature; III, preparatory; IV, maturing; V, mature; VI, spent), and dorsal mantle length frequency (in percentage of the total sample assessed) of each sex with 0.5 cm size class (C; n= 708).

3.3.3 *Doryteuthis gahi* (former *Loligo gahi*) – Falkland calamari – LOL (Figure 25)

The total catch of Falkland calamari was 968 kg. It was caught at 90 of the 97 trawl stations sampled throughout the research cruise (Figure 25A). Catches ranged from 0.02 to 76.9 kg. Among the 90 stations, 31 yielded >10 kg and two >50 kg. Densities ranged from 0.12 to 378 kg·km^{-2}. (CPUE ranged 0.02 – 76.9 kg·h^{-1}). Falkland calamari was caught almost throughout the survey and densities were not that variable between stations given that during this year's survey we did not sample any station in the *Loligo* box (Figure 25A). The number of squid sampled for dorsal mantle length frequency was 7,520 (eight juveniles, 3,974 females, 3,517 males, and 21 unsexed), 281 were sampled for length–weight and 351 for statoliths (including three non–randomly selected individuals). Dorsal mantle length ranged from 5.5 to 8 cm for juveniles, from 4 to 17.5 cm for females, from 3.5 to 21.5 cm for males, and from 4.5 to 11 for unsexed individuals (Figure 25C). One cohort appeared on the length frequency histogram (mode at 7.5 cm) (Figure 25C). Females were young (35%), immature (62%), preparatory (2%), maturing (0.5%), and mature (0.5%) (Figure 25B). Males were young (42%), immature (48 %), preparatory (6%), maturing (2%), and mature (2%) (Figure 25B).

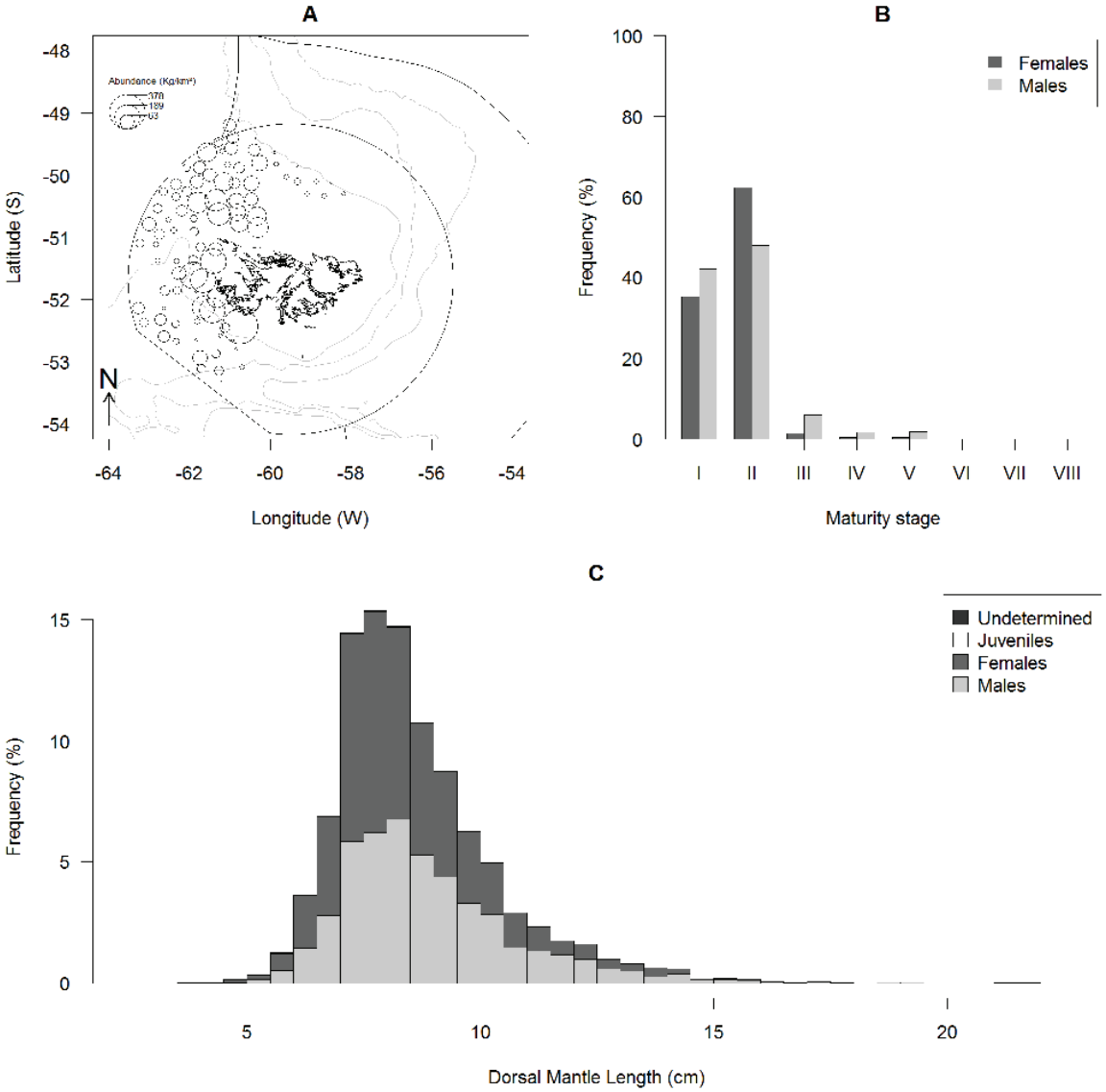

Figure 25: Biological data of *Doryteuthis gahi* (Falkland calamari; LOL), map of the densities in kg·km^{-2} (A), percentage of specimens of each sex per maturity stage (B; I, young; II, immature; III, preparatory; IV, maturing; V, mature; VI, spent), and dorsal mantle length frequency (in percentage of the total sample assessed) of each sex with 0.5 cm size class (C; n= 7,520).

3.4 Biological information of skates

3.4.1 *Bathyraja albomaculata* – white spotted skate – RAL (Figure 26)

The total catch of white spotted skate was 46 kg. It was caught at 18 out of the 97 trawl stations sampled through the research cruise (Figure 26A). Catches ranged from 0.02 to 5.92 kg. Of the 18 stations, three yielded >5 kg. Densities ranged from 0.09 to 28.23 kg·km^{-2} (CPUE ranged 0.02 to 5.92 kg·h^{-1}). Highest densities were observed in the northern part of the survey zone (Figure 26A). The number of skate sampled for total length, disc–width and weight was 28 (53.6% male). Disc width ranged from ten to 53 cm for females and from ten to 45 cm for males (Figure 26C). The histogram exhibits a juvenile and an adult cohort. Females (n = 13) were juvenile (23%), adolescent, maturing (23%), adult, developing (15%), adult, mature (23%), adult, laying (8), and adult, resting (8%) (Figure 26B). Males (n = 15) were juvenile (7%), adolescent, maturing (20%), adult, developing (20%), adult, mature (40%), and adult, running (13%) (Figure 26B).

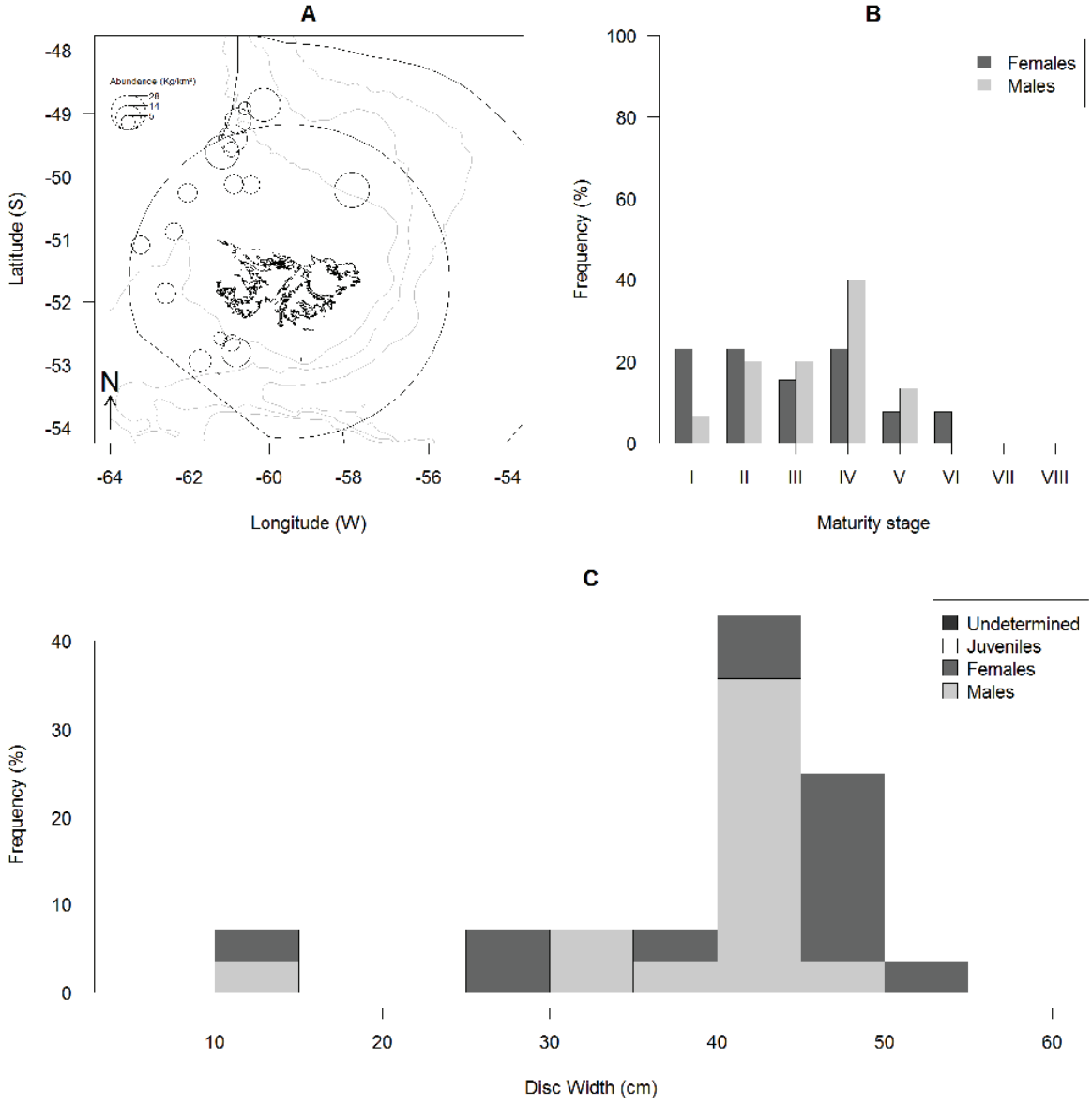

Figure 26: Biological data of *Bathyraja albomaculata* (white spotted skate, RAL), map of the densities in kg/km² (A), percentage of specimens of each sex per maturity stage (B; I, juvenile; II, adolescent maturing; III, adult, developing; IV, adult, mature; V, adult laying/running; VI, adult resting), and length frequency (in percentage of the total sample assessed) of each sex with 5 cm size class (C; n= 28).

3.4.2 *Bathyraja brachyurops* – blonde skate – RBR (Figure 27)

The total catch of blonde skate was 337 kg. It was caught at 61 out of the 97 trawl stations sampled throughout the research cruise (Figure 27A). Catches ranged from 0.02 to 62.76 kg. Of the 61 stations, 66 yielded >10 kg, and one >50 kg. Densities ranged from 0.10 to 342.02 kg·km^{-2} (CPUE ranged 0.02 to 62.76 kg·hr^{-1}). Highest densities were observed in the NE part of the survey zone (Figure 27A). The number of skate sampled for total length, disc–width and weight was 177 (50.8% males). Disc widths ranged from six to 77 cm for females and from seven to 67 cm for males (Figure 27C). The histogram exhibits a single clear juvenile cohort in the 10–14cm size class (Figure 27C). Females (n = 87) were observed juvenile (25%), adolescent, maturing (43%), adult, developing (12%), adult, mature (9%), adult, laying (1%) and adult, resting (10%) (Figure 27B). Males (n = 90) were juvenile (26%), adolescent, maturing (31%), adult, developing (14%), adult, mature (22%), adult, running (7%) (Figure 27B).

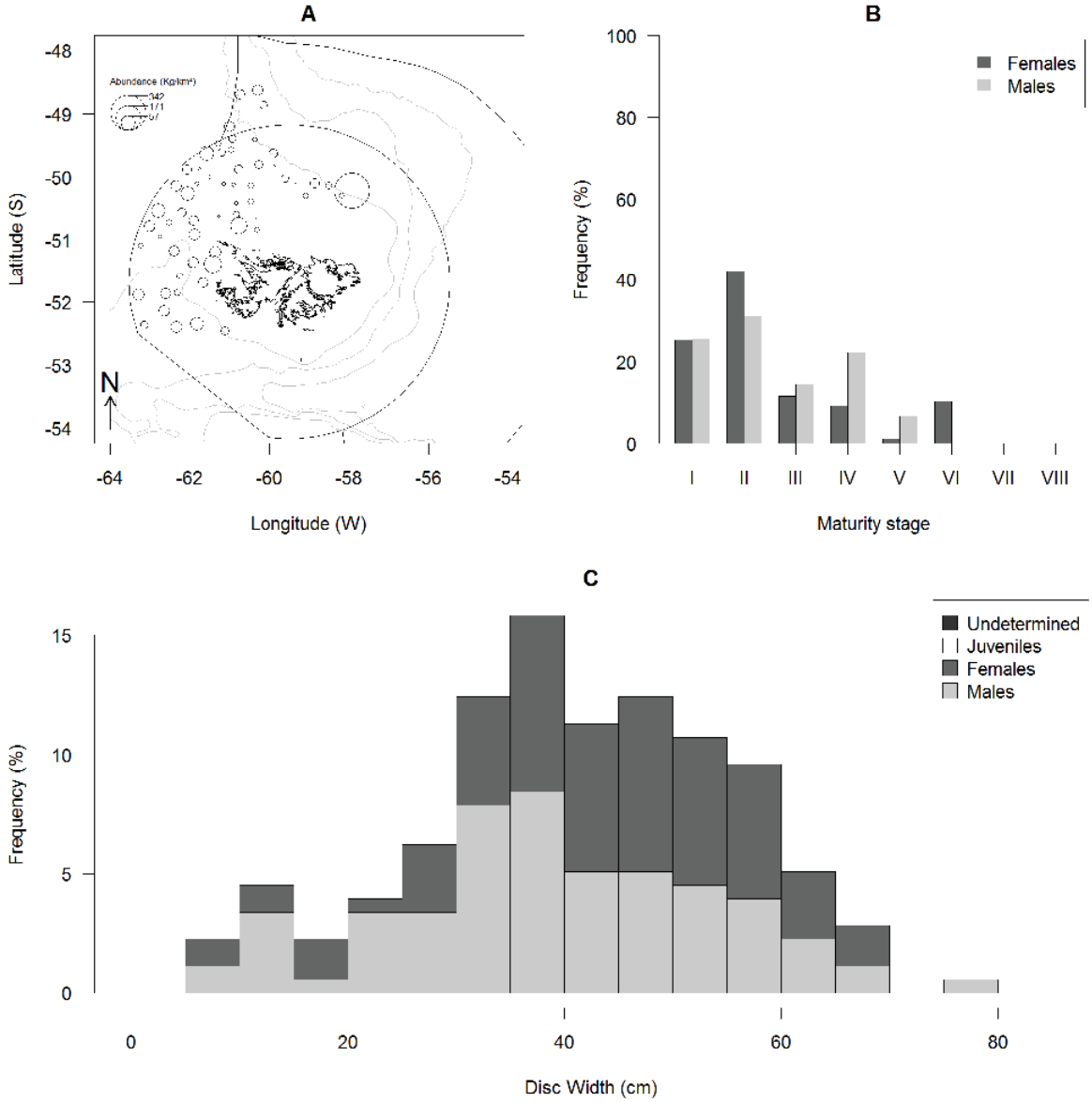

Figure 27: Biological data of *Bathyraja brachyurops* (blonde skate, RBR), map of the densities in kg/km² (A), percentage of specimens of each sex per maturity stage (B; I, juvenile; II, adolescent maturing; III, adult, developing; IV, adult, mature; V, adult laying/running; VI, adult resting), and size frequency frequency (in percentage of the total sample assessed) of each sex with 5 cm size classes (C; n= 177).

3.4.3 *Bathyraja cousseauae* – joined–fin skate – RBZ (Figure 28)

The total catch of joined–fin skate was 112 kg. It was caught at nine out of the 97 trawl stations sampled throughout the research cruise (Figure 28A). Catches ranged from 1.02 to 28.70 kg. Of the nine stations, five yielded >10 kg. Densities ranged from 4.41 to 156.40 kg·km^{-2} (CPUE ranged 1.02 to 28.70 kg·hr^{-1}). Highest densities were observed in the northern, NE, and SW part of the survey zone (Figure 28A). The number of skate sampled for total length, disc–width and weight was 24 (54.2% male). Disc width ranged from 27 to 74 cm for females and from 28 to 84 cm for males (Figure 28C). Females were juvenile (27%), adolescent, maturing (27%), adult, developing (37%), and adult, mature (9%) (Figure 28B). Males were juvenile (38%), adolescent, maturing (8%), adult, developing (23%), and adult, running (31%) (Figure 28B).

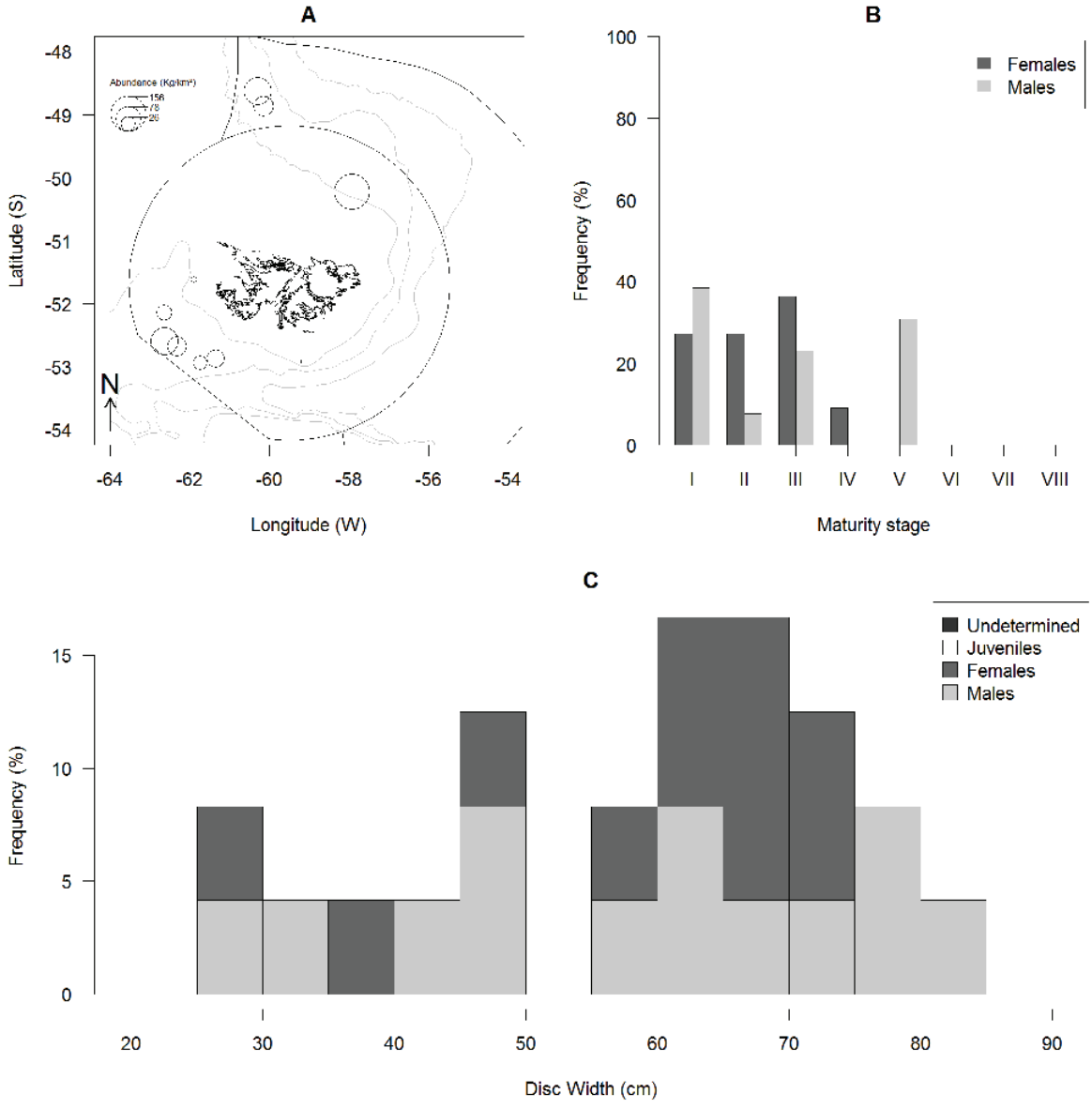

Figure 28: Biological data of *Bathyraja cousseauae* (joined–fin skate, RBZ), map of the densities in kg/km² (A), percentage of specimens of each sex per maturity stage (B; I, juvenile; II, adolescent maturing; III, adult, developing; IV, adult, mature; V, adult laying/running; VI, adult resting), and length frequency (in percentage of the total sample assessed) of each sex with 5 cm size class (C; n= 24).

3.4.4 *Zearaja argentinensis* – Black Skate – RDA (Figure 29)

There was one catch of black skate of 11.3 kg. It was caught at 1 out of the 97 trawl stations sampled through the research cruise (Figure 29A). Density was 61.58 kg·km^{-2}, and the CPUE was 11.3 kg·hr^{-1}). The single juvenile female specimen caught from the NE part of the survey was taken back to Stanley for detailed analyses.

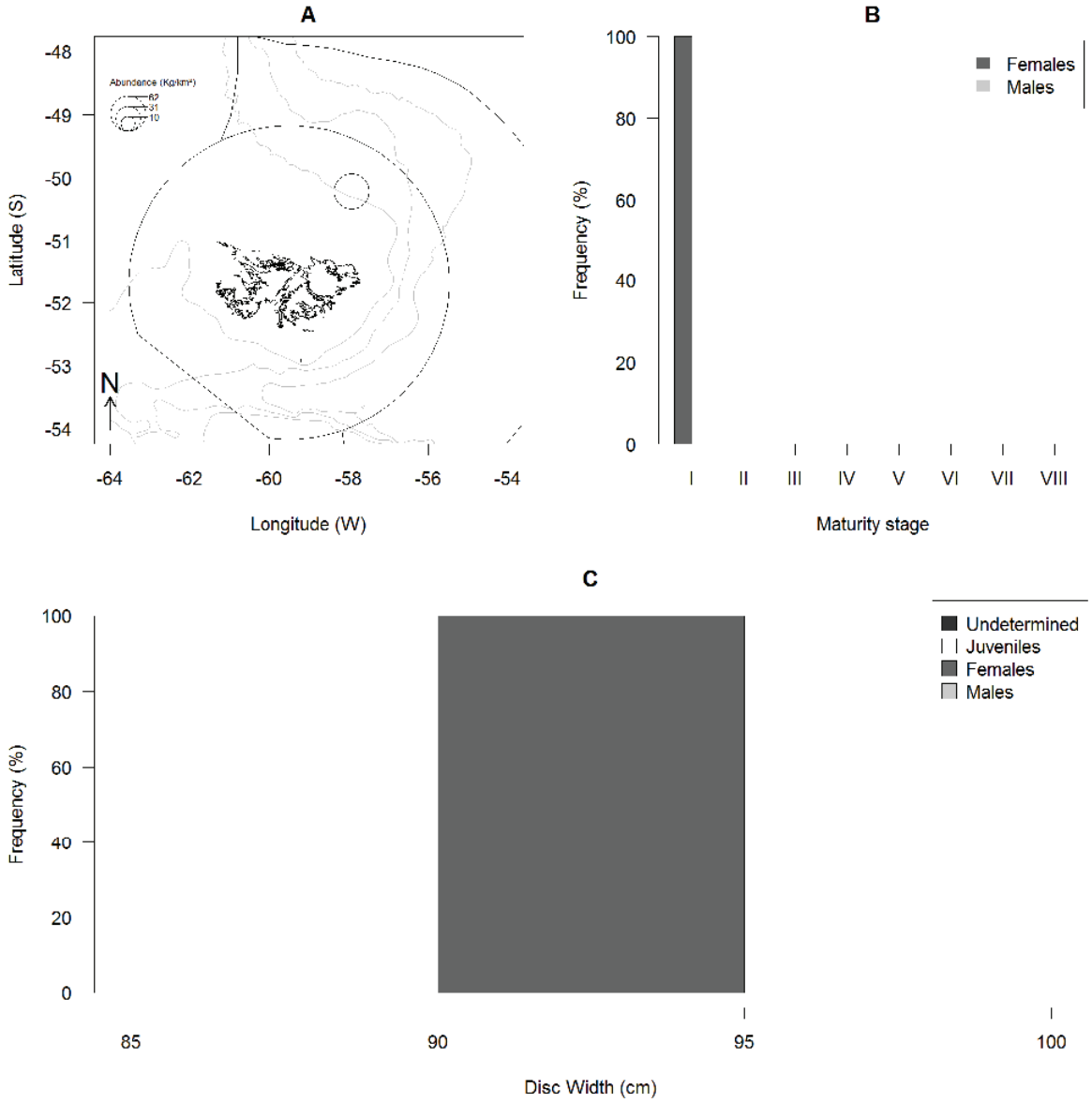

Figure 29: Biological data of *Zearaja argentinensis* (Black skate, RDA), map of the densities in kg/km² (A), percentage of specimens of each sex per maturity stage (B; I, juvenile; II, adolescent maturing; III, adult, developing; IV, adult, mature; V, adult laying/running; VI, adult resting), and length frequency (in percentage of the total sample assessed) of each sex with 5 cm size class (C; n= 1).

3.4.5 *Amblyraja doellojuradoi* – Starry Skate – RDO (Figure 30)

The total catch of starry skate was three kg. It was caught at 11 out of the 97 trawl stations sampled through the research cruise (Figure 30A). Catches ranged from 0.01 to 1.06 kg. Densities ranged from 0.04 to 4.96 kg·km^{-2} (CPUE ranged 0.01 to 1.06 kg·hr^{-1}). Highest densities were observed in the northern and western parts of the survey zone in deeper waters (Figure 30A). The number of skate sampled for total length, disc–width and weight was 14 (50% female). Disc width ranged from eight to 33 cm for females and from seven to 35 cm for males (Figure 30C). Females were juvenile (71%), adult, mature (14%), and adult, laying (14%) (Figure 30B). Males were juvenile (86%), and adult, mature (14%) (Figure 30B).

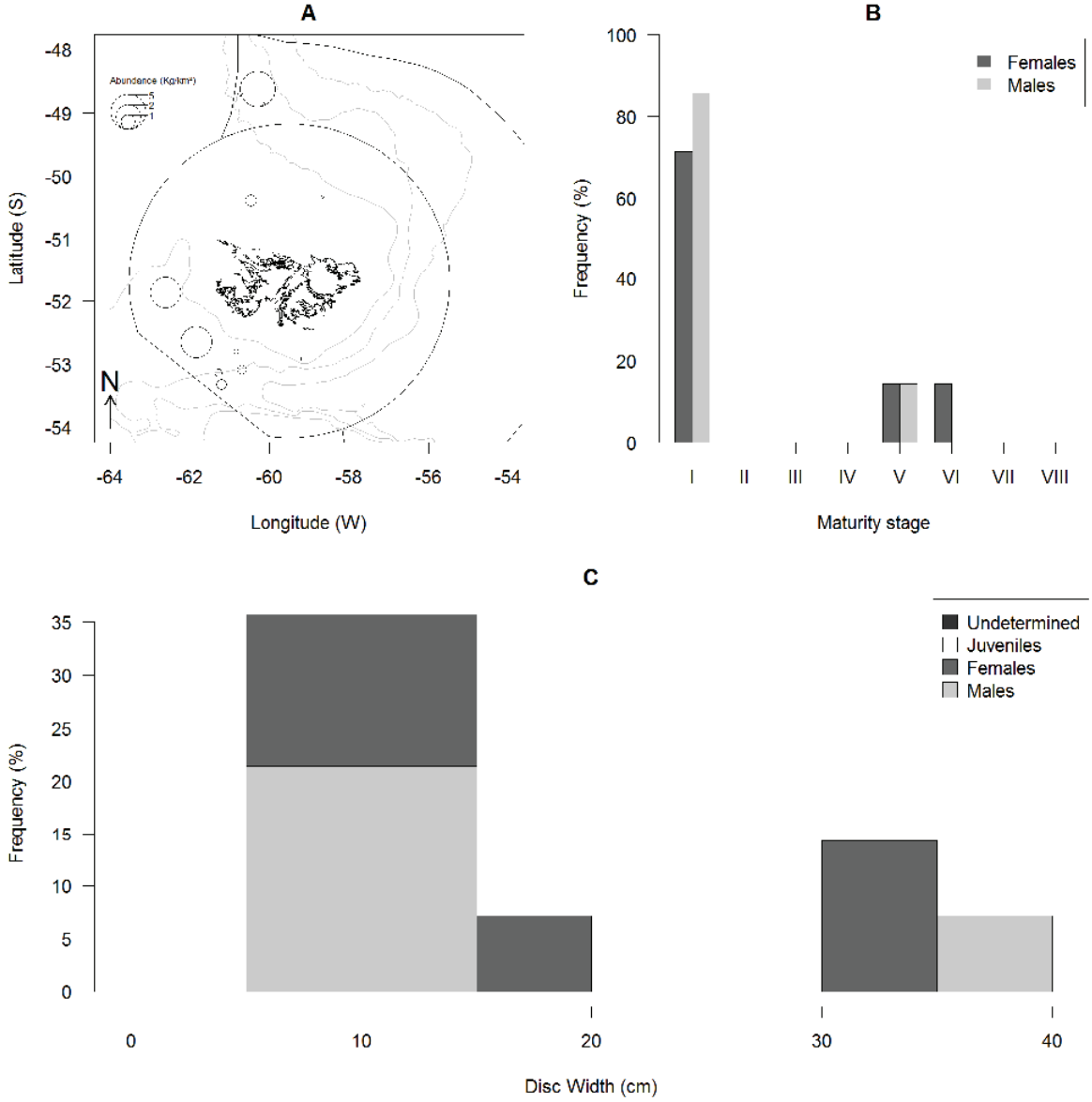

Figure 30: Biological data of *Amblyraja doellojuradoi* (Starry skate, RDO), map of the densities in kg/km² (A), percentage of specimens of each sex per maturity stage (B; I, juvenile; II, adolescent maturing; III, adult, developing; IV, adult, mature; V, adult laying/running; VI, adult resting), and length frequency (in percentage of the total sample assessed) of each sex with 5 cm size class (C; n= 14).

3.4.6 *Zearaja chilensis* – yellow nose skate – RFL (Figure 31)

The total catch of yellow nose skate was 361 kg. It was caught at 50 out of the 97 trawl stations sampled throughout the research cruise (Figure 31A). Catches ranged from 0.76 to 48.94 kg. Of the 50 stations, nine yielded >10 kg. Densities ranged from 3.44 to 227.68 $kg \cdot km^{-2}$ (CPUE ranged 0.76 to 48.94 $kg \cdot hr^{-1}$). Highest densities were observed in the NW part of the survey zone (Figure 31A). The number of skate sampled for total length, disc–width and weight was 114 (80.7% female). Disc width ranged from 35 to 84 cm for females and from 36 to 65 cm for males (Figure 31C). The histogram exhibits no clear cohorts. Females (n = 92) were observed juvenile (14%), adolescent, maturing (65%), adult, developing (20%), and adult, resting (1%) (Figure 31B). Males (n = 21) were juvenile (9%), adolescent, maturing (33%), adult, developing (30%), adult, mature (9%), adult, running (19%) (Figure 31B).

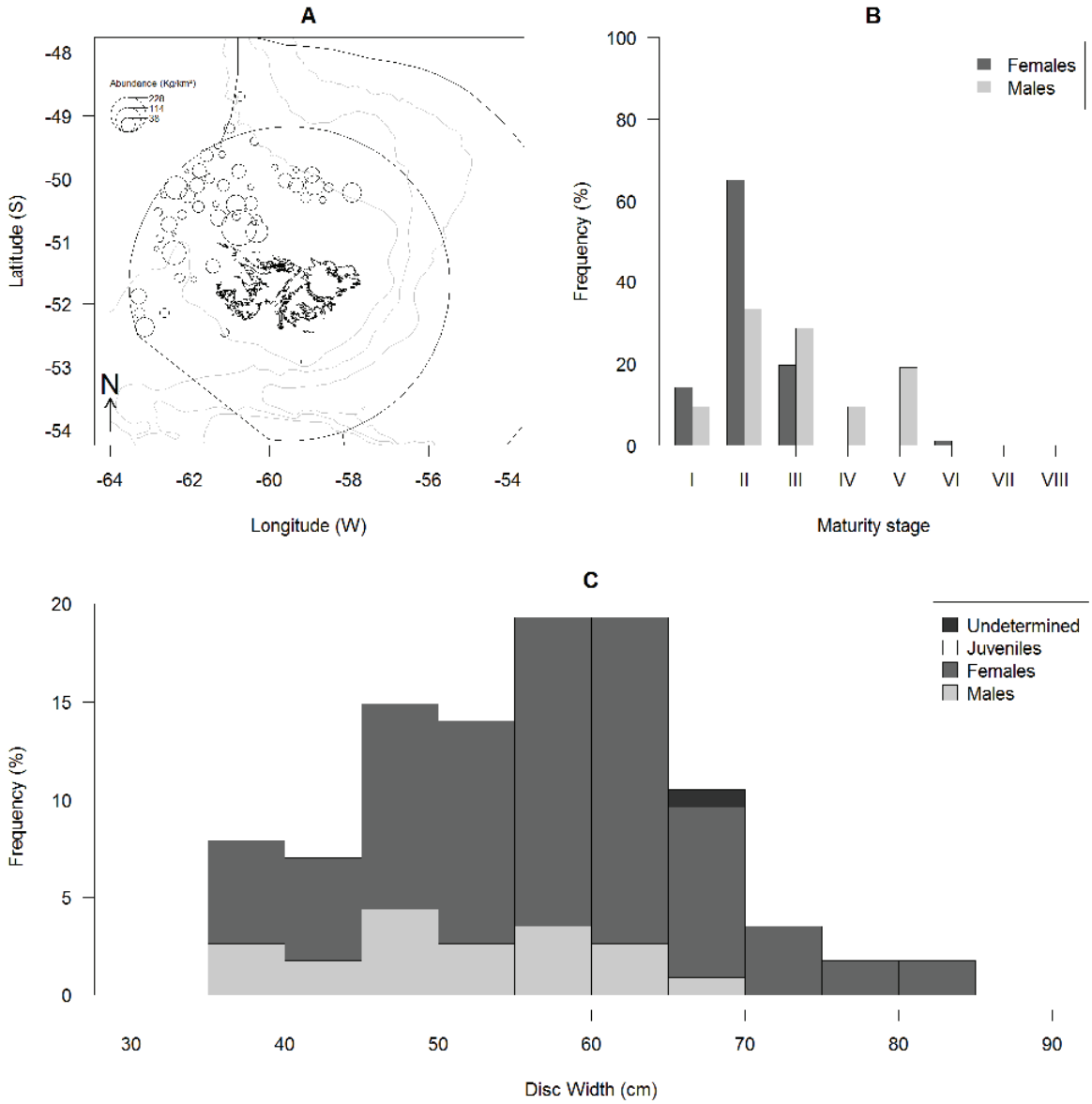

Figure 31: Biological data of *Zearaja chilensis* (yellow nose skate, RFL), map of the densities in kg/km² (A), percentage of specimens of each sex per maturity stage (B; I, juvenile; II, adolescent maturing; III, adult, developing; IV, adult, mature; V, adult laying/running; VI, adult resting), and length frequency (in percentage of the total sample assessed) of each sex with 5 cm size class (C; n= 114).

3.4.7 *Bathyraja griseocauda* – grey tailed skate – RGR (Figure 32)

The total catch of grey tailed skate was 814 kg. It was caught at 30 out of the 97 trawl stations sampled through the research cruise (Figure 32A). Catches ranged from 0.38 to 114.00 kg. Of the 30 stations, 24 yielded >10 kg, and one >100 kg. Densities ranged from 1.73 to 621.26 kg·km^{-2} (CPUE ranged 0.38 to 114.00 kg·hr^{-1}). Highest densities were observed in the northern, NE, and SW part of the survey zone (Figure 32A). The number of skate sampled for total length, disc–width and weight was 122 (50.8% male). Disc width ranged from 15 to 102 cm for females and from 21 to 90 cm for males (Figure 32C). The histogram exhibits no clear cohorts (Figure 32C). Females (n = 60) were observed juvenile (43%), adolescent, maturing (27%), adult, developing (7%), adult, mature (13%), adult, laying (3%) and adult, resting (7%) (Figure 32B). Males (n = 62) were juvenile (32%), adolescent, maturing (18%), adult, developing (18%), adult, mature (11%), and adult, running (21%) (Figure 32B).

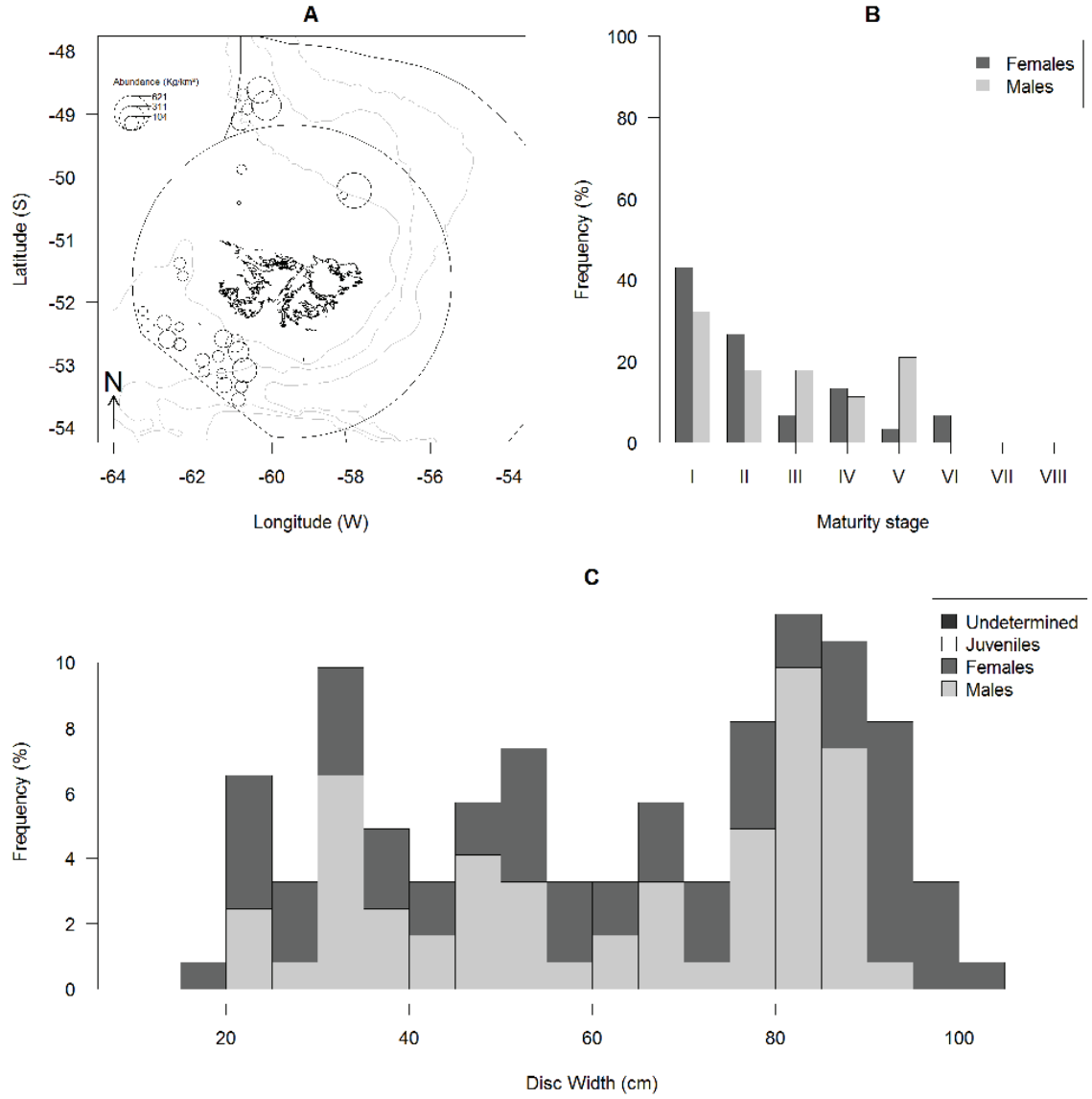

Figure 32: Biological data of *Bathyraja griseocauda* (grey tailed skate, RGR), map of the densities in kg/km² (A), percentage of specimens of each sex per maturity stage (B; I, juvenile; II, adolescent maturing; III, adult, developing; IV, adult, mature; V, adult laying/running; VI, adult resting), and length frequency (in percentage of the total sample assessed) of each sex with 5 cm size class (C; n= 122).

3.4.8 *Bathyraja macloviana* – Falkland skate – RMC (Figure 33)

The total catch of Falkland skate was 45 kg. It was caught at 28 out of the 97 trawl stations sampled throughout the research cruise (Figure 33A). Catches ranged from 0.43 to 6.49 kg. Among the 28 stations, one yielded >5 kg. Densities ranged from 2.03 to 29.82 kg·km^{-2} (CPUE ranged 0.43 to 6.49 kg·hr^{-1}). Highest densities were observed to the NW of the Jason Islands (Figure 33A). The number of skate sampled for total length, disc–width and weight was 40 (65% male). Disc width ranged from 14 to 40 cm for females and from 21 to 39 cm for males (Figure 33C). Females (n = 14) were juvenile (7%), adolescent, maturing (14%), adult, developing (29%), adult, mature (29%), adult, laying (7%) and adult, resting (14%) (Figure 33B). Males (n = 26) were juvenile (4%), adolescent, maturing (23%), adult, developing (12%), adult, mature (15%), and adult, running (46%) (Figure 33B).

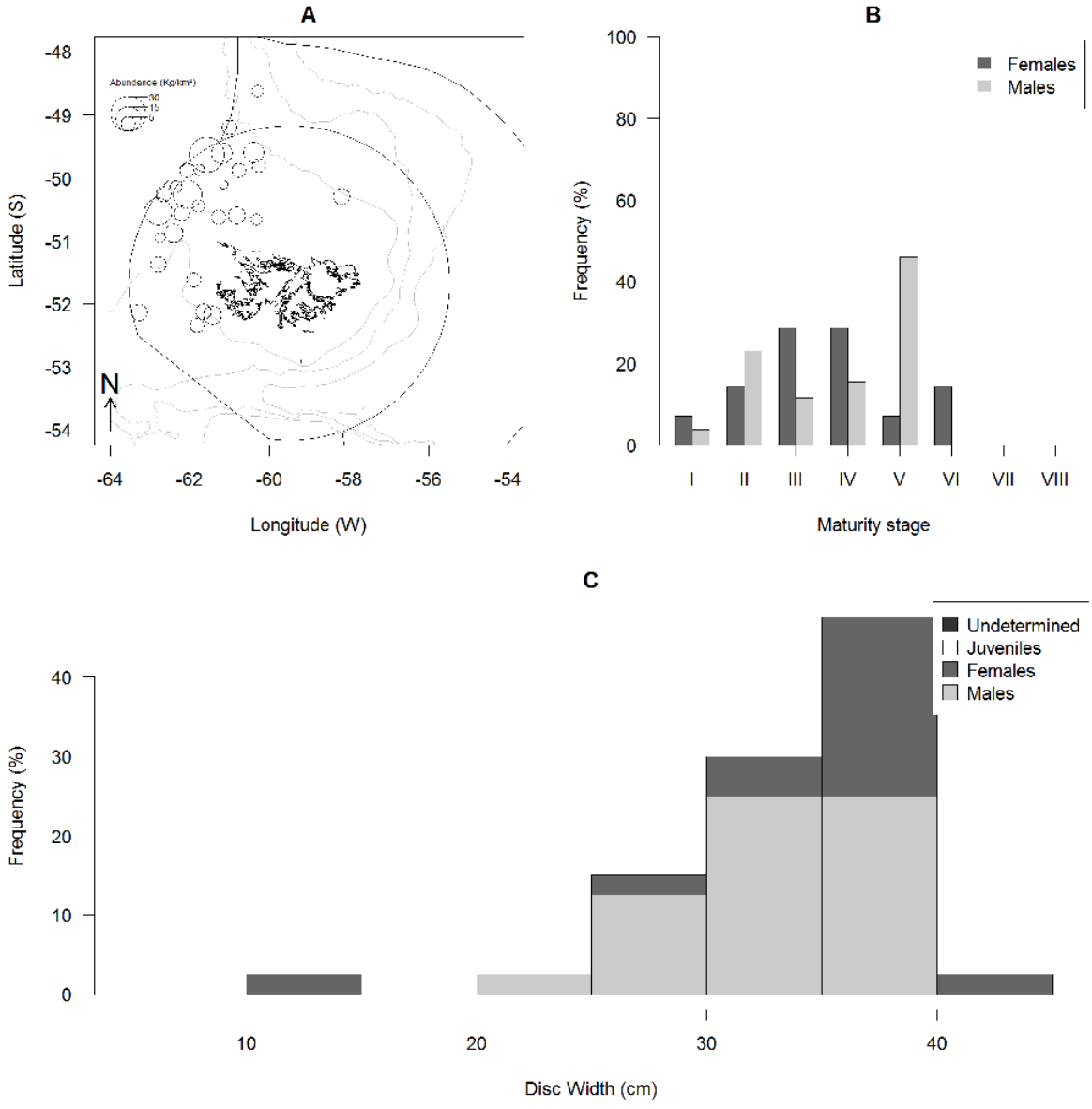

Figure 33: Biological data of *Bathyraja macloviana* (Falkland skate, RMC), map of the densities in kg/km² (A), percentage of specimens of each sex per maturity stage (B; I, juvenile; II, adolescent maturing; III, adult, developing; IV, adult, mature; V, adult laying/running; VI, adult resting), and length frequency (in percentage of the total sample assessed) of each sex with 5 cm size class (C; n= 40).

3.4.9 *Bathyraja magellanica* – Magellanic skate – RMG (Figure 34)

There was one catch of Magellanic skate of 0.35 kg (Figure 34A). Density was 1.9 kg·km^{-2}, and the CPUE was 0.35 kg·hr^{-1}). The single juvenile female specimen caught from the western part of the survey was taken back to Stanley for detailed analyses.

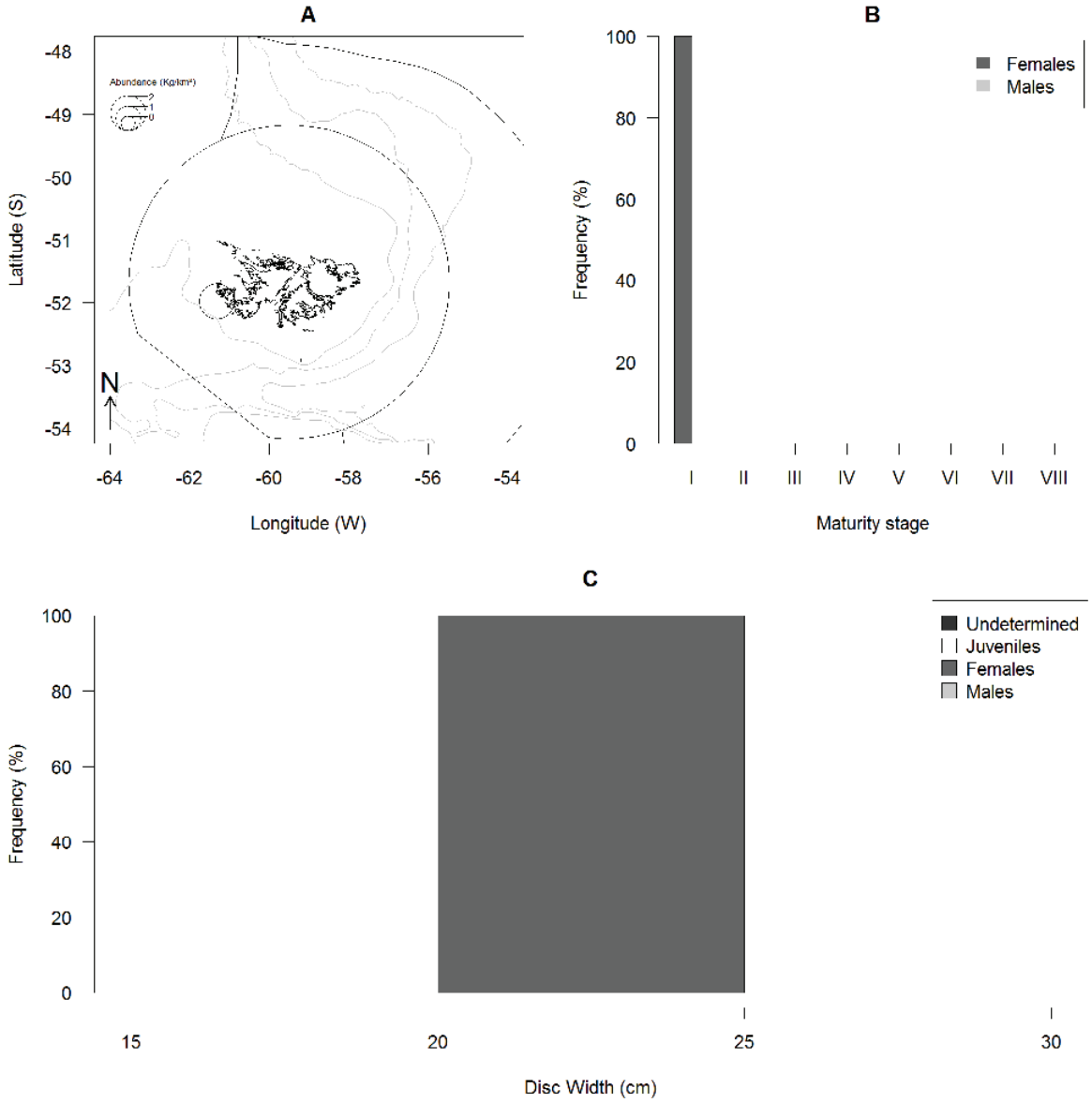

Figure 34: Biological data of *Bathyraja magellanica* (Magellanic skate, RMG), map of the densities in kg/km² (A), percentage of specimens of each sex per maturity stage (B; I, juvenile; II, adolescent maturing; III, adult, developing; IV, adult, mature; V, adult laying/running; VI, adult resting), and length frequency (in percentage of the total sample assessed) of each sex with 5 cm size class (C; n= 1).

3.4.10 *Bathyraja multispinis* – multispined skate – RMU (Figure 35)

The total catch of multispined skate was 59 kg. It was caught at eight out of the 97 trawl stations sampled through the research cruise (Figure 35A). Catches ranged from 2.56 to 29.57 kg. Of the eight stations, one yielded >10 kg. Densities ranged from 11.24 to 161.16 kg·km^{-2} (CPUE ranged 2.56 to 29.57 kg·hr^{-1}). Highest densities were observed in the NE part of the survey zone (Figure 35A). The number of skate sampled for total length, disc–width and weight was 11 (63.6% female). Disc width ranged from 36 to 85 cm for females and from 48 to 74 cm for males (Figure 35C). Females were observed juvenile (29%), adolescent, maturing (29%), adult, developing (29%), and adult, mature (14%) (Figure 35B). Males were adolescent, maturing (75%) and adult, developing (25%) (Figure 35B).

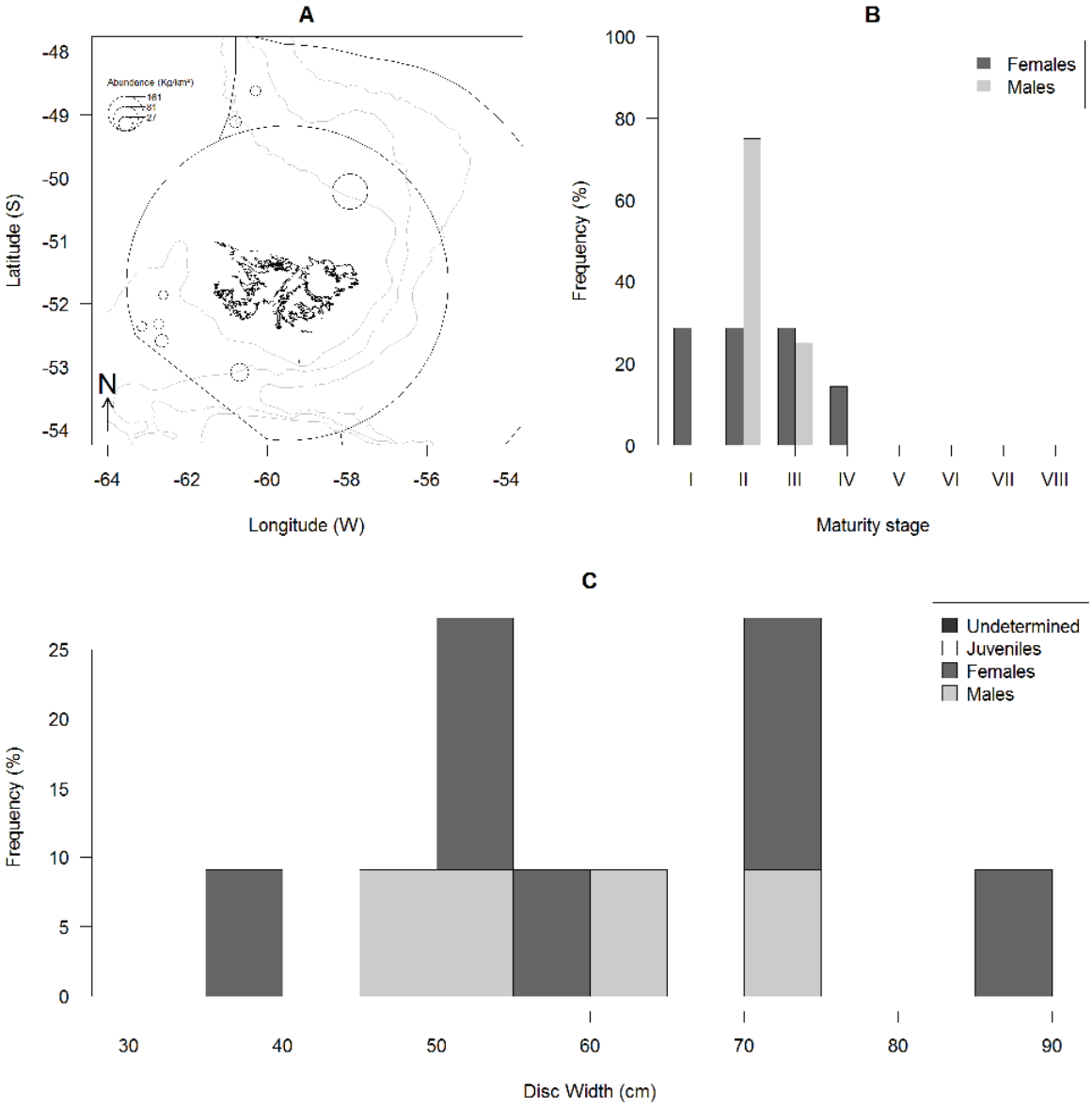

Figure 35: Biological data of *Bathyraja multispinis* (multispined skate, RMU), map of the densities in kg/km² (A), percentage of specimens of each sex per maturity stage (B; I, juvenile; II, adolescent maturing; III, adult, developing; IV, adult, mature; V, adult laying/running; VI, adult resting), and length frequency (in percentage of the total sample assessed) of each sex with 5 cm size class (C; n= 11).

3.4.11 *Pasmmobatis spp.* – Sandray Unidentified – RPX (Figure 36)

The total catch of sandrays was 12 kg. It was caught at 17 out of the 97 trawl stations sampled through the research cruise (Figure 36A). Catches ranged from 0.02 to 1.38 kg. Densities ranged from 0.10 to 6.18 kg·km^{-2} (CPUE ranged 0.02 to 1.38 kg·hr^{-1}). Highest densities were observed in the NW part of the survey zone (Figure 36A). The number of skate sampled for total length, disc–width and weight was 21 (52.4% female). Disc width ranged from 14 to 29 cm for females and from six to 28 cm for males (Figure 36C). Females (n = 11) were observed juvenile (9%), adolescent, maturing (27%), adult, developing (9%), adult, mature (27%), and adult, resting (27%) (Figure 36B). Males (n = 10) were juvenile (30%), adult, developing (30%), adult, mature (20%), and adult, running (20%) (Figure 36B).

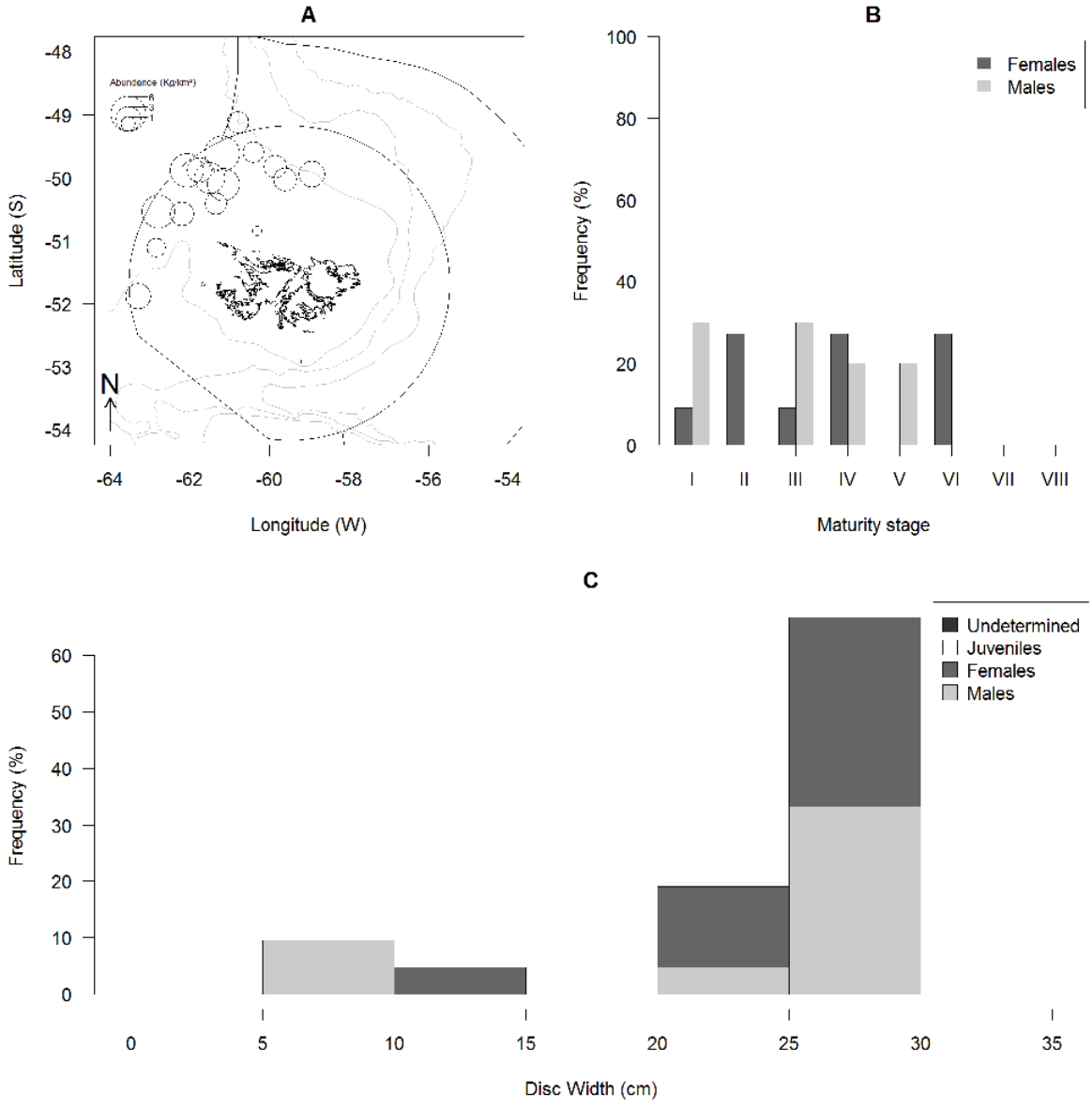

Figure 36: Biological data of *Psammobatis spp*. (Sandray Unidentified, RPX), map of the densities in kg/km² (A), percentage of specimens of each sex per maturity stage (B; I, juvenile; II, adolescent maturing; III, adult, developing; IV, adult, mature; V, adult laying/running; VI, adult resting), and length frequency (in percentage of the total sample assessed) of each sex with 5 cm size class (C; n= 21).

3.4.12 *Bathyraja scaphiops* – cuphead skate – RSC (Figure 37)

The total catch of cuphead skate was 33 kg. It was caught at 13 out of the 97 trawl stations sampled throughout the research cruise (Figure 37A). Catches ranged from 0.96 to 6.63 kg. Of the 13 stations, one yielded >5 kg. Densities ranged from 4.27 to 30.05 kg·km^{-2} (CPUE ranged 0.96 to 6.63 kg·hr^{-1}). Highest densities were observed in the north and SW parts of the survey zone (Figure 37A). The number of skate sampled for total length, disc–width and weight was 16 (50% female). Disc width ranged from 45 to 57 cm for females and from 36 to 50 cm for males (Figure 37C). The histogram exhibits primarily an adult cohort (Figure 37C). Females (n = 8) were observed adolescent, maturing (13%), adult, developing (13%), adult, mature (62%), and adult, resting (13%) (Figure 37B). Males (n = 8) were juvenile (13%), adolescent, maturing (62%), adult, and mature (25%).

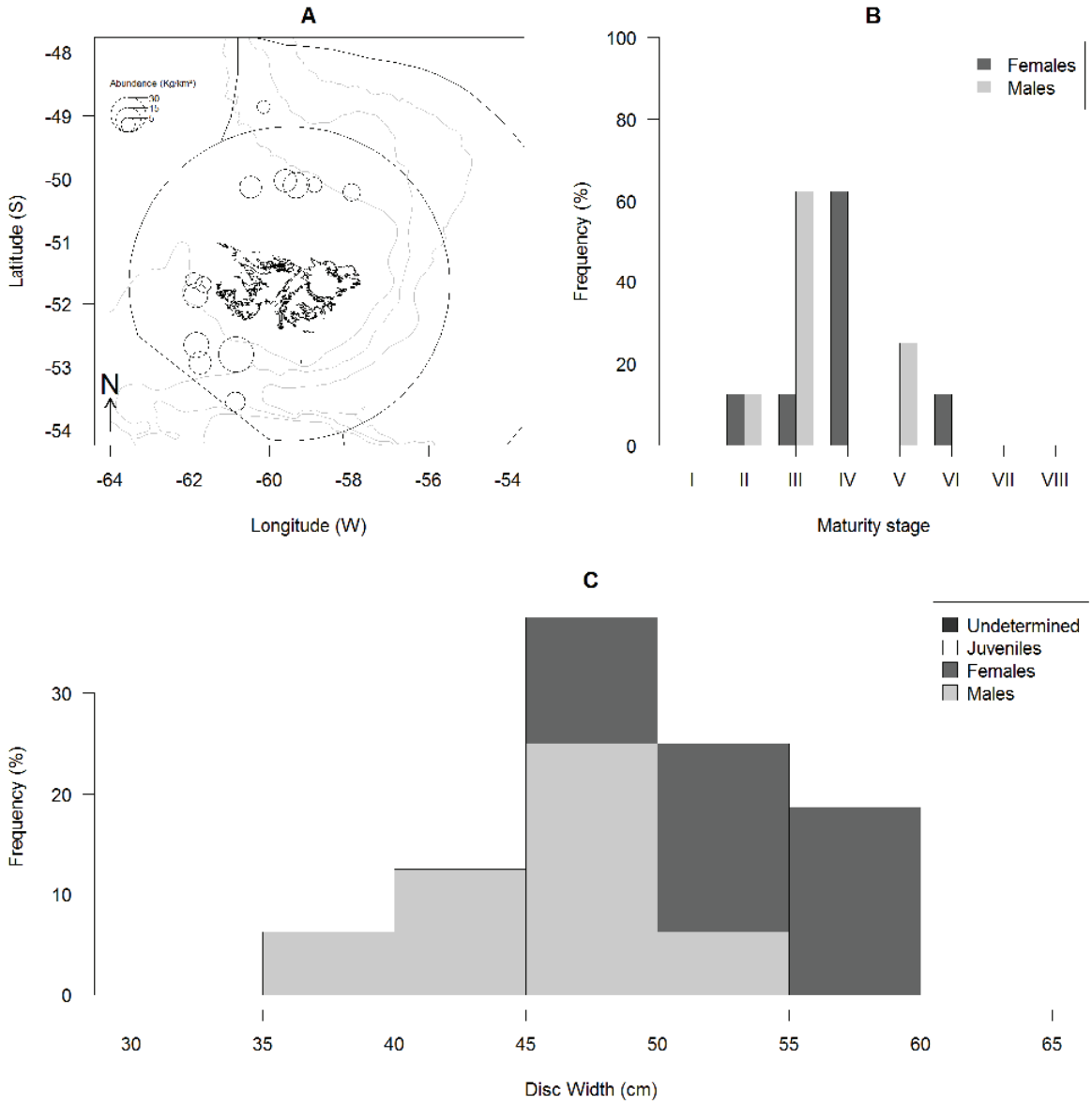

Figure 37: Biological data of *Bathyraja scaphiops* (cuphead skate, RSC), map of the densities in kg/km² (A), percentage of specimens of each sex per maturity stage (B; I, juvenile; II, adolescent maturing; III, adult, developing; IV, adult, mature; V, adult laying/running; VI, adult resting), and length frequency (in percentage of the total sample assessed) of each sex with 5 cm size class (C; n= 16).

3.5 Biomass estimation and cohort analysis

3.5.1 Red cod (Figure 38 and Figure 39)

Red cod observed densities ranged from 0.1 kg·km^{-2} to 34.5 t·km^{-2} (Figure 38B). These densities were Box–Cox (λ=0.5) transformed and used to plot the semi–variogram using 25 distance classes (Figure 38A). The best variogram model was spherical and reached the sill (2,037) at a range of 35 km. The average kriged density was 643 kg·km^{-2} and the biomass estimation was 78,797 t (Figure 38C). The kriged map showed one hot spot of red cod in the FICZ to the west of West Falkland. The hot spots that were observed in previous years were not seen in 2018. From the temporal perspective, red cod biomass increased from 2010 to 2011 (from 103,566 t to 161,707 t) (Figure 38C). From 2011 to 2017 a decreasing trajectory was observed to 75,979 t (Figure 38C). This decrease was non–significant until 2016 and became significant in 2017. In 2018 a non–significant increase of the biomass was seen (Figure 38C). The abundance followed the same trajectory as the biomass from 2010 to 2015 and from 2016 to 2017 (Figure 38C). From 2015 to 2016 the abundance increased while the biomass decreased (Figure 38C) a consequence of the decrease in the average length of fish in the stock (Figure 39). The opposite trend was observed between 2017 and 2018 which shows that the stock consisted of bigger fish (Figure 38C). That could be further observed on the length frequency histogram (Figure 39).

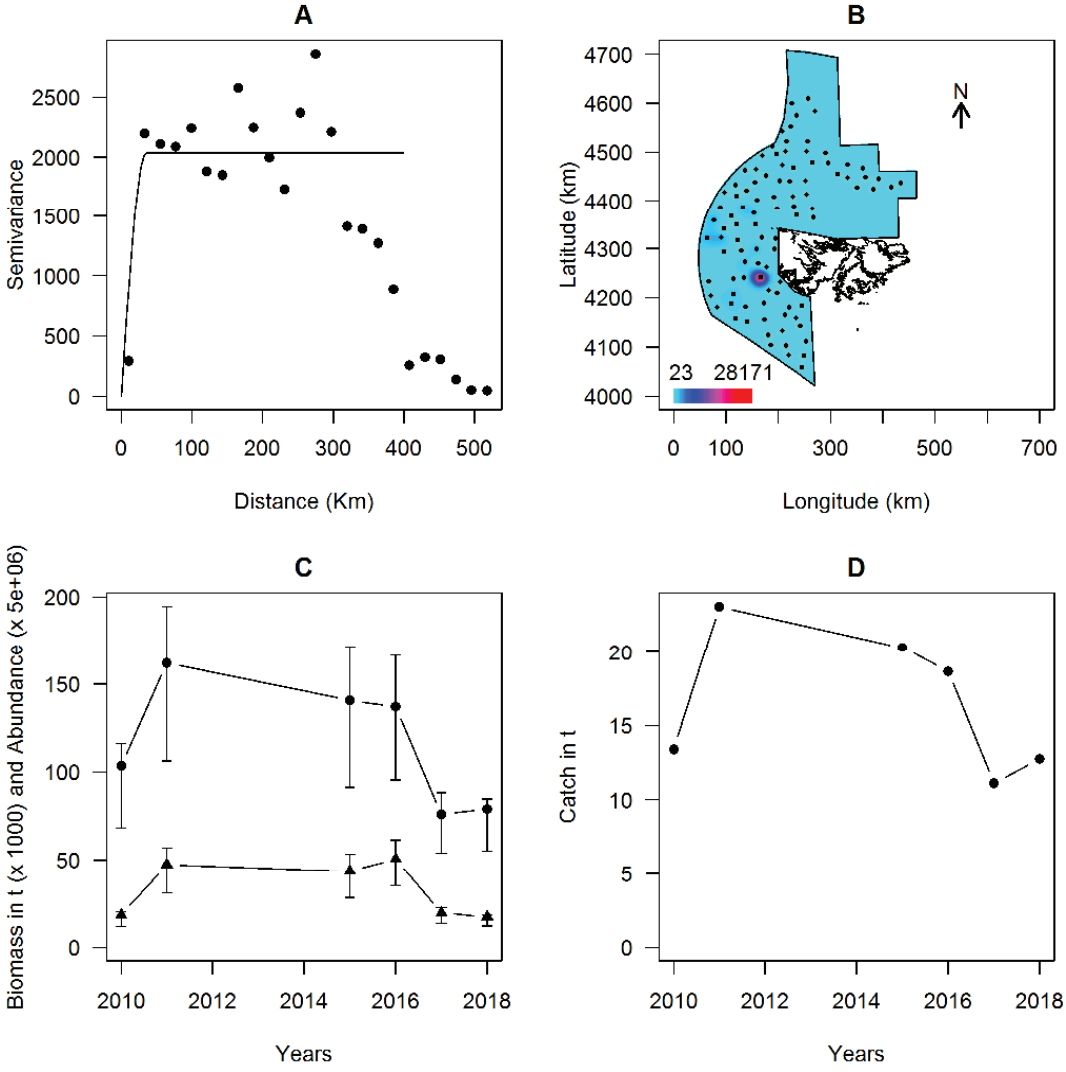

Figure 38: Experimental variogram with spherical model fitted (A), kriged map of red cod density (B), time series of estimated biomass and numbers of fish (with associated 95% confidence intervals) using the February ground fish survey conducted from 2010 (C) and total catch of each survey (D).

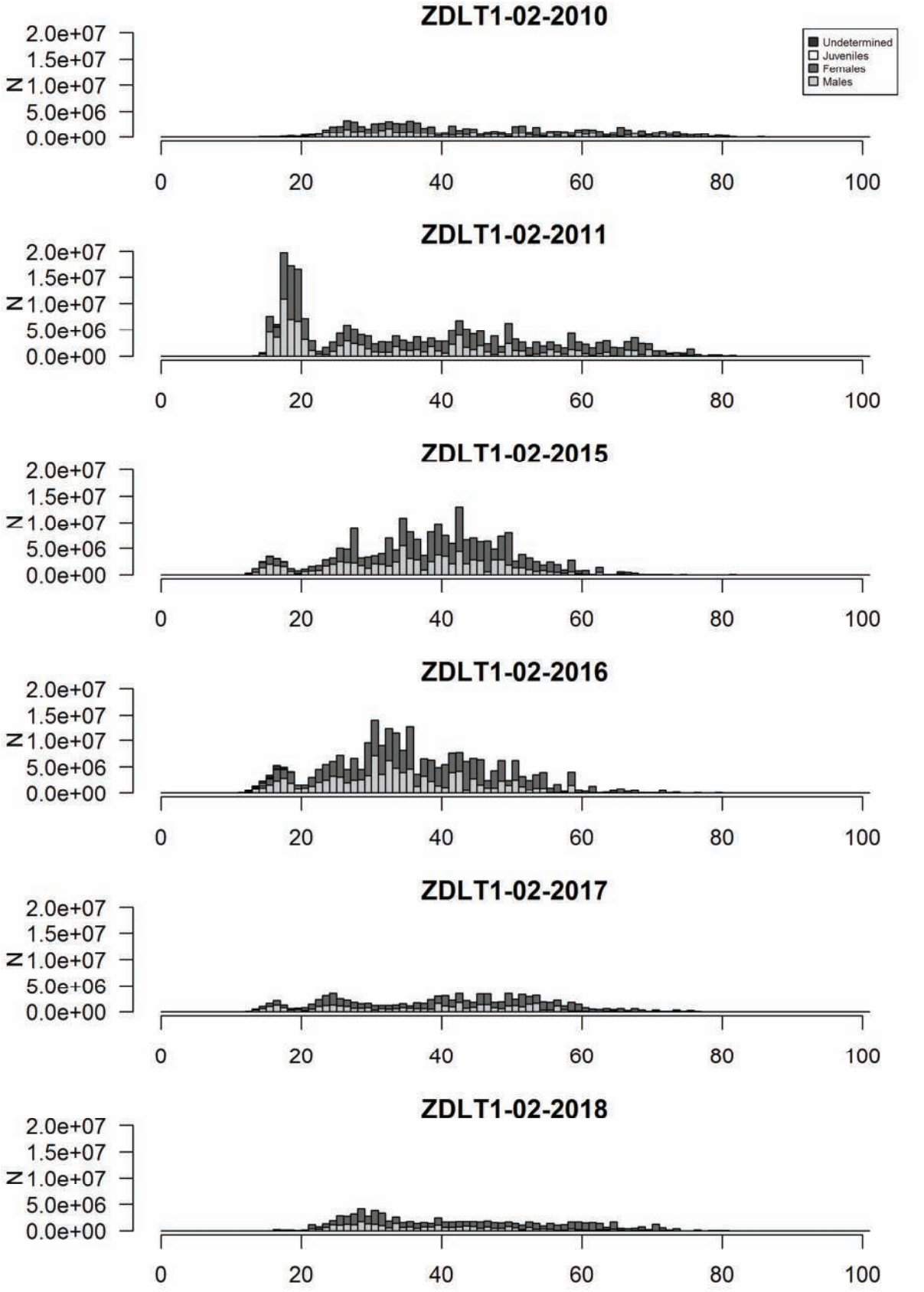

Figure 39: Length frequency histograms of red cod extrapolated to the estimated total biomass for years 2010–2011 and 2015–2018.

3.5.2 Southern blue whiting (Figure 40 and Figure 41)

Southern blue whiting was caught at a limited number of stations. The observed densities ranged from 0.04 kg·km^{-2} to 2,017 kg·km^{-2} (Figure 40B). Observed densities were used to plot a semi–variogram after Box–Cox transformation (λ=0.5) and using 29 distance classes (Figure 40A). The model that best fitted the data was the exponential model without any nugget effect. The variogram was fitted to a maximum distance of 250 km. The model reached the sill (250) at a range of 115 km (Figure 40A). The kriged density ranged from 2 to 1,927 kg·km^{-2}, averaging 103 kg·km^{-2} (Figure 40B). The biomass estimation for 2018 was 12,647 t (Figure 40C). In 2018, unlike in previous years, the survey went to the south in deeper waters where southern blue whiting is most abundant. As a result, the hot spot of that species was found in the southwest of the FICZ Figure 40B). Southern blue whiting biomass decreased from 2010 to 2017 (from 36,512 to 1,974 t) and rebounded in 2016 (39,051 t) (Figure 40C). Over the 2010–2017 the survey area did not cover well the southern blue whiting stock and conclusions about trend in biomass should be interpreted carefully. The abundance of the stock did not follow the same trajectory as the biomass (Figure 40 C) and as shown by the length frequency, the composition of the stock highly varied from year to year (Figure 41). This was probably again the consequence of a survey design that did not cover well the stock prior to 2018.

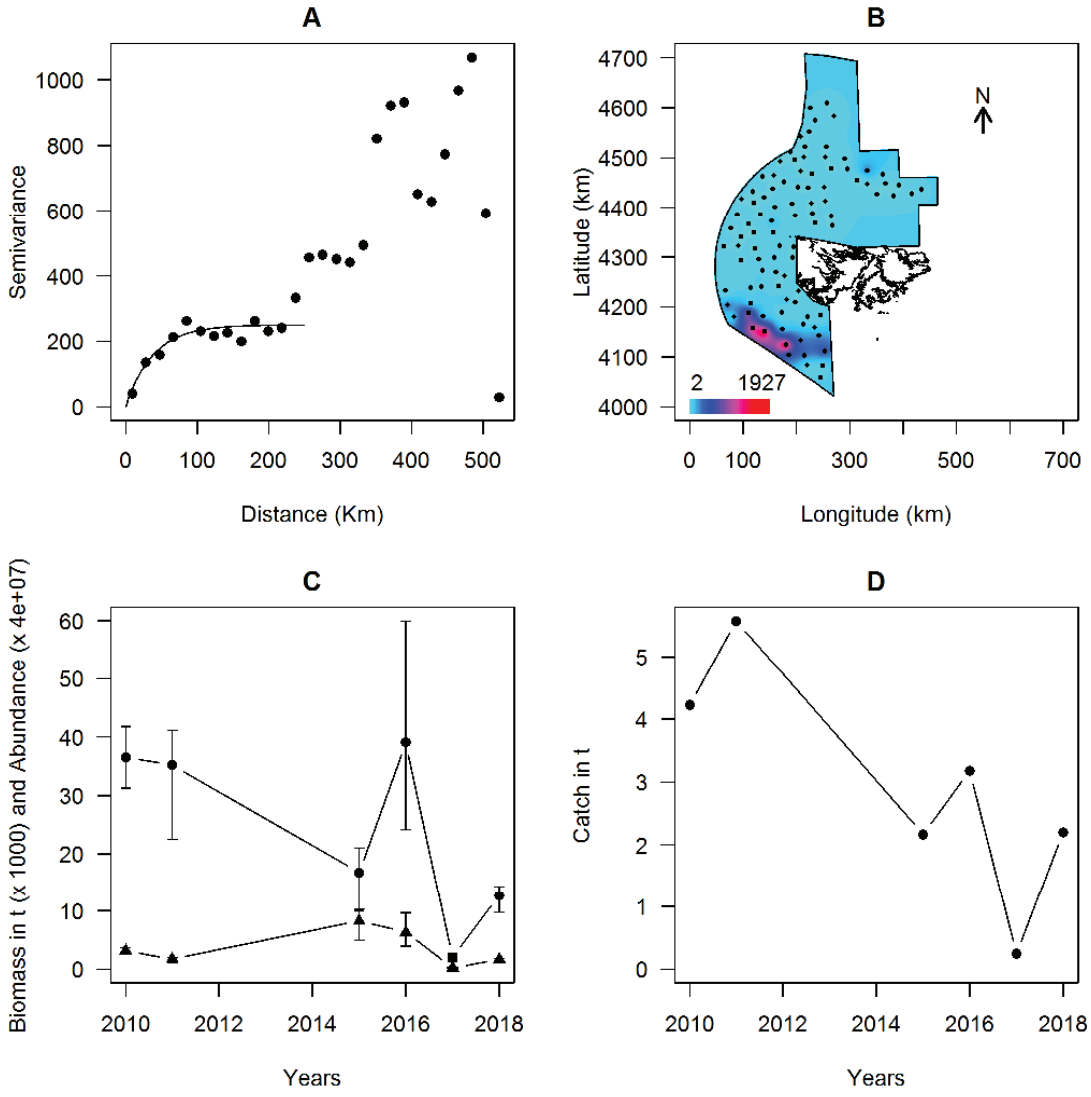

Figure 40: Experimental variogram with exponential model fitted (A), kriged map of southern blue whiting density (B), time series of estimated biomass and numbers of fish (with associated 95% confidence intervals) using the ground fish survey conducted from 2010 (C) and total catch of each survey (D).

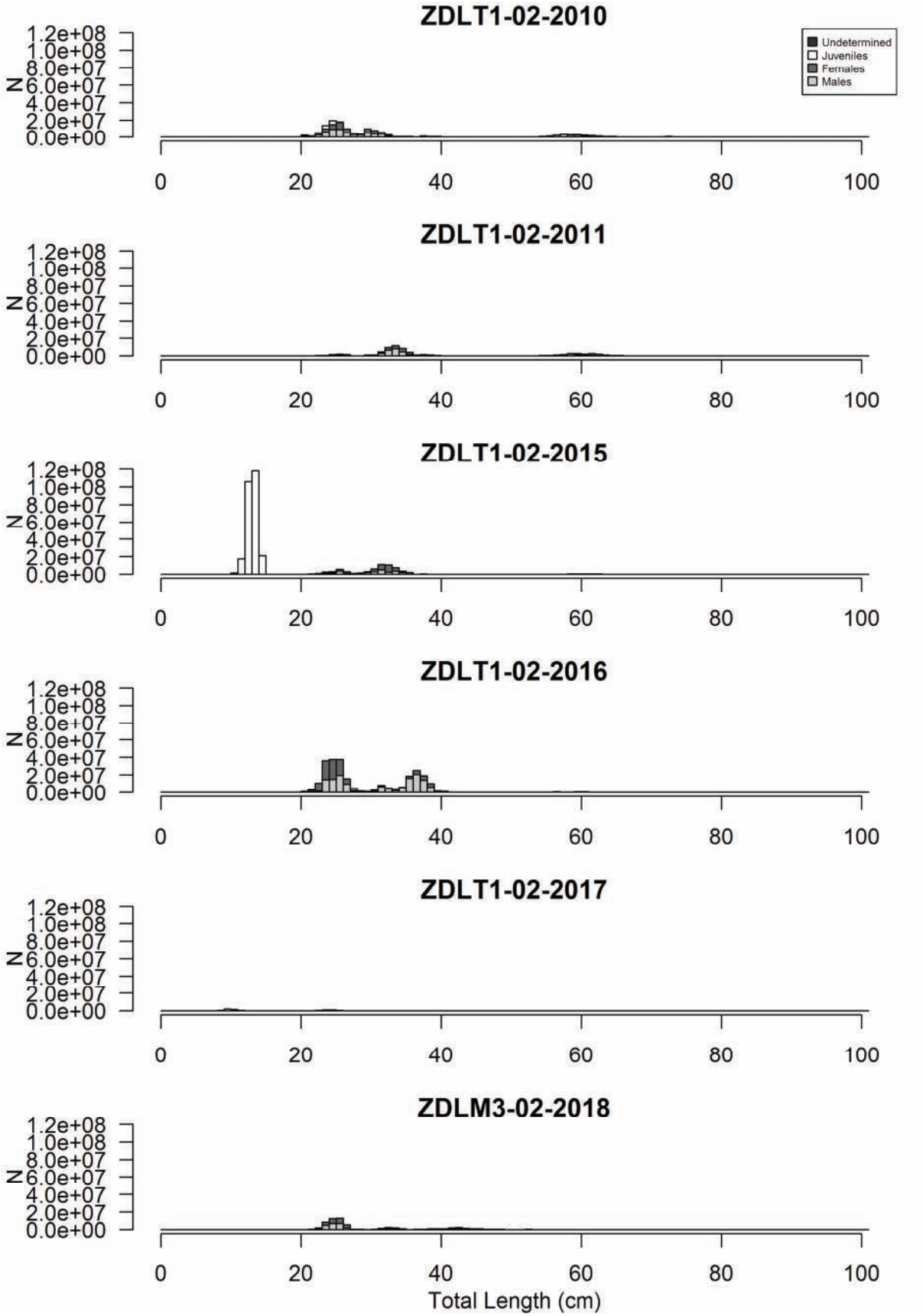

Figure 41: Length frequency histograms of southern blue whiting extrapolated to the estimated total biomass for years 2010–2011 and 2015–2018.

3.5.3 Common Hake (Figure 42 and Figure 43)

Observed densities of common hake ranged from 1.07 kg·km^{-2} to 1.046 t·km^{-2} (Figure 42B) and were Box–Cox transformed (λ=0.5). The semi–variogram was plotted with 33 distance classes and a spherical model with no nugget effect fitted to the observed values (Figure 42A). The model reached the sill (302) at 258 km (Figure 42A). Kriged densities ranged from 1 to 955 kg·km^{-2} and averaged 81.6 kg·km^{-2} (Figure 42B). The estimated biomass was 9,997 t (Figure 42C). Over the years that the ground fish surveys have been conducted, hake biomass first increased from 8,586 t to 20,714 t from 2010 to 2015 (Figure 42C). After reaching its maximum in 2015, the biomass followed a decreasing trajectory until 2018 when it was estimated at 9,996 t (Figure 42C). The lowest biomass was observed in 2016 (4,798 t) (Figure 42C). Even if hake is present in Falkland waters in February, it is not the ideal time to assess this species as this research cruise occurs prior to the period of migration from spawning to feeding grounds, which is suspected to occur around April each year. The abundance of hake roughly followed the same trajectory as the biomass. The length frequency histograms showed a variability of the modal total length of fish (Figure 43). However, this figure does not show a trend in the stock structure as the specimens sampled during the survey were smaller and not representative of the stock.

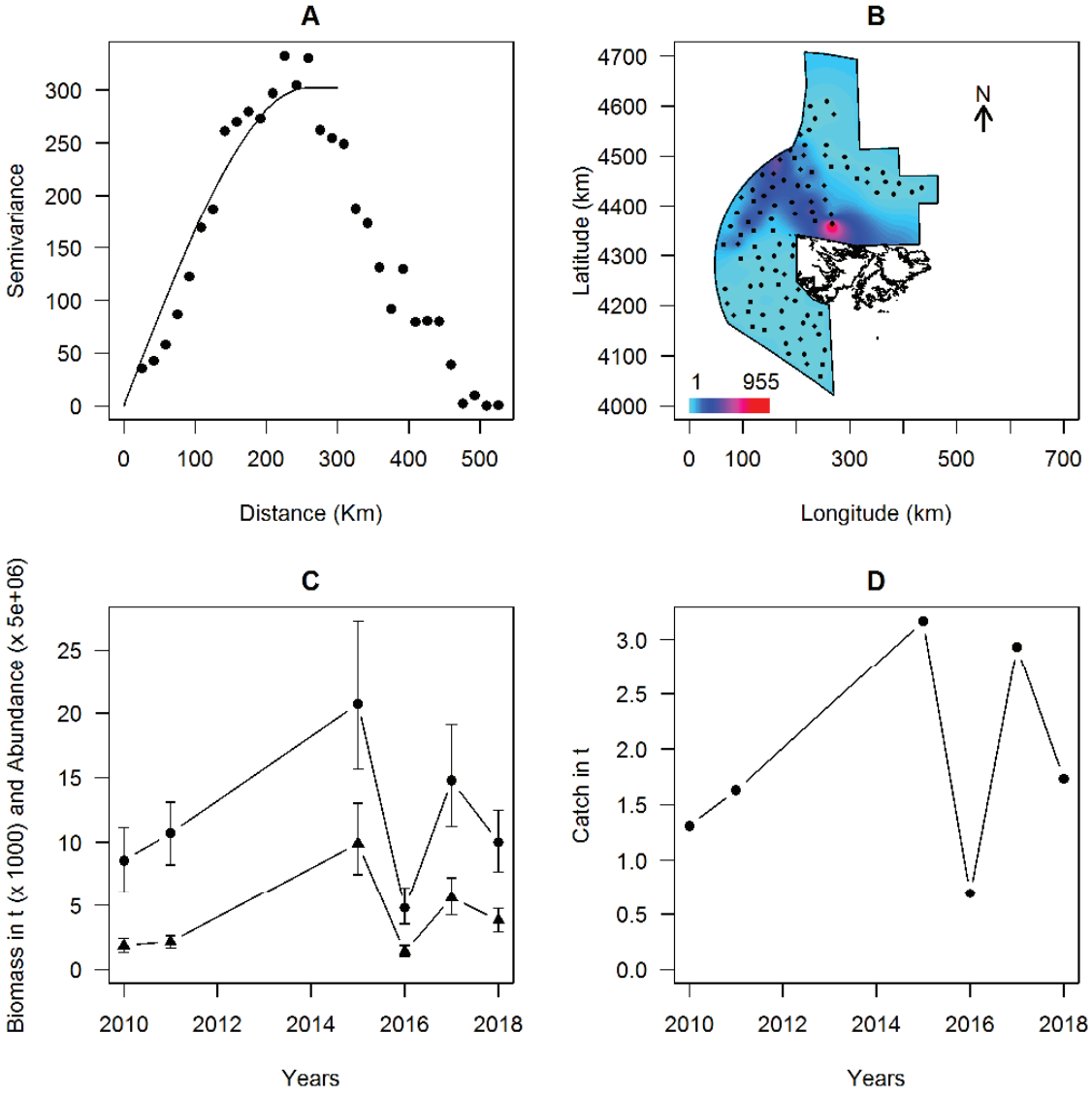

Figure 42: Experimental variogram with spherical model fitted (A), kriged map of red cod density (B), time series of estimated biomass and numbers of fish (with associated 95% confidence intervals) using the ground fish survey conducted from 2010 (C) and total catch of each survey (D).

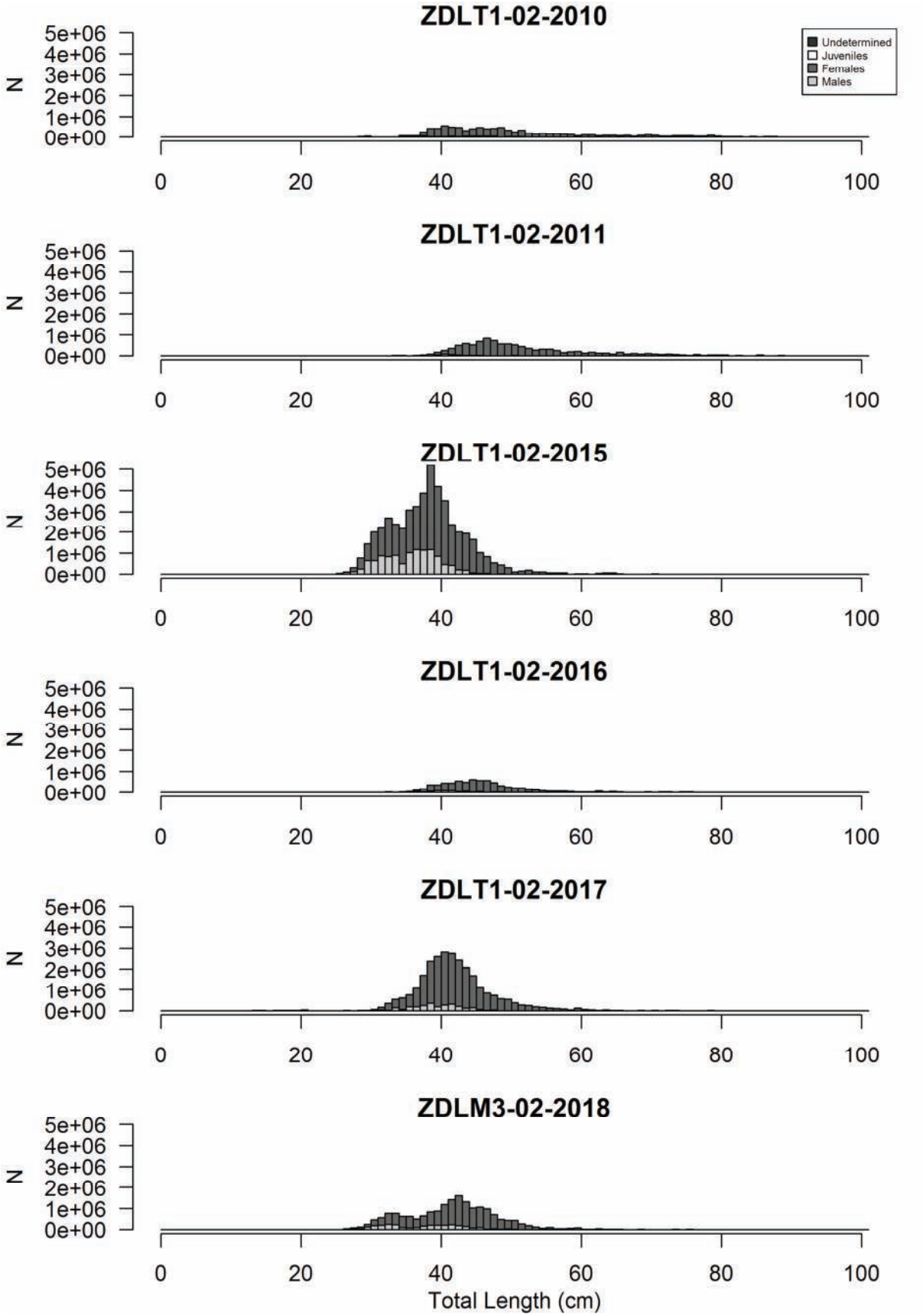

Figure 43: Length frequency histograms of common hake extrapolated to the estimated total biomass for years 2010–2011 and 2015–2017.

3.5.4 Argentine shortfin squid (Figure 44 and Figure 45)

Observed densities of Argentine shortfin squid ranged from 0.09 kg·km^{-2} to 8.7 t·km^{-2} (Figure 44B). The semi–variogram was plotted with 35 distance classes and an exponential model with no nugget effect was fitted (Figure 44A). It reached the sill (1483) at 178 km (Figure 44A). The averaged kriged density was 427 kg·km^{-2} ranging from 8 to 8,191 kg·km^{-2} (Figure 44B). The total estimated biomass was 52,283 t (Figure 44C). In 2018 two areas exhibited higher densities, one to the north (along the border between the FICZ and the FOCZ) and one to the west of West Falkland (Figure 44A). From the temporal perspective, the shortfin squid biomass in Falkland waters was initially estimated at 7,193 t in 2010 and increased to 12,578 t a year later (Figure 44C). In 2015, when the survey was conducted again prior to the record catches, 259,935 t were estimated (Figure 44C). In 2016, the biomass dropped to 295 t (Figure 44C). An increasing trend over the following two years to 16,389 t and 52,283 t was observed (Figure 44C). Such inter–annual variability is common in squid stocks as they have an annual life cycle and the recruitment is highly dependent on environmental conditions. The stock structure (Figure 45) also shows a high inter–annual variability that is again dependent on environmental conditions.

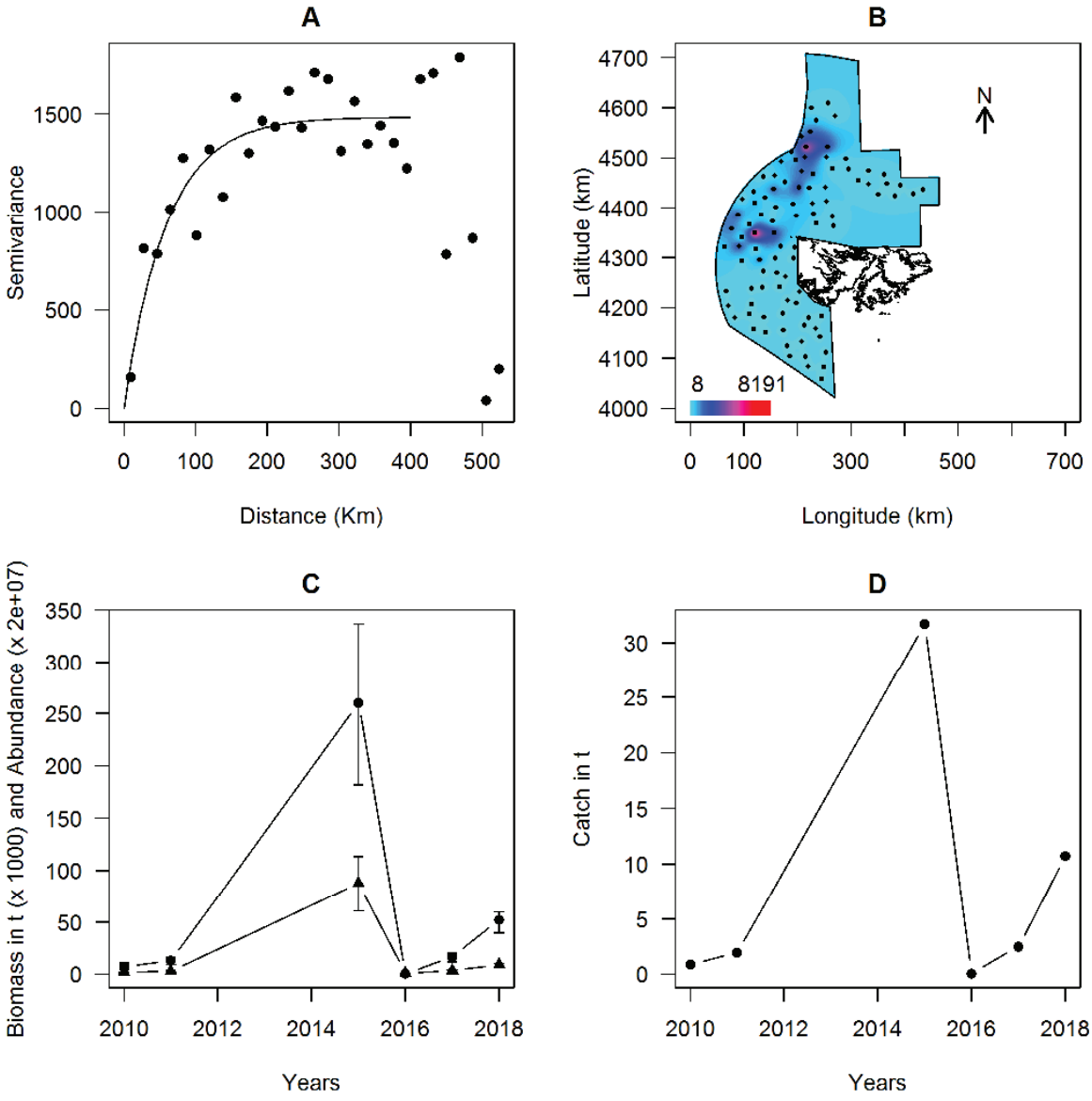

Figure 44: Experimental variogram with spherical model fitted (A), kriged map of common hake density (B) and time series of estimated biomass using the ground fish survey conducted from 2010.

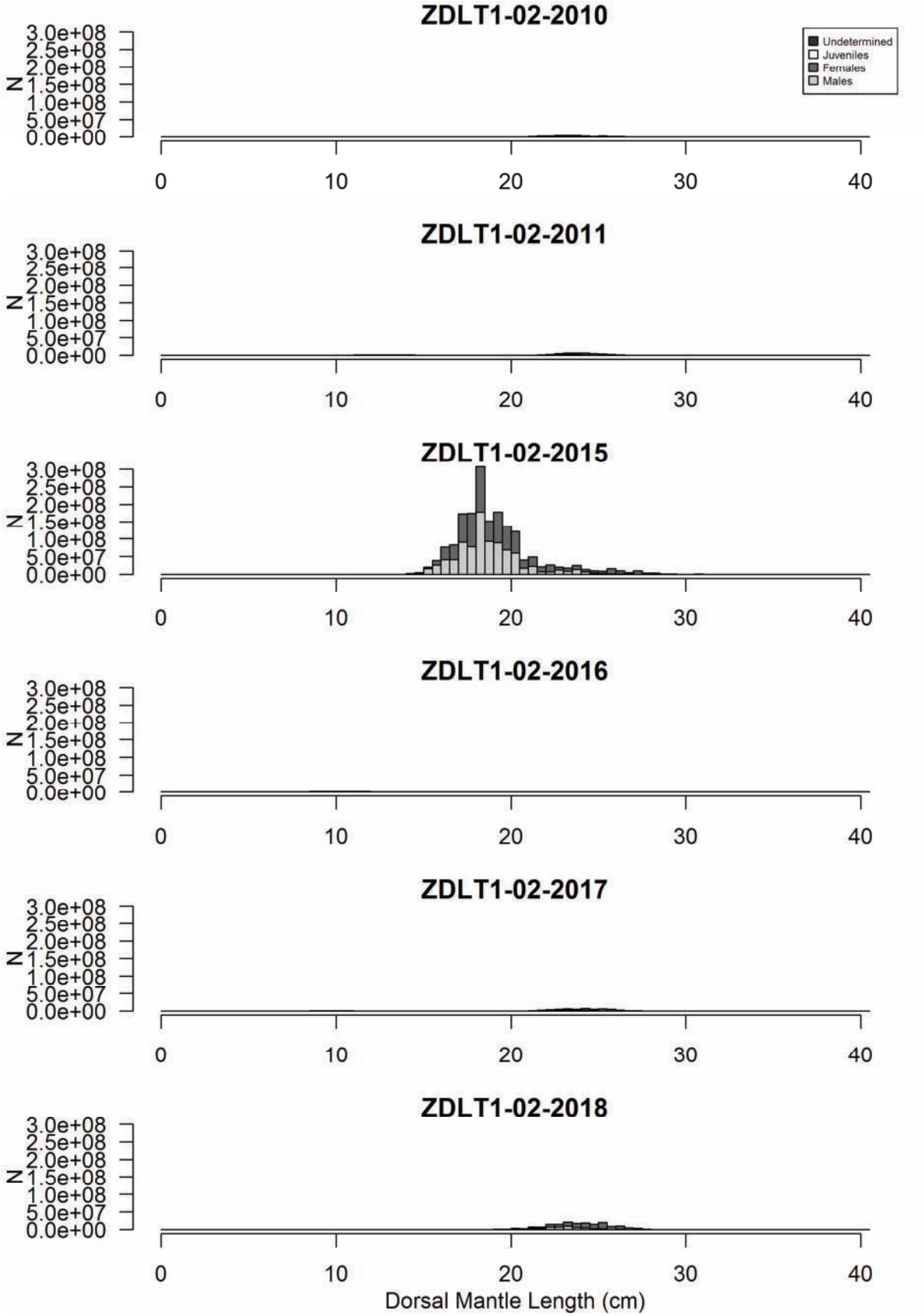

Figure 45: Length frequency histograms of Argentine short–finned squid extrapolated to the estimated total biomass for years 2010–2011 and 2015–2017.

3.5.5 Kingclip (Figure 46 and Figure 47)

Observed densities for kingclip ranged from 2.1–1,667 kg·km^{-2} (Figure 46B). These densities were Box–Cox transformed (λ=0.5) and used to plot a semi–variogram with 32 distance classes (Figure 46A). The best model that fitted the data was exponential with no nugget effect. The model reached the sill (304) at 67 km. The kriged densities ranged from 5 kg·km^{-2} to 1.38 t·km^{-2} and averaged 146 kg·km^{-2}. The biomass estimation was 17,841 t (Figure 46C), a significant decrease compared to 2017 when the biomass was 27,142 t (Figure 46C). Two areas of higher abundances were identified in the finfish zone, one in the north along the limit between the FICZ and FOCZ not far from Argentine waters, the second area was to the west of West Falkland (Figure 46B). From a temporal perspective, kingclip abundance increased by more than two folds from 2010 to 2011 (24,192 t and 55,025 t respectively) (Figure 46C). In 2015, the highest abundance of the series was observed (116,049 t) and the abundances then decreased until February 2018 (Figure 46C). The abundance followed the same trajectory as the biomass from 2010 to 2016 (Figure 46C). However in 2017 and 2018, the biomass decrease was steeper than the abundance (Figure 46C). This is the result of a shift in the length frequency of the stock towards smaller individuals (Figure 47). It is further shown in Figure 47 where the length frequency mode is observed at *c.* 50 cm while it was always >50 cm prior to 2018.

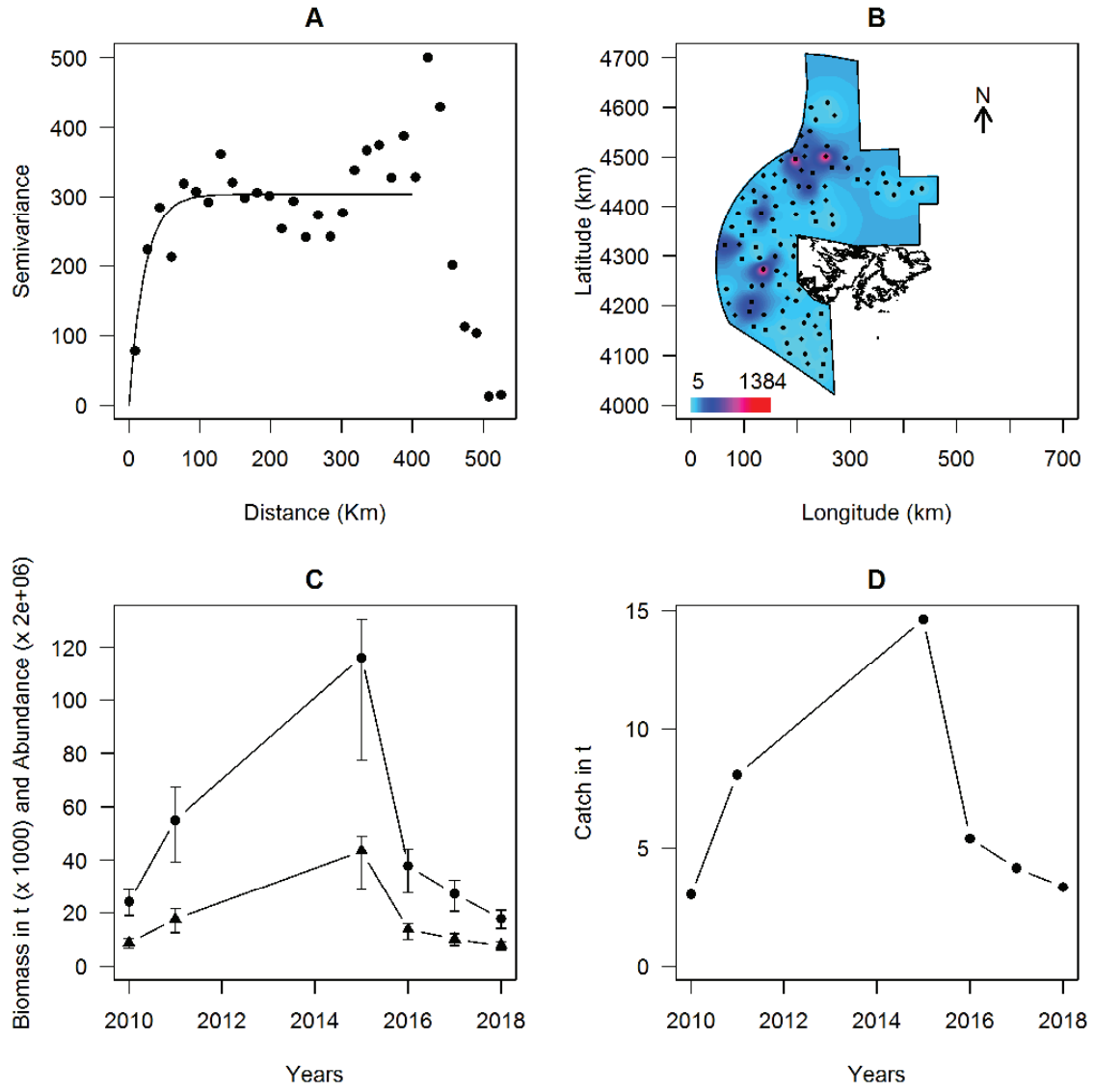

Figure 46: Experimental variogram with spherical model fitted (A), kriged map of kingclip density (B) and time series of estimated biomass using the ground fish survey conducted from 2010.

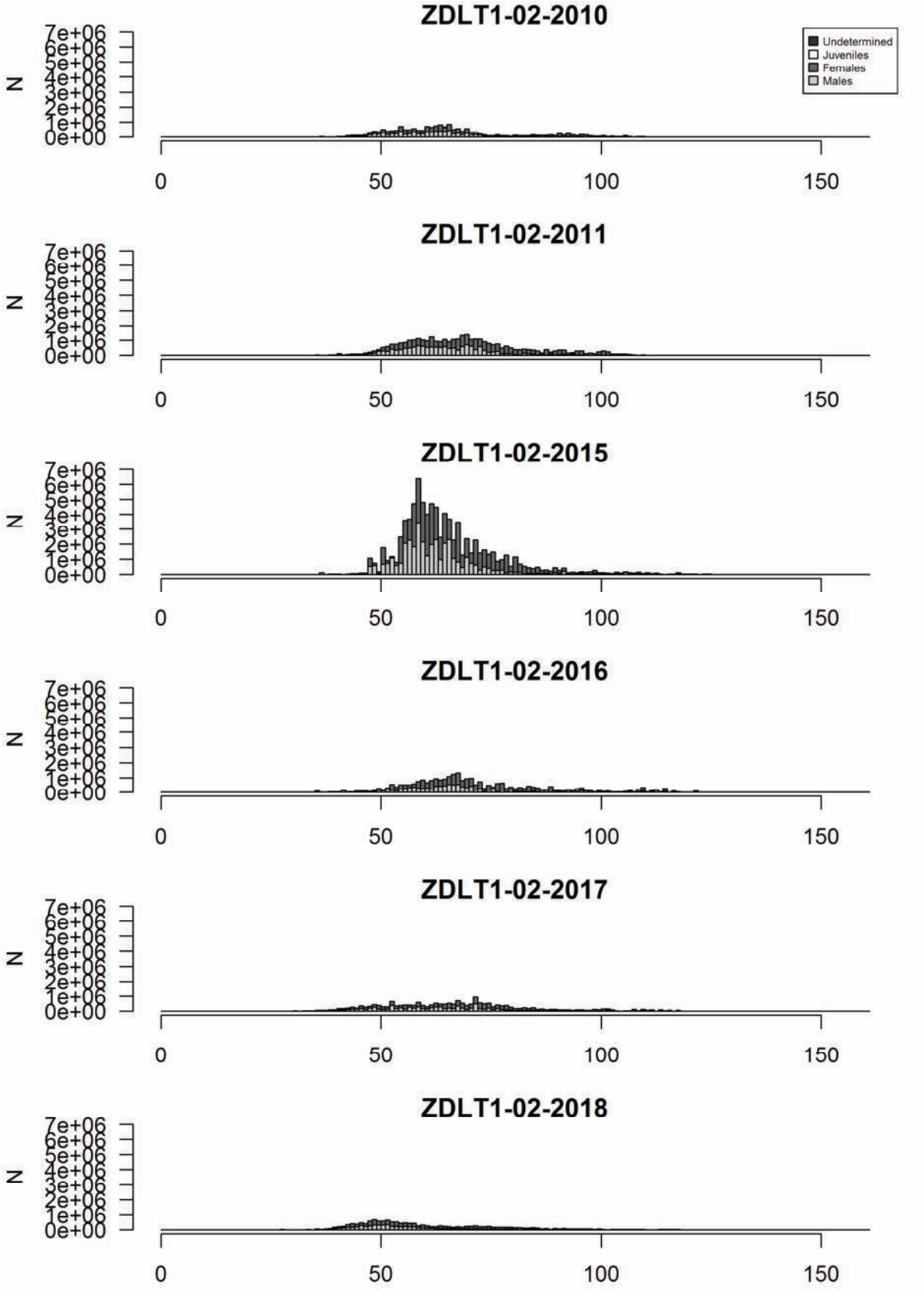

Figure 47: Length frequency histograms of kingclip extrapolated to the estimated total biomass for years 2010–2011 and 2015–2018.

3.5.6 Common rock cod (Figure 48 and Figure 49)

Common rock cod biomass was estimated using density–at–station ranging from 0.56 kg·km^{-2} to 8,753 kg·km^{-2} (Figure 48B). Observed densities were Box–Cox transformed (λ=0.5) and the experimental variogram was plotted with 29 distance classes (Figure 48A). The covariance model that best fitted the data was exponential with no nugget effect, a range of 43 km and reached the sill at 981. The average kriged density was 537 kg·km^{-2} and ranged from 14 kg·km^{-2} to 8.35 t·km^{-2}. Finally, the estimated total biomass on the survey zone was 65,811 t (Figure 48C). Biomass of rock cod first increased from 2010 to 2011, from 752,836 t to 870,932 t, then decreased significantly to 237,168 t in 2015, followed by a non–significant decrease to 230,992 t a year later (Figure 48C). The decreasing trend carried on in 2017 and 2018 to reach 95,242 t and 64,948 t, respectively (Figure 48C). The abundance of rock cod also followed a decreasing trend since 2010 (Figure 48C). However, the decrease was not as extensive as the biomass, which highlights a shift in the length composition of the stock. In 2010 and 2011 the length frequency histograms showed that the stock consisted of fish >15 cm (Figure 49). In 2015 when the survey was repeated after 4 years, the length frequency histogram showed an abundant cohort of pre–recruits with a mode at 14 cm (Figure 49). This cohort appeared again a year later (mode at 19 cm) and disappeared in 2017 (Figure 49). That year a new cohort of pre–recruits was identified (mode at 14 cm too) (Figure 49). However, in 2018, this cohort was not seen and neither was the pre–recruit cohort (Figure 49).

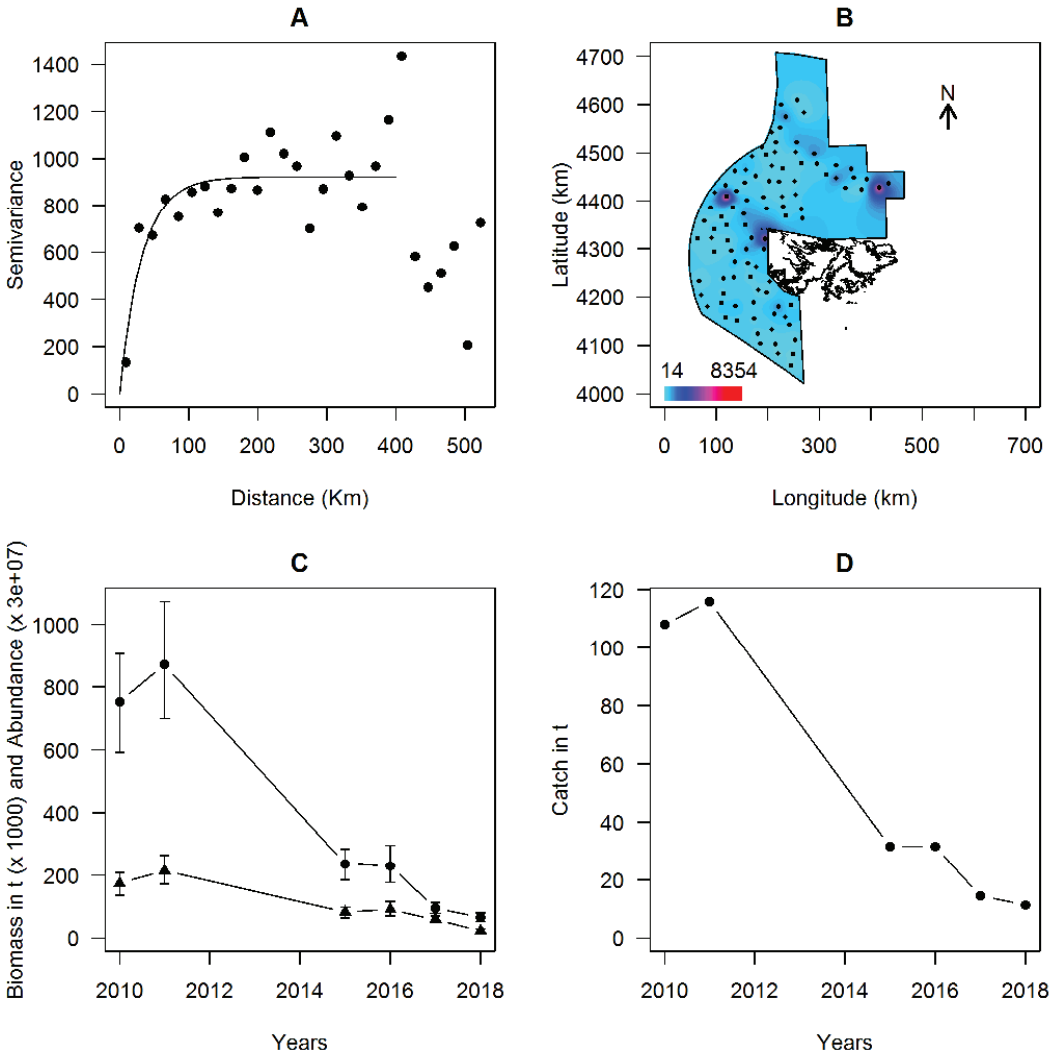

Figure 48: Experimental variogram with exponential model fitted (A), kriged map of common rock cod density in kg·km^{-2} (B), time series of estimated biomass and abundance (with associated 95% confidence intervals) using the ground fish February surveys conducted from 2010 to 2018 (C) and total catch of each ground fish survey (D).

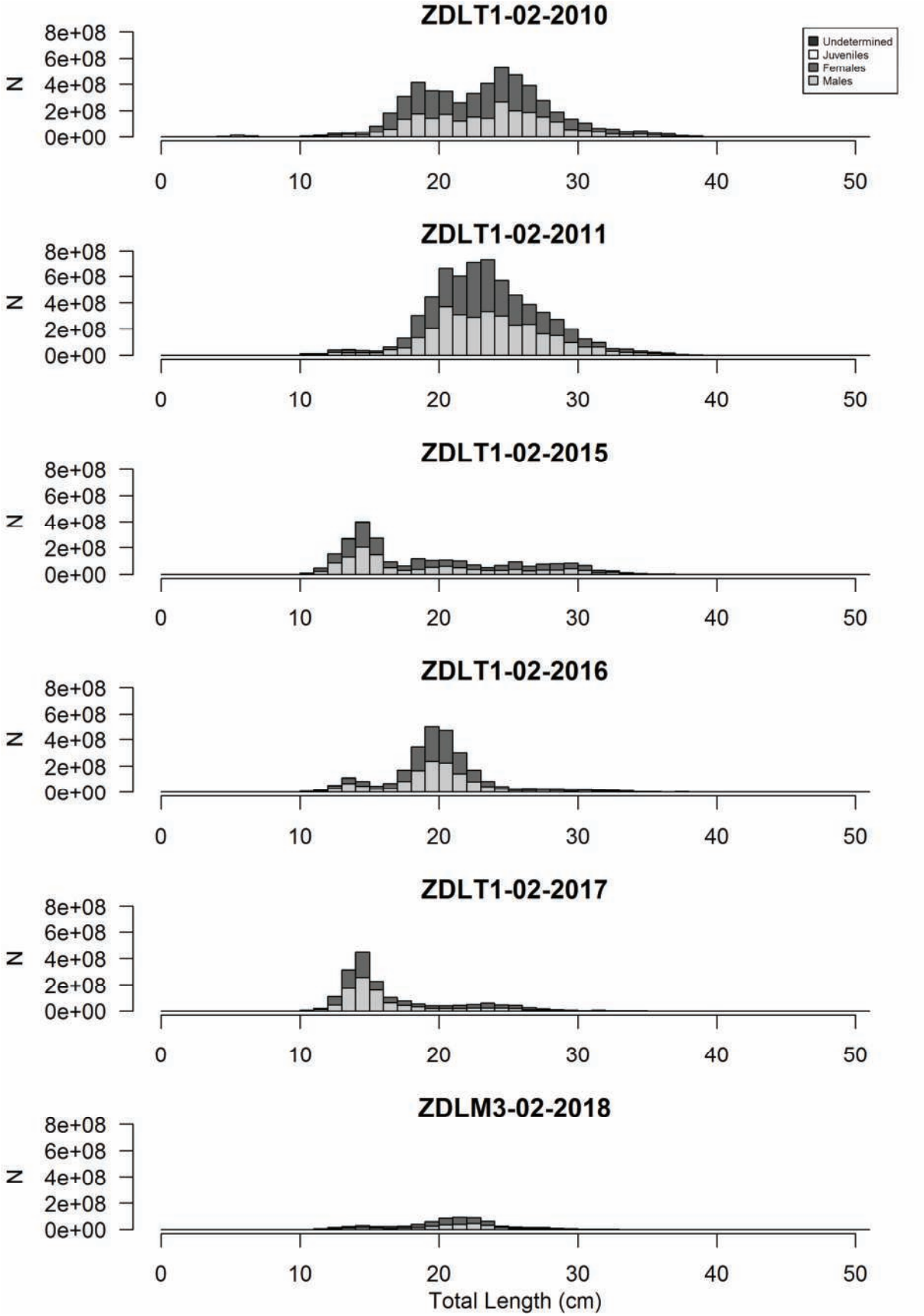

Figure 49: Length frequency histograms of common rock cod extrapolated to the estimated total biomass for years 2010–2011 and 2015–2018.

3.5.7 Toothfish (Figure 50 and Figure 51)

Toothfish observed densities ranged from 1. 71–902 kg·km^{-2} (Figure 50B) and were Box–Cox transformed (λ=0.5) prior to using them to plot a semi–variogram with 31 distance classes (Figure 50A). The best model that fitted the data was exponential with no nugget effect. It reached the sill (150) at 158 km (Figure 50A). Using this variogram model, the kriged density averaged 69.8 kg·km^{-2} ranging from 1 to 791 kg·km^{-2} (Figure 50B). The total biomass was estimated to be 8,551 t (Figure 50C). Higher biomasses of toothfish appeared in three different areas. The first one was inshore to the south of the Jason Islands (Figure 50B), an area where young toothfish has been observed over the years. Two other areas were also sampled, one along the 200 m isobath and another in the west next to the western FICZ border (Figure 50B). At these deeper stations, larger toothfish were sampled. Biomass as well as abundance decreased from 2010 to 2015 when the minimum of each variable was reached (Figure 50C). From 2015 to 2018, both indices increased (Figure 50C). The increase observed in 2018 could also be the result of the addition of 20 stations in the south of the survey area. These stations enabled data collection of deeper areas where toothfish are older. On the length frequency histogram on Figure 51 two to three cohorts can be identified depending on the year. It seems that in 2010 larger specimens were more abundant than in 2011, 2015–2017 (Figure 51).

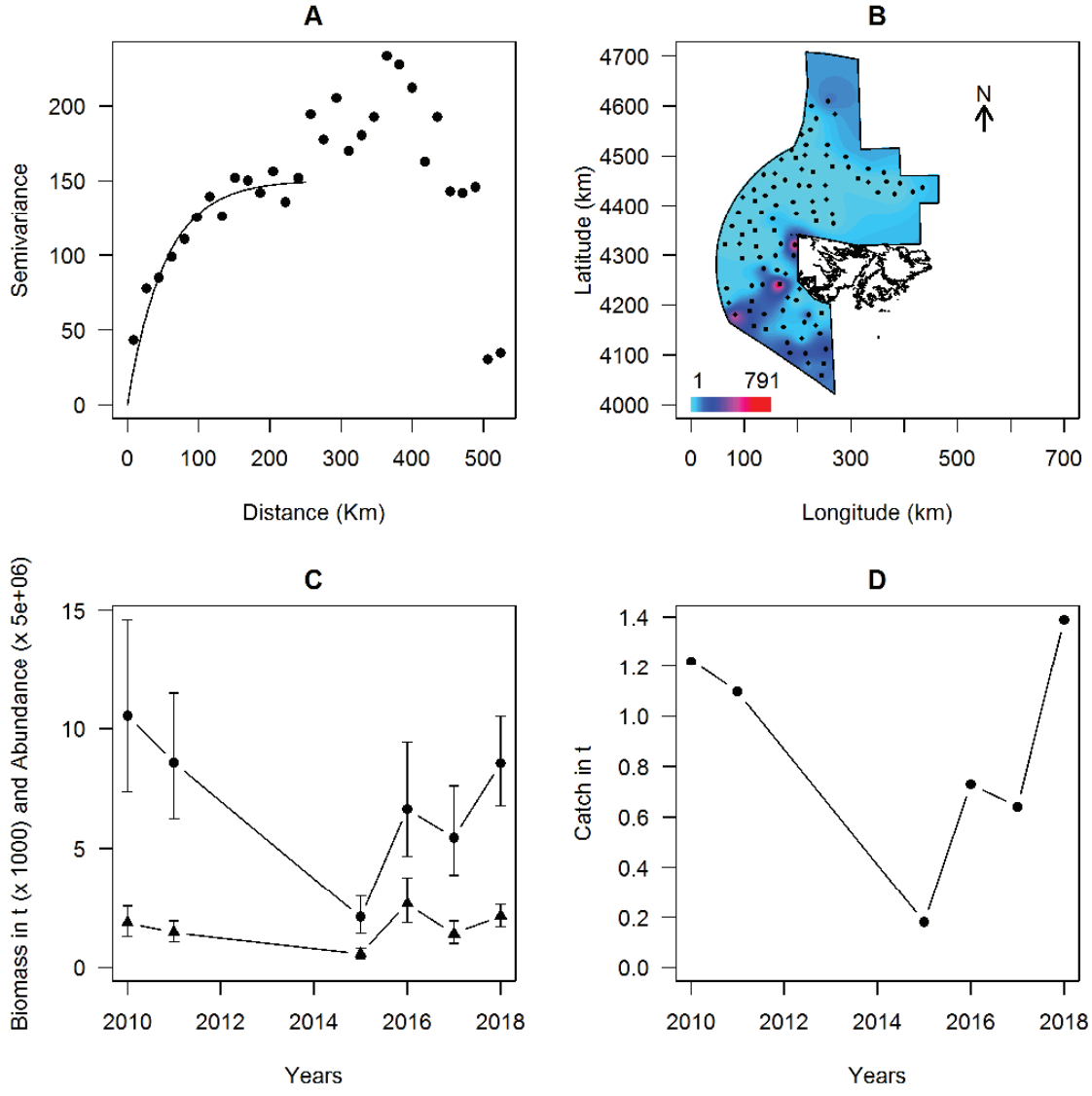

Figure 50: Experimental variogram with spherical model fitted (A), kriged map of toothfish density (B) and time series of estimated biomass using the ground fish survey conducted from 2010.

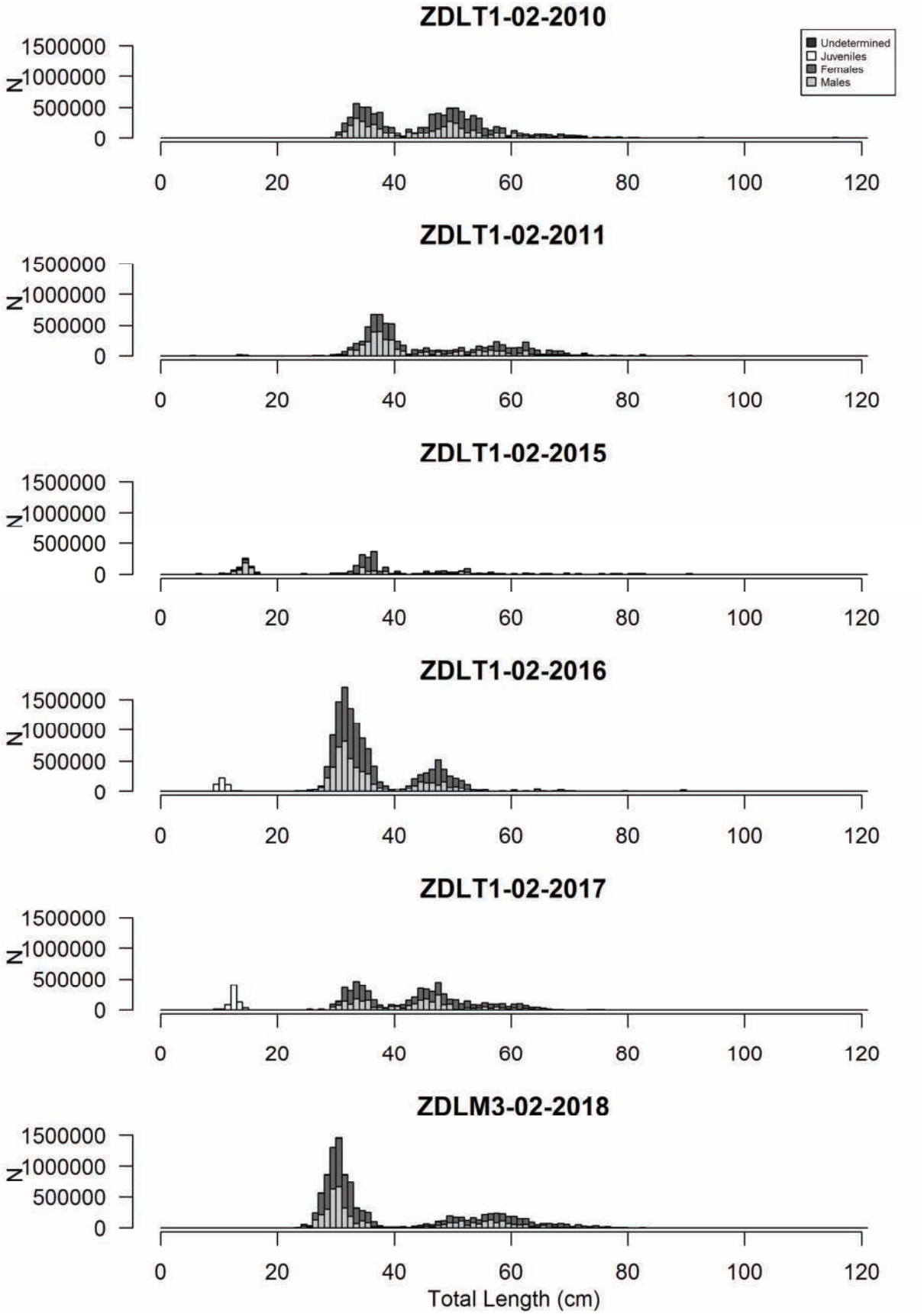

Figure 51: Length frequency histograms of toothfish extrapolated to the estimated total biomass for years 2010–2011 and 2015–2017.

3.5.8 Hoki (Figure 52 and Figure 53)

Hoki densities varied from 1 kg·km^{-2} to 21.2 t·km^{-2} (Figure 52B). After Box–Cox transformation with λ=0.5, a semi–variogram was plotted with 29 distance classes and the best model that fitted the data was exponential with no nugget effect (Figure 52A). The sill (4593) was reached at a distance of 196 km (Figure 52A). Taking into account the auto–correlation, the estimated kriged density averaged 1,333 kg·km^{-2} (ranging from 26 to 20,325 kg·km^{-2}) (Figure 52B). The total biomass accross the survey area was 163,263 t (Figure 52C). Most of the hoki was observed in the southwest of the survey zone in deep waters (>200 m) where hoki is usually abundant, especially along the limit between the FICZ and Argentine waters (Figure 52B). Biomass and abundance of hoki decreased from 296,890 t to 24,944 t over the period 2010–2017 (Figure 52C). In 2018, an increase of the biomass and the abundance was observed to 163,262 t (Figure 52C). As in the case of toothfish and southern blue whiting the 20 new stations added to the 2018 survey brought information from areas that were surveyed prior to 2017 and where hoki is abundant. The structure of the stock described by Figure 53 highlights a decrease in abundance of old animals that were observed in 2010 and 2015 at 25–30 cm pre–anal length (Figure 53). The majority of the stock now consists of specimens <20 cm (Figure 53).

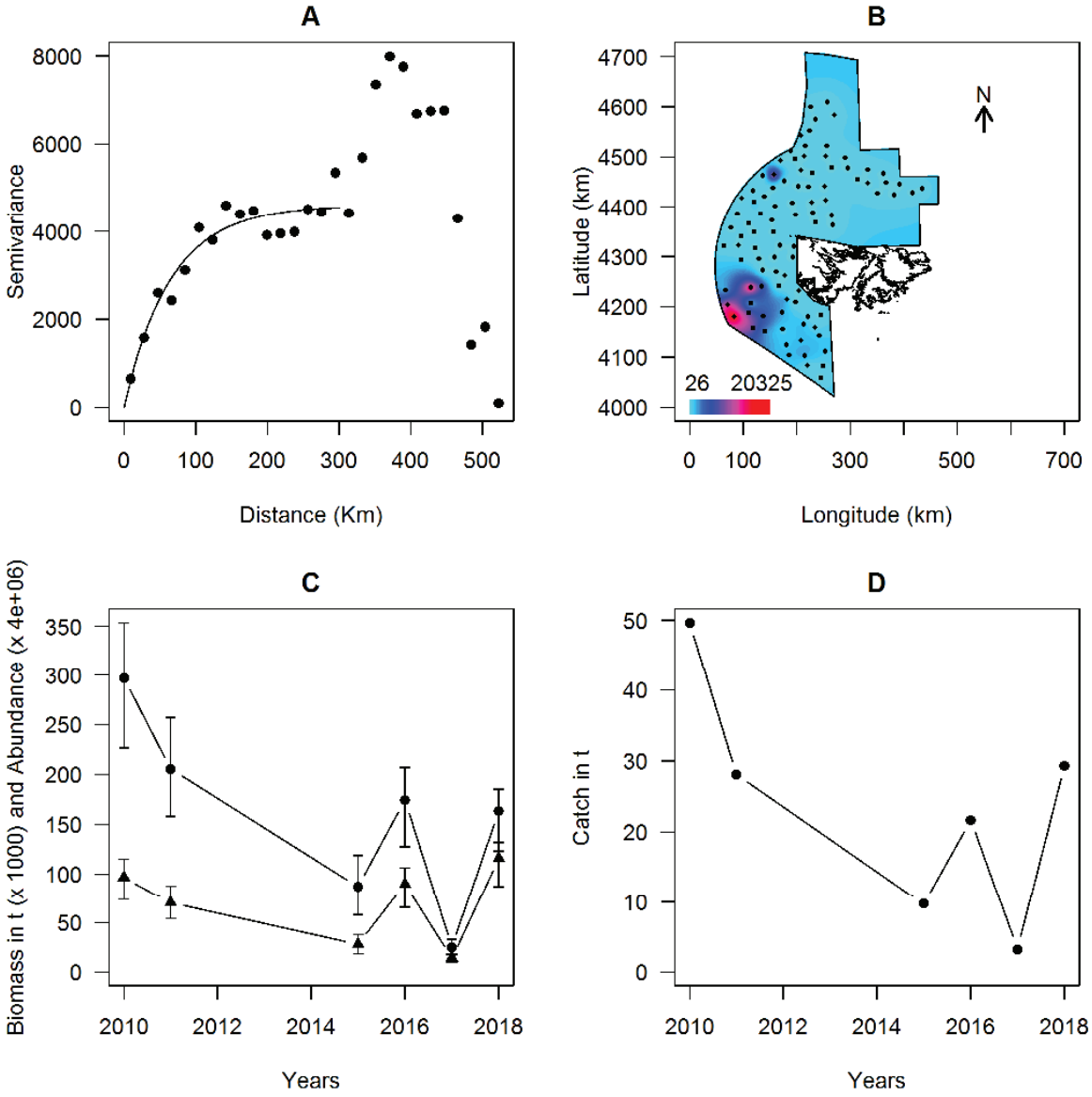

Figure 52: Experimental variogram with spherical model fitted (A), kriged map of hoki density (B) and time series of estimated biomass using the ground fish survey conducted from 2010.

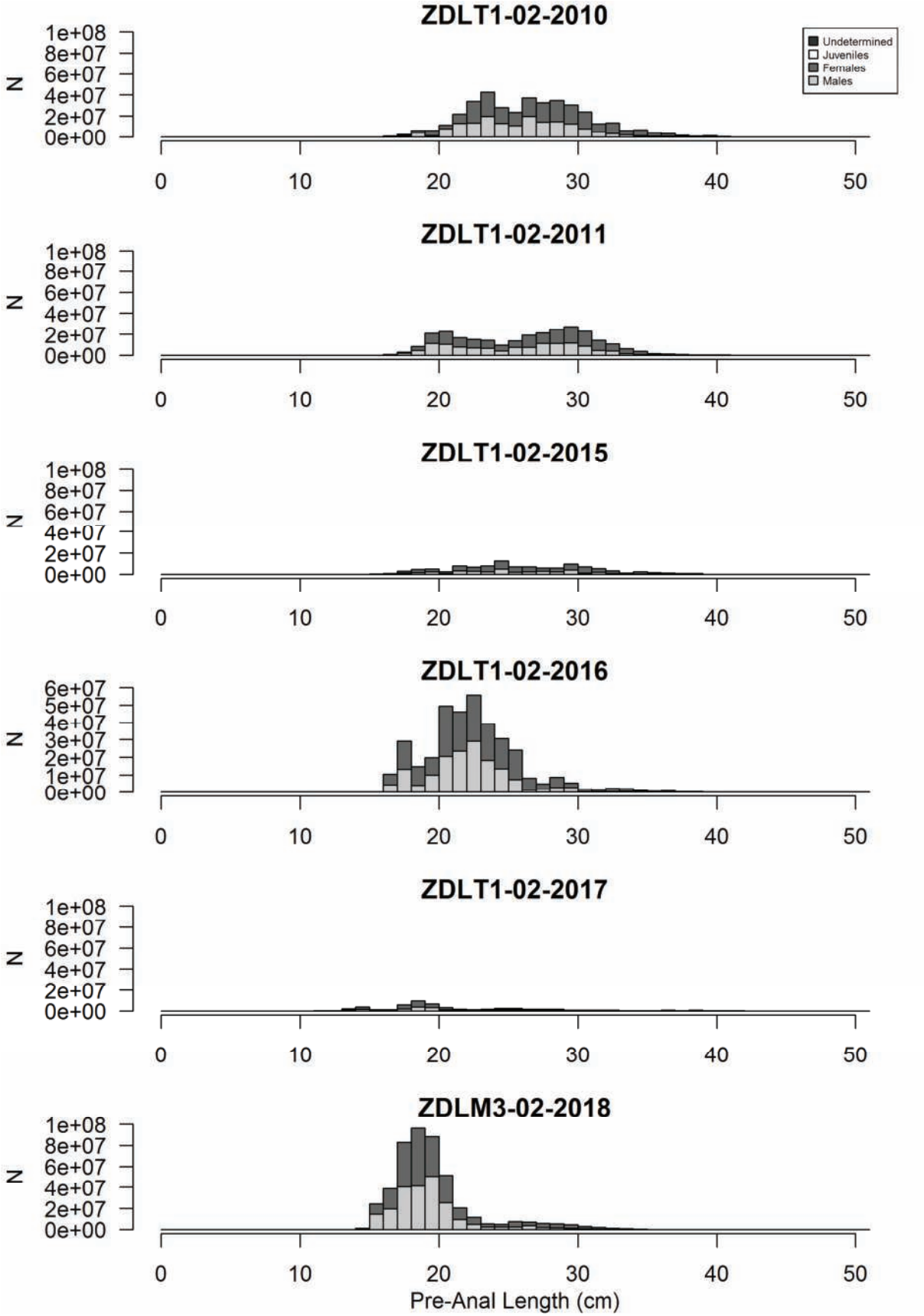

Figure 53: Length frequency histograms of hoki extrapolated to the estimated total biomass for years 2010–2011 and 2015–2018.

3.6 Oceanography

Oceanographic data were collected at 101 stations. The area covered ranged from 48° 37.9'S to 53° 34.4'S and 57° 52.7'W to 63° 17.8'W. Good data were collected at all bar one station, all the down-casts at these stations were good, and so up-cast data were removed.
Figure 54 below shows the location of the stations.

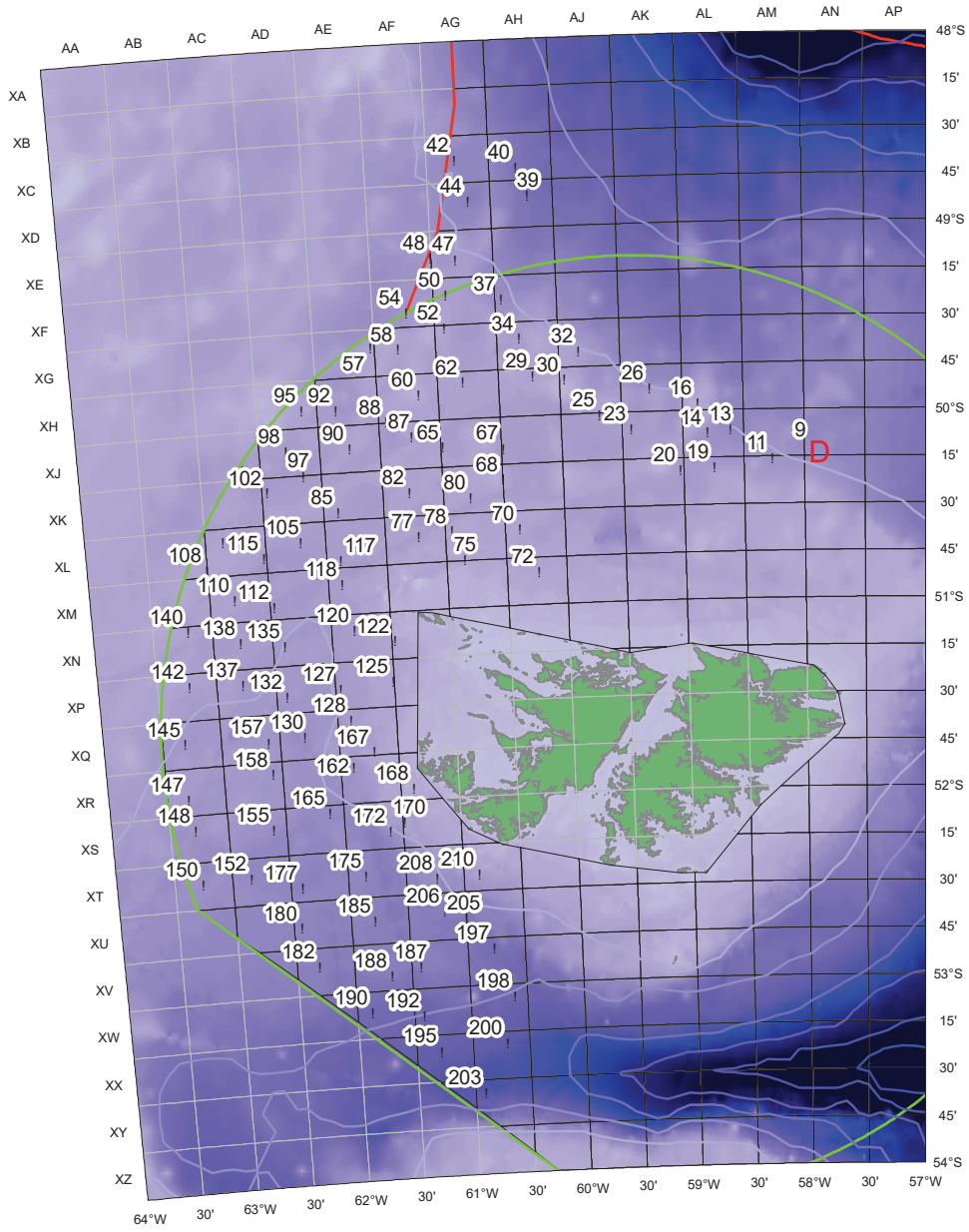

Figure 54 Location and number of CTD stations

Figure 55, Figure 56 Figure 57 show the temperature, salinity and σ-t density, respectively, gridded using ODV4 DIVA[1] gridding algorithm, at depths of 10, 50, 100 m and the seabed. The first layer at 10m is the shallowest depth common to all CTD casts. The surveyed area covered depths ranging from 117 to 697 m; with the extension of the survey to the south west, data acquisition extends to deeper waters relative to previous cruises.

The temperature data (in Figure 55) show 2 patterns. The first shows a warm water mass at the surface along the edge of the shelf with a cooler water mass pushing north from the south-

[1] DIVA is a gridding software developed at the University of Liege (http://modb.oce.ulg.ac.be/projects/1/diva)

west. The second is apparent as depth increases, showing considerable mixing at 50 m, 100 m, and at the seabed where the western branch of the Falklands Current pushes north to meet with the return of the eastern branch of the Falklands Current. This pattern is also repeated in the salinity maps (Figure 56, Figure 57).

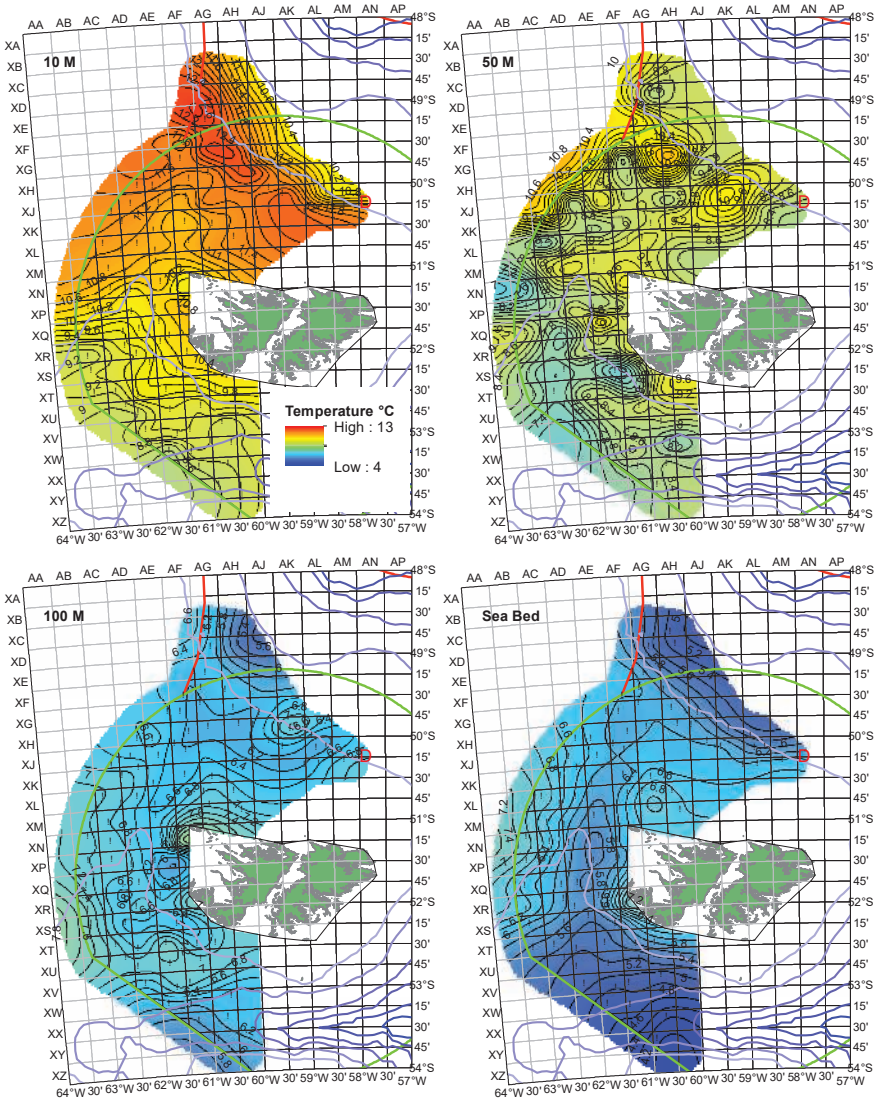

Figure 55. Temperatures at 10m, 50m, 100m, and the seabed (contours at 0.25°C).

Figure 58 shows the change in temperature from 2018, relative to 2015, 2016, and 2017 (reds indicating warmer, whereas blues representing cooler temperatures, respectively). The comparison has been undertaken only in areas where the 2018 survey overlapped previous surveys, thus exclude the south west of the zone. At the surface, waters were generally warmer in 2018 than in 2015 and 2016, whilst they were cooler in 2018 than in 2017, especially to the north and considerably cooler in the north-east. At the seabed the water was generally warmer in 2018 relative to all three years, with only areas of the seabed close to the eastern branch of the Falklands Current being slightly cooler in 2018.

Figure 56 shows the salinity over the surveyed area. At the surface, the salinity is relatively stable between 33.6 and 33.8 PSU. As depth increases there is a greater variation, with significant differences nearer the seabed. At the seabed salinity is greater in water masses closest to the two branches of the Falklands Current. The water mass to the north east along the shelf and in the Trough to the south west show measured salinities greater than 34.1 PSU.

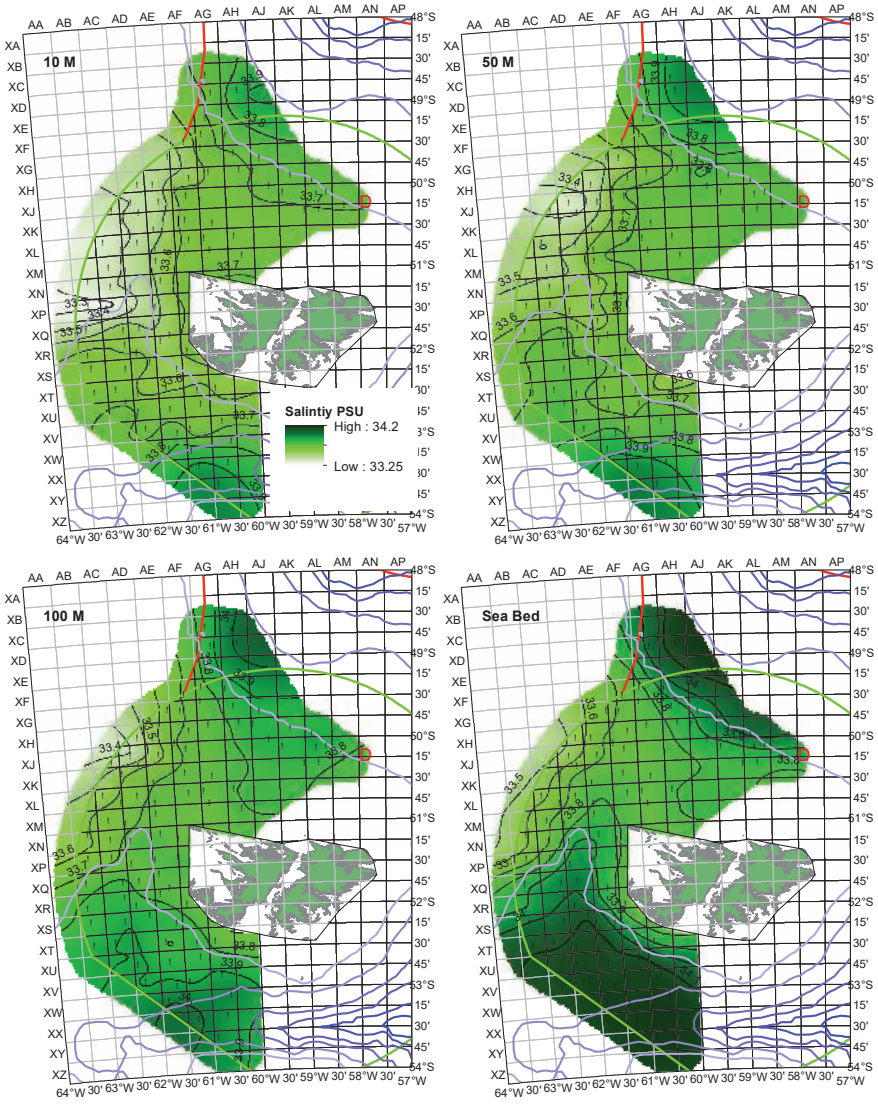

Figure 56. Salinities at 10m, 50m, 100m, and the seabed (contours at 0.05 PSU).

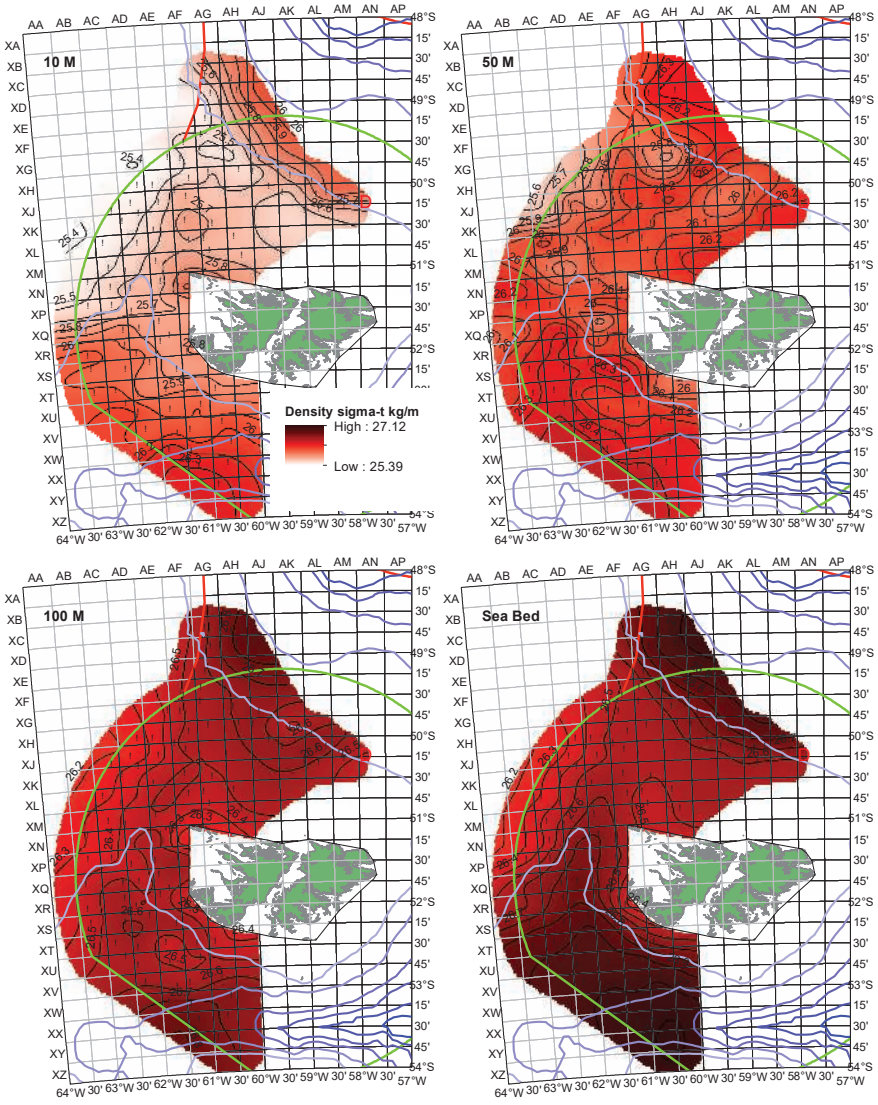

Figure 57. Density at 10m, 50m, 100m, and the seabed (contours at 0.05 sigma-t).

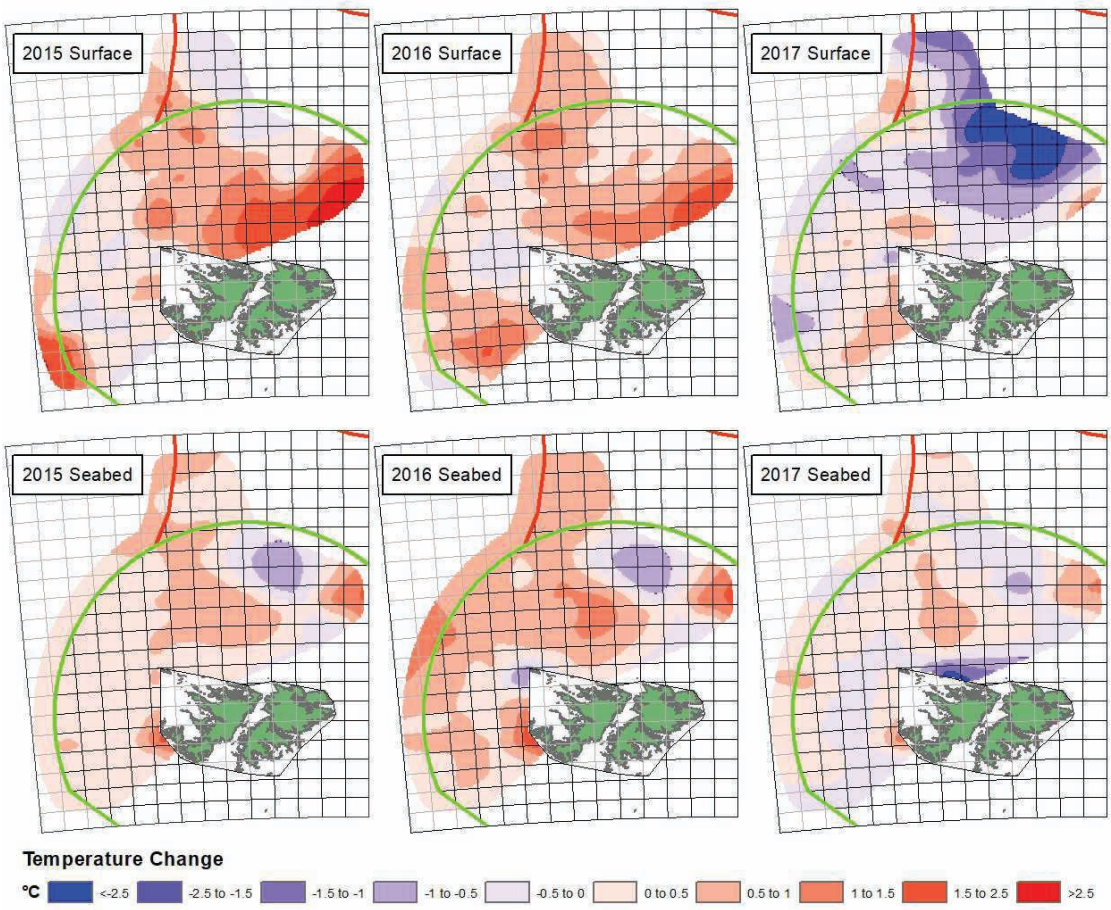

Figure 58. Temperature differences, 2018 relative to 2015, 2016, and 2017 at 10 m and the seabed.

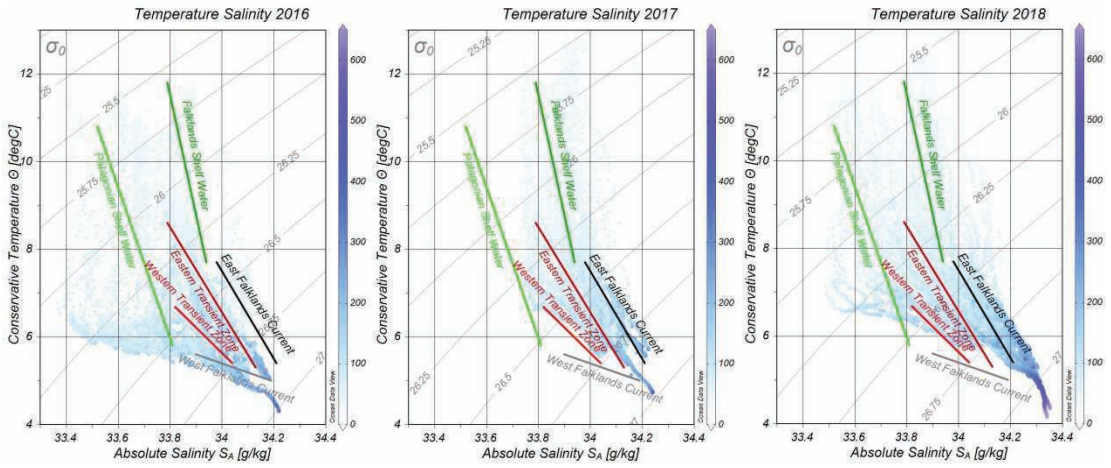

Figure 59. Temperature-Salinity plots, 2016 data on the left, 2017 in the center, and 2018 on the right (water mass terminology from Arkhipkin et al., 2013)

A plot of conservative temperature against absolute salinity is shown in Figure 59 comparing 2018 to the surveys undertaken in February 2016 and 2017. Whilst the salinity range was limited in 2017, the 2018 data show a slight increase in the temperature recorded at the different salinities. Also, the survey indicates that the Falklands Current occurs at greater depths in 2018 relative to previous years as seen in the data in the lower right of the 2018 scatter plot.

The density map, Figure 57, shows lowest density water at 10 metres over the shelf, reflecting higher temperatures and lower salinities (seen in Figure 55 and Figure 56, respectively). At 50 m there is more mixing with the denser water from the West Branch of the Falklands Current moving north and mixing with Falklands Shelf water. At 100 m the denser west Falkland Current can be seen moving north and meeting the eastern branch of the Falklands Current. There is only a weak counter clock-wise gyre over the shelf to the north of the Islands (inferred from the interpolated values). In the seabed layer away from the Falklands, there is a greater density water mass pushing from the south west up the west of the Falklands to join the eastern branch of the Falklands Current. The density is slightly lower to the north of the Falklands in the vicinity of XKAG/XLAH and significantly less dense to the east of the Current.

Figure 60 shows the oxygen concentrations at 10, 50, 100 m, and at the seabed in ml/L of water. Oxygen concentration is greatest at the surface, with levels of 6.0 to 6.5 ml/L over the majority of the survey area. Subsurface oxygen concentration is highest at each depth interval over the west branch of the Falklands Current. This greater oxygenated water pushes to the north of the Falklands. The eastern branch of the Falklands Current does not show greater levels of oxygenation.

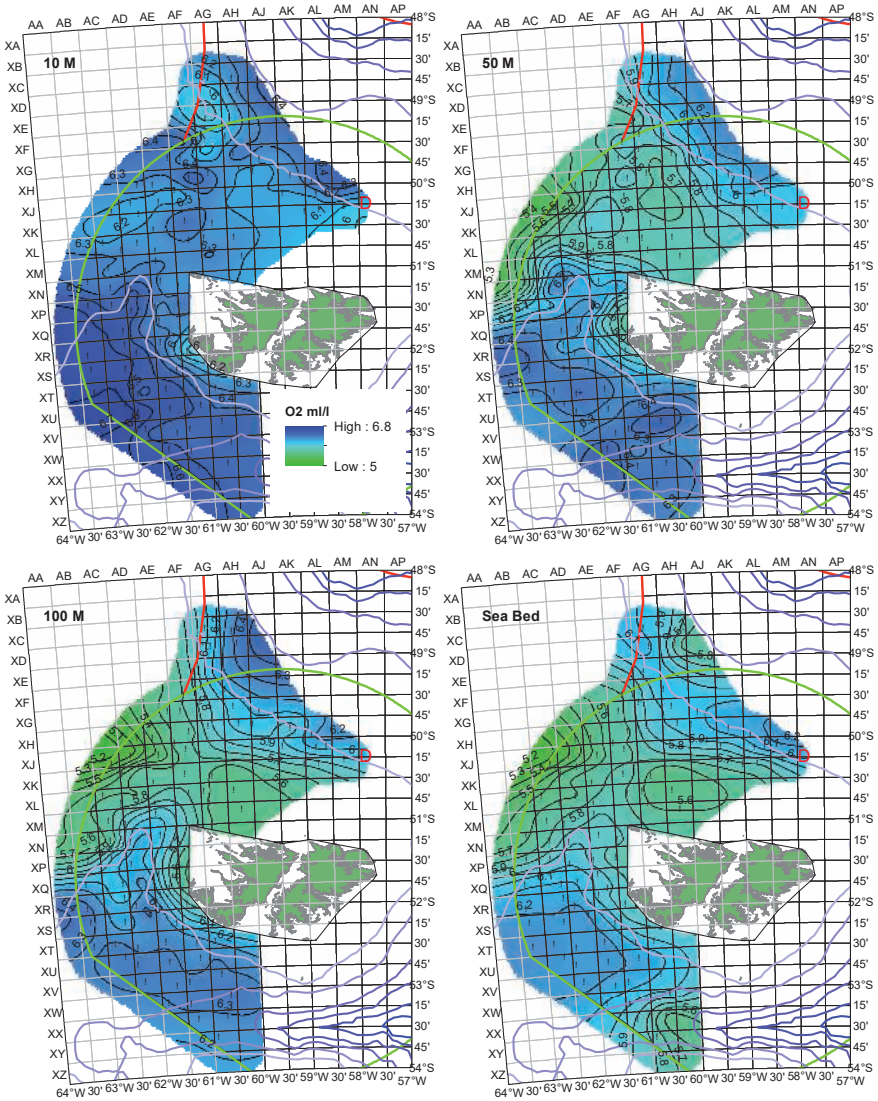

Figure 60. Oxygen concentrations at 10m, 50m, 100m, and 200m (contours at 0.1ml/L).

4.0 Discussion

The February ground fish survey has been conducted for the sixth time since 2010, every time concurrently with the first season *Loligo* pre–recruitment survey. Since 2011, the same stations were repeated to ease comparisons between years. To improve the data collection towards the implementation of an ecosystem–based framework for fisheries management in the Falkland Islands, the survey was extended 23 stations to the south of the finfish zone, thus increasing the number of stations from 89 to 102 (10 stations were removed in the north of the *Loligo* box as this area is already covered by the *Loligo* pre–recruitment survey). The southward expansion of the survey enabled collecting data that was not feasible with the survey design used until 2017 (inclusively). Southern blue whiting, hoki, toothfish, and skates were better covered in the 2018 survey than by previous ones. In 2018, hot spots for southern blue whiting and hoki were identified to the south of the southern limit of the previous survey area. Furthermore, data were collected for the first time during this survey on grenadier–ridge scaled rattail (GRC), a species that was targeted by some bottom trawlers over the last three years especially in late-spring and early-summer and whose distribution consists of waters deeper than 400 m to the north and south of the finfish area.

Rock cod biomass decreased over the years 2011–2017 (Figure 48C). In 2018 a further decrease (30%) was observed relative to 2017 (Figure 48C). A decrease in abundance was also observed over the years, but until 2017 that decrease was not steep as the biomass (Figure 48C). This is the result of a shift in the structure of the stock towards smaller animals (Figure 49). The situation observed in 2018 is quite worrisome. As opposed to previous years, no highly abundant pre–recruited cohort was observed (Figure 49). High abundances of rock cod on the high seas north of the FOCZ were reported during the 2017-18 summer by trawlers. However, no quantitative data were collected to estimate the biomass available outside Falkland waters. Considering the importance of this stock to the finfish bottom trawl fleet (A–, G– and W–licensed) and its regulation by vessel units, annual monitoring of this species is paramount. Moreover, as rock cod is most likely an important prey item for most of the commercial species such as toothfish, kingclip, red cod, hakes, and skates, studying trophic relationships and competition with other species is imperative in order to gain insights into the decrease of this stock. Furthermore, the extension of the survey to the south showed that rock cod was found at stations as deep as 733 m, the deepest station sampled during the survey, which is much deeper than the 500 m limit mentioned reported on Fishbase (Froese and Pauly, 2018).

The total toothfish catch during this research cruise was the highest since 2010 (Figure 50D) and has resulted in a significant increase in estimated biomass relative to 2017 (Figure 50C). However, this is most likely an artefact to extending the survey to the south in deeper waters as the highest densities of toothfish were observed in waters exceeding 300 m in depth to the south and southwest of the survey area (Figure 50B). Of note, toothfish bycatch levels at the ten deepest stations (340 to 733 m) averaged 3.5% (range 0.3 to 7.7%) with eight stations exceeding the 1.5% toothfish bycatch threshold. Given the current interest and restrictions placed on toothfish by-catch, it is recommended that the extension to the south of the finfish area be maintained for future demersal fish surveys. As aforementioned, this would further benefit our knowledge concerning other species, in addition to toothfish, such as southern blue whiting, hoki, grenadiers, and skates. However, of concern is the absence of the pre-recruit cohort in 2018 for the first time since 2011. Although a greater proportion of larger individuals were caught and sampled from the extended area of the survey to the south, we would have expected to catch smaller individuals from this pre-recruit cohort in shallow waters surrounding the Jason Islands to the northwest of the survey area. Unfortunately, these were not and indicate that the Department will need to monitor and manage future

recruitment into the longline fisheries carefully over the coming years. This provides further support to the continuation of this survey, in its extended form, beyond 2018.

As observed in previous ground fish surveys conducted in February (Gras et al., 2015; 2016; 2017), Argentine shortfin squid was already present in Falkland waters. Interestingly catches and biomass of this species were high in 2015 (year of record catches, 357,722 t) and almost nil in 2016 (2,360 t). However, from 2017 to 2018, biomass estimations derived from catches of the ground fish survey increased from 16,389 to 52,283 while commercial catches decreased from 67,445 to 54,387 t (at the time of finalising this report). Although the relationship between the estimated biomass in February and total catches is most likely not a simple linear regression, the ground fish survey that is conducted prior to the start of the fishing season could be used as a pre–recruitment survey for *I. argentinus*. Combined with oceanographic data, this survey could provide us with an indication of recruitment timing into the FICZ/FOCZ. Throughout the season a depletion model (Basson et al., 1996) could be used to monitor *I. argentinus* biomass and forecast the Spawning Stock Biomass at the end of the season like what is already done to monitor *D. gahi* (Roa-Ureta and Arkhipkin, 2007). Although access to Argentine data would improve the forecasting, Basson et al., 1996 showed that the stock could be monitored with Falkland data alone.

Kingclip biomass has decreased substantially from a high in 2015, now reaching a biomass lower than that estimated in 2010 (Figure 46C). Despite kingclip abundance following a similar trend, similarly to rock cod, the recent decline in kingclip abundance is not as steep as the one observed for biomass (Figure 46C), thus suggesting a shift in length frequency towards smaller individuals. This can indeed be seen in the length frequency histograms where the 2018 modal length can be observed at 50 cm, where it used to lie closer to 55 cm (Figure 47). Furthermore, very few individuals >100 cm in length were observed this year relative to 2010-2017 (Figure 47). Age length keys for 2010 to 2018 need to be constructed and compared once the age validation exercise for kingclip is completed to determine whether length at age has shifted.

Red cod biomass has increased from 2017, albeit not significantly, while abundance has decreased (Figure 39C). This indicates a shift in length distribution of the species at this time of the year. Although a shift is not clearly observed on the basis of the length frequency histograms, what is noticeable is the absence of the first pre-recruit cohort for the first time since 2010 (Figure 39). Additionally it is interesting to notice that the highest densities of red cod are near the spawning grounds (Figure 39B) in areas that would be closed to fishing during the spawning season (October).

Regarding the sampling strategy, it seems that some adjustments could be done to improve the biological sampling. For the bigger fish such as toothfish, red cod, kingclip, southern blue whiting and hake, it appeared that a random sample of 100 specimens per station was not necessarily representative of the whole catch. Sampling the whole catch would improve the sampling for these species that are important both from the commercial and ecosystem perspective. A paper that gives more insight in this topic has been published recently (Moriarty et al., 2018) and could be of use in guiding us towards best practice.

The survey that was conducted in July was an opportunity to have a second snapshot of the ecosystem in 2017, but during winter months. It (i) enabled the biomass estimation of some species that are not abundant in Falkland waters in summer, and (ii) gave an opportunity to have an inter–seasonal comparison for all the commercial stocks. Given that it is not possible to compare July 2017 to January 2018 without a time series for stock biomass during the winter months, it is recommended that the FIFD commit to creating a time series with this

July survey to determine whether changes in biomass between summer and winter months are simply attributable to seasonal migrations. Understanding seasonal patterns in species biomass is imperative to gaining insights into temporal patterns in ecosystem dynamics to inform an ecosystem–based framework to managing our Fisheries resources.

Changes in relative abundance and biomass of skate assemblages were observed during this survey relative to previous years. However, given the extension of the survey to the south, the elimination of ten stations overlapping with the pre–recruitment survey to the northeast, and the shortened "skate stations" in deeper waters to the north, direct comparisons are simply not possible or desirable. As such, continuing the February demersal survey for at least two more years under the same protocol as 2018 would enable using data from this research cruise towards the annual skate stock assessment and replace the "skate cruise" that is meant to occur every three years, but has been skipped several times to date due to limited days set aside for research cruises and other departmental priorities.

The February ground fish survey has brought a lot of information to understand the dynamics of marine populations in the finfish zone. Data collected during this survey can be used to derive fisheries independent indices of abundance for all the finfish species surveyed. These data can also be used for an *Illex* pre–recruitment survey and for annual skate stock assessment. Moreover, ages and maturities collected during this survey could help derive age–structured indices of abundance that could be used to tune age–structured models such as virtual population analysis or statistical catch–at–age. Finally, as every finfish species was sampled such data could be used as input data in an ecosystem model such as Ecopath with Ecosim (Ewe, 2018).

References

Arkhipkin, A. I., Bakanev, S., and Laptikhovsky, V. V. 2011. Rock cod biomass survey. Stanley, Falkland Islands. 37 pp.

Arkhipkin, A., Brickle, P., and Laptikhovsky, V. V. 2013. Links between marine fauna and oceanic fronts on the Patagonian Shelf and Slope. Life and Marine Sciences, 30: 19–37.

Bakun, A. 1993. The California current, Benguela current, and southwestern Atlantic shelf ecosystems: A comparative approach to identifying factors regulating biomass yields. *In* Large Marine Ecosystems: Stress, Mitigation, and Sustainability, pp. 199–221. Ed. by K. Sherman, L. M. Alexander, and B. D. Gold. Washington D. C., USA.

Bax, N. J. 1998. The significance and prediction of predation in marine fisheries. ICES Journal of Marine Science, 55: 997–1030.

Basson, M., Beddington, J. R., Crombie, J. A., Holden, S. J., Purchase, L. V., and Tingley, G. A. (1996). Assessment and management techniques for migratory annual squid stocks: the *Illex argentinus* fishery in the Southwest Atlantic as an example. *Fisheries Research* **28**, 3–27.

Bivand, R., Keitt, T., Rowlingson, B., Pebesma, E., Summer, M., Hijmans, R., Rouault, E., and Ooms, J. 2017. Package 'rgdal'. Bindings for the 'Geospatial' data abstraction library. R Package 1.2–13. https://cran.r-project.org/web/packages/rgdal/rgdal.pdf.

Brickle, P., and Laptikhovsky, V. V. 2010. Rock cod biomass survey. Stanley, Falkland Islands. 31 pp.

Brickle, P., and Winter, A. 2011. First cod end mesh size experiments. Stanley, Falkland Islands. 57 pp.

Corrales, X., Coll, M., Tecchio, S., Bellido, J. M., Fernandez, A. M., and Palomera, I. 2015. Ecosystem structure and fishing impacts in the northwestern Mediterranean Sea using a food web model with a comparative approach. Journal of Marine Systems, 148: 183-199.

EwE, 2018. Ecopath with Ecosim website. www.ecopath.org. (accessed May 2018)

Falkland Islands Fisheries Department. 2014. Vessel Units, allowable Effort, and Allowable Catch 2015. Fisheries Department, Directorate of Natural Resources. Stanley, Falkland Islands. 54 pp.

Falkland Islands Fisheries Department. 2015. Vessel units, allowable effort and allowable catch 2016. Fisheries Department, Directorate of Natural Resources. Stanley, Falkland Islands. 54 pp.

Falkland Islands Fisheries Department. 2016. Vessel units, allowable effort and allowable catch 2017. Fisheries Department, Directorate of Natural Resources. Stanley, Falkland Islands. 100 pp.

Falkland Islands Fisheries Department. 2017. Vessel units, allowable effort and allowable catch 2018. Fisheries Department, Directorate of Natural Resources. Stanley, Falkland Islands.

Froese, R., and Pauly, D. (Eds.) 2018. FishBase. World Wide Web electronic publication. www.fishbase.org. version (02/2018).

Gras, M. 2016. Linear models to predict the horizontal net opening of the DNR Fisheries trawl. Stanley, Falkland Islands. 5 pp.

Gras, M., Blake, A., Pompert, J., Jürgens, L., Visauta, E., Busbridge, T., Rushton, H., *et al.* 2015. Rock cod biomass survey 2015 ZDLT1-02-2015. Stanley, Falkland Islands. 46 pp.

Gras, M., Pompert, J., Blake, A., Boag, T., Grimmer, A., Iriarte, V., and Sanchez, B. 2016. Finfish and rock cod biomass survey. Stanley, Falkland Islands. 72 pp.

Gras, M., Pompert, J., Blake, A., Busbridge, T., Derbyshire, C., Keningale, B., and Thomas, O. 2017. Ground Fish Survey. Stanley, Falkland Islands. 84 pp.

Laptikhovsky, V. V., Arkhipkin, A. I., and Brickle, P. 2013. From small bycatch to main commercial species: Explosion of stocks of rock cod Patagonotothen ramsayi (Regan) in the Southwest Atlantic. Fisheries Research, 147: 399–403.

Link, J. S. 2002. What does ecosystem-based fisheries management mean. Fisheries, 27: 18-21.

Lipiński, M. R. 1979. Universal maturity scale for the commercially important squids (Cephalopoda: Teuthoidea). The results of maturity classification of \textit{Illex illecebrosus} (Le Sueur 1821) population for years 1973-1977. 40 pp.

McEachran, J. D. 1983. Results of the research cruises of FRV 'Walther Herwig' to South America. LXI. Revision of the South American skate genus Psammobatis Günther, 1870. (Elasmobranchii: Rajiformes, Rajidae). Archiv fur Fischeriwissenschaf Bundesforschungsanstalt fur Fischerie, 34: 23–80.

Moriarty, M., Sell, A. F., Trenkel, V. M., Lynam, C. P., Burns, F., Clarke, E. D., Greenstreet, S. P. R., and McGonigle, C. *In* press. Resolution of biodiversity and assemblage structure in demersal fisheries surveys: the role of tow duration. ICES Journal of Marine Science, doi: 10.1093/icesjms/fsy050.

Pompert, J., Gras, M., Blake, A., and Visauta, E. 2014. Rock cod biomass and biological survey. Stanley, Falkland Islands. 50 pp.

Ribeiro Jr., P. J., and Diggle, P. J. (2016) Package 'geoR'. Analysis of geostatistical data. R Package 1.7-5.2. https://cran.r-project.org/web/packages/geoR/geoR.pdf.

Rivoirard, J., Simmonds, J., Foote, K. G., Fernandes, P., and Bez, N. 2000. Geostatistics for estimating fish abundance. John Wiley & Sons. 206 pp.

Roa-Ureta, R. and Arkhipkin, A. I. 2007. Short-term stock assessment of *Loligo gahi* at the Falkland Islands: sequential use of stochastic biomass projection and stock depletion models. ICES Journal of Marine Science, 64, 3–17.

Roux, M., Brewin, P., Jürgens, L., Winter, A., and James, R. 2013. Square mesh panel (SMP) trials - 2. Stanley, Falkland Islands. 49 pp.

Roux, M.-J., Laptikhovsky, V. V., Brewin, P., Arkhipkin, A. I., and Winter, A. 2012. Second cod end mesh size experiment. Stanley, Falkland Islands. 54 pp.

Roux, M., Laptikhovsky, V. V., Brewin, P., and Winter, A. 2013. Square mesh panel (SMP) trials - 1. 45 pp.

Roux, M., Laptikhovsky, V. V., Brewin, P., and Winter, A. 2013. Third cod end mesh size experiment. Stanley, Falkland Islands. 45 pp.

Roux, M., Winter, A., and James, R. 2013. Square mesh panel (SMP) trials - 3. Stanley, Falkland Islands. 53 pp.

Schlitzer, R. 2013. Ocean data view. http://odv.awi.de.

Vaudo, J., and Heithaus, M. 2011. High-trophic-level consumers: elasmobranchs. *In* Treatise on Estuarine and Coastal Science, pp. 203-225. Ed. by Wolanski, E., and McClusky, D., Academic Press, London, UK.

Winter, A., Laptikhovsky, V. V., Brickle, P., and Arkhipkin, A. I. 2010. Rock cod (Patagonotothen ramasyi (Regan, 1913)) stock assessment in the Falkland Islands. Stanley, Falkland Islands. 12 pp.

Appendix

Table 2: Catch table ZDLM3-02-2018

Species	Latin Name	Total Catch (kg)	Total Sample (kg)	Total Discard (kg)	Proportion (%)
MED	Medusae	37,476.08	7.17	37,474.00	28.74%
WHI	*Macruronus magellanicus*	29,334.80	1,716.72	6.88	22.50%
BAC	*Salilota australis*	12,733.50	2,298.81	107.03	9.76%
PAR	*Patagonotothen ramsayi*	11,383.25	977.52	5,729.26	8.73%
ILL	*Illex argentinus*	10,693.70	1,338.68	1.48	8.20%
GRF	*Coelorhynchus fasciatus*	6,854.33	413.26	5,069.05	5.26%
GRC	*Macrourus carinatus*	3,944.98	1,348.58	175.09	3.03%
KIN	*Genypterus blacodes*	3,350.93	3,299.15	6.81	2.57%
MUN	*Munida* spp.	2,522.11	-	2,522.05	1.93%
BLU	*Micromesistius australis*	2,200.67	659.56	337.87	1.69%
HAK	*Merluccius hubbsi*	1,731.75	1,307.87	19.01	1.33%
TOO	*Dissostichus eleginoides*	1,388.92	1,240.69	18.59	1.07%
LOL	*Doryteuthis gahi*	968.41	167.62	43.50	0.74%
RGR	*Bathyraja griseocauda*	814.06	813.99	0.38	0.62%
PYM	*Physiculus marginatus*	807.36	73.67	442.43	0.62%
ING	*Moroteuthis ingens*	397.25	303.23	311.85	0.30%
RFL	*Zearaja chilensis*	360.94	360.94	-	0.28%
RBR	*Bathyraja brachyurops*	336.69	336.65	4.61	0.26%
MUG	*Munida gregaria*	304.39	1.44	304.39	0.23%
MXX	Myctophid spp.	274.11	2.24	274.11	0.21%
PAT	*Merluccius australis*	267.96	267.96	-	0.21%
CGO	*Cottoperca gobio*	255.37	255.32	233.85	0.20%
SPN	Porifera	210.87	2.56	208.73	0.16%
SAR	*Sprattus fuegensis*	208.47	13.83	208.46	0.16%
DGS	*Squalus acanthias*	188.87	1.04	188.87	0.14%
DGH	*Schroederichthys bivius*	177.13	4.87	172.25	0.14%
BUT	*Stromateus brasiliensis*	168.70	168.70	164.82	0.13%
CHE	*Champsocephalus esox*	129.05	48.68	-	0.10%
PAU	*Patagolycus melastomus*	117.33	13.20	114.46	0.09%
RBZ	*Bathyraja cousseauae*	112.08	112.08	-	0.09%
RMU	*Bathyraja multispinis*	59.35	53.88	5.47	0.05%
SQT	Ascidiacea	46.12	-	46.12	0.04%
RAL	*Bathyraja albomaculata*	45.62	45.62	3.13	0.03%
RMC	*Bathyraja macloviana*	45.44	45.44	7.01	0.03%
SHT	Mixed invertebrates	43.53	3.04	43.53	0.03%
ANG	*Anthoptilum grandiflorum*	39.03	-	39.03	0.03%
GYN	*Gymnoscopelus nicholsi*	35.60	2.29	35.44	0.03%
COP	*Congiopodus peruvianus*	33.44	27.04	33.44	0.03%
RSC	*Bathyraja scaphiops*	32.59	32.59	0.96	0.02%
HYD	Hydrozoa	31.57	0.08	31.57	0.02%
STA	*Sterechinus agassizi*	22.86	0.01	22.86	0.02%
GOC	*Gorgonocephalus chilensis*	22.29	-	22.29	0.02%
NEM	*Neophyrnichthys marmoratus*	18.08	16.97	16.97	0.01%
ALF	*Allothunnus fallai*	16.78	16.78	5.26	0.01%
RED	*Sebastes oculatus*	16.12	16.12	2.14	0.01%
COT	*Cottunculus granulosus*	15.23	14.59	15.23	0.01%
RAY	Rajiformes	13.32	13.31	-	0.01%

ICA	*Icichthys australis*	12.64	1.69	0.04	<0.01%
RPX	*Psammobatis* spp.	11.72	11.72	7.46	<0.01%
RDA	*Dipturus argentinensis*	11.30	11.30	-	<0.01%
PSM	*Pseudocyttus maculatus*	8.70	-	-	<0.01%
XXX	Unidentified animal	7.85	7.54	0.25	<0.01%
BDU	*Brama dussumieri*	7.09	7.09	3.45	<0.01%
ANM	Anemone	6.48	-	6.48	<0.01%
MAN	*Mancopsetta* sp.	5.89	5.89	-	<0.01%
OCT	*Octopus* spp.	4.56	-	3.69	<0.01%
EGG	Eggmass	4.46	-	4.46	<0.01%
FUM	*Fusitriton m. magellanicus*	4.43	0.10	2.38	<0.01%
WRM	*Chaetopterus variopedatus*	4.20	-	4.20	<0.01%
CAS	*Campylonotus semistriatus*	4.19	1.68	1.40	<0.01%
CTA	*Ctenodiscus australis*	3.91	0.02	3.86	<0.01%
OPV	*Ophiacanta vivipara*	3.58	0.16	3.58	<0.01%
ALC	*Alcyoniina*	3.30	0.01	3.30	<0.01%
RDO	*Amblyraja doellojuradoi*	3.11	3.00	1.20	<0.01%
COS	*Coryphaenoides subserrulatus*	2.91	0.24	0.24	<0.01%
ALG	Algae	2.73	-	2.73	<0.01%
COG	*Patagonotothen guntheri*	2.66	2.62	2.26	<0.01%
AUC	*Austrocidaris canaliculata*	2.15	-	2.15	<0.01%
ANR	*Antimora rostrata*	2.09	2.09	2.09	<0.01%
PTE	*Patagonotothen tessellata*	1.97	1.97	-	<0.01%
MLA	*Muusoctopus longibrachus akambei*	1.96	0.22	1.96	<0.01%
ZYP	*Zygochlamys patagonica*	1.79	-	1.79	<0.01%
MAM	*Mancopsetta milfordi*	1.76	1.76	-	<0.01%
UHH	Heart urchin	1.75	0.01	1.75	<0.01%
POA	*Porania antarctica*	1.49	0.02	1.49	<0.01%
AST	Asteroidea	1.48	0.01	1.43	<0.01%
ODM	*Odontocymbiola magellanica*	1.35	-	0.66	<0.01%
PES	*Peltarion spinosulum*	1.32	-	1.32	<0.01%
MUU	*Munida subrugosa*	1.08	-	1.08	<0.01%
SRP	*Semirossia patagonica*	1.00	0.01	1.00	<0.01%
COL	*Cosmasterias lurida*	0.89	-	0.89	<0.01%
OPH	Ophiuroidea	0.81	-	0.80	<0.01%
SEP	*Seriolella porosa*	0.79	0.79	0.79	<0.01%
ASA	*Astrotoma agassizii*	0.77	-	0.77	<0.01%
ODP	*Odontaster pencillatus*	0.76	0.01	0.76	<0.01%
CAZ	*Calyptraster* sp.	0.75	-	0.75	<0.01%
NUD	Nudibranchia	0.69	0.01	0.68	<0.01%
BRY	Bryozoa	0.68	-	0.68	<0.01%
SUN	*Labidaster radiosus*	0.64	0.07	0.64	<0.01%
EUL	*Eurypodius latreillei*	0.63	0.01	0.63	<0.01%
CEX	*Ceramaster* sp.	0.61	-	0.61	<0.01%
UCH	Sea urchin	0.59	-	0.59	<0.01%
PYX	Pycnogonida	0.56	0.01	0.56	<0.01%
OPL	*Ophiuroglypha lymanii*	0.55	0.01	0.55	<0.01%
THB	*Thymops birsteini*	0.51	-	0.51	<0.01%
ANT	Anthozoa	0.42	-	0.42	<0.01%
BAO	*Bathybiaster loripes*	0.41	-	0.41	<0.01%

RMG	*Bathyraja magellanica*	0.35	0.35	-	<0.01%
ISO	Isopoda	0.33	0.01	0.33	<0.01%
MUO	*Muraenolepis orangiensis*	0.29	0.26	0.29	<0.01%
MAT	*Achiropsetta tricholepis*	0.26	0.20	-	<0.01%
ILF	*Iluocoetes fimbriatus*	0.23	0.01	0.16	<0.01%
CRY	*Crossaster* sp.	0.20	-	0.20	<0.01%
LIA	*Lithodes antarcticus*	0.19	-	0.19	<0.01%
EUO	*Eurypodius longirostris*	0.18	-	0.18	<0.01%
BAL	*Bathydomus longisetosus*	0.18	-	0.12	<0.01%
MAV	*Magellania venosa*	0.16	-	0.16	<0.01%
COK	*Coelorinchus kaiyomaru*	0.14	0.14	0.14	<0.01%
CYX	*Cycethra* sp.	0.11	-	0.11	<0.01%
HOL	Holothuroidea	0.07	-	0.07	<0.01%
LOS	*Lophaster stellans*	0.06	-	0.06	<0.01%
AGO	*Agonopsis chilensis*	0.05	-	0.05	<0.01%
HCR	Paguroidea	0.04	-	0.04	<0.01%
GYM	*Gymnoscopelus* spp.	0.04	-	0.04	<0.01%
OPS	*Ophiactis asperula*	0.04	-	0.04	<0.01%
POL	Polychaeta	0.04	-	0.04	<0.01%
CRI	Crinoidea	0.03	-	0.03	<0.01%
ACS	*Acanthoserolis schythei*	0.02	-	0.02	<0.01%
OPD	*Ophiacantha densispina*	0.02	-	0.02	<0.01%
NUH	*Nuttallochiton hyadesi*	0.01	-	0.01	<0.01%
STS	*Stereomastis suhmi*	0.01	-	0.01	<0.01%
CAV	*Campylonotus vagans*	0.01	-	0.01	<0.01%
EEL	*Iluocoetes/Patagolycus* mix	0.01	-	-	<0.01%
FIN	Unidentified finfish	0.01	-	-	<0.01%
PGR	*Paradiplospinus gracilis*	<0.01	<0.01	<0.01	<0.01%
		130,402.05	17,904.80	54,551.33	

Table 3: Sample numbers by sample type

Code	Species Name	N	R	S	Total	
PAR	*Patagonotothen ramsayi*	82	6,741	2,252	9,075	23.9%
LOL	*Doryteuthis gahi*	1	8,228	103	8,332	22.0%
BAC	*Salilota australis*	13	2,817	1,104	3,934	10.4%
HAK	*Merluccius hubbsi*	4	1,572	1,448	3,024	8.0%
ILL	*Illex argentinus*	30	2,838	96	2,964	7.8%
KIN	*Genypterus blacodes*	1	1,032	1,279	2,312	6.1%
WHI	*Macruronus magellanicus*	3	664	570	1,237	3.3%
TOO	*Dissostichus eleginoides*	8	456	366	830	2.2%
PTE	*Patagonotothen tessellata*		805		805	2.1%
GYN	*Gymnoscopelus nicholsi*		754		754	2.0%
CHE	*Champsocephalus esox*		323	270	593	1.6%
CGO	*Cottoperca gobio*	16	433	61	510	1.3%
BLU	*Micromesistius australis*	3	335	103	441	1.2%
BUT	*Stromateus brasiliensis*		408		408	1.1%
GRF	*Coelorhynchus fasciatus*		271	103	374	1.0%
RBR	*Bathyraja brachyurops*		373	1	374	1.0%
PAU	*Patagolycus melastomus*		62	274	336	0.9%
SAR	*Sprattus fuegensis*		335		335	0.9%
PYM	*Physiculus marginatus*		171	99	270	0.7%
RFL	*Zearaja chilensis*		244		244	0.6%
RED	*Sebastes oculatus*		106	2	108	0.3%
RGR	*Bathyraja griseocauda*		54	48	102	0.3%
PMC	*Protomictophum choriodon*		85		85	0.2%
PAT	*Merluccius australis*		65	6	71	0.2%
RMC	*Bathyraja macloviana*		71		71	0.2%
COT	*Cottunculus granulosus*		59		59	0.2%
RAL	*Bathyraja albomaculata*		41		41	0.1%
RPX	*Psammobatis spp.*		38		38	0.1%
RMG	*Bathyraja magellanica*		32		32	0.1%
ILF	*Iluocoetes fimbriatus*		9	17	26	0.1%
RSC	*Bathyraja scaphiops*		25		25	0.1%
DGS	*Squalus acanthias*		20	2	22	0.1%
SEP	*Seriolella porosa*		19		19	0.1%
COP	*Congiopodus peruvianus*		18		18	<0.01%
RBZ	*Bathyraja cousseauae*		9	5	14	<0.01%
NEC	*Neorossia caroli*		9		9	<0.01%
MUO	*Muraenolepis orangiensis*		8		8	<0.01%
RMU	*Bathyraja multispinis*		2	5	7	<0.01%
LYB	*Lycenchelys bachmanni*		6		6	<0.01%
COG	*Patagonotothen guntheri*		5		5	<0.01%
OIB	*Oidiphorus brevis*		5		5	<0.01%
RDO	*Amblyraja doellojuradoi*		5		5	<0.01%
ALF	*Allothunnus fallai*		3	1	4	<0.01%
MLA	*Muusoctopus longibrachus akambei*		4		4	<0.01%
POE	*Pogonolycus elegans*		4		4	<0.01%
GON	*Gonatus antarcticus*		2		2	<0.01%
PLS	*Plesienchelys stehmanni*		2		2	<0.01%
SEC	*Seriolella caerulea*		2		2	<0.01%
THN	*Thysanopsetta naresi*		2		2	<0.01%
ING	*Moroteuthis ingens*		1		1	<0.01%
MMA	*Mancopsetta maculata*		1		1	<0.01%
PAV	*Patagonotothen brevicauda*	1			1	<0.01%
POR	*Lamna nasus*		1		1	<0.01%
RTR	*Dipturus trachydermus*		1		1	<0.01%
SYB	*Symbolophorus boops*		1		1	<0.01%
					37,954	